A THEORETICAL STUDY OF THE SUBSTITUENT EFFECTS ON SOME SPECTROSCOPIC AND BONDING PARAMETERS OF SOME METAL β-DIKETONATES AND OTHER MACROCYCLIC COMPLEXES.

By

HARUNA MORO

B.Sc. (Hons.) Chemistry, Kumasi

A Thesis submitted to the Department of Chemistry,

Kwame Nkrumah University of Science and Technology

In partial fulfillment of the requirements for the degree of

MASTER OF SCIENCE

College of Science.

September, 2012.

CERTIFICATION

I hereby declare that this submission is my own work towards the MSc. and that, to the best of my knowledge, it contains no material previously published by another person nor material which has been accepted for the award of any other award of any other degree of the university, except where due acknowledgement has been made in the text.

……..	……	……
Student Name	Signature	Date

Certified by,

……	……	…….
Supervisor(s) Name	Signature	Date

Certified by,

……	……	…….
Head of Dept. Name	Signature	Date

ABSTRACT

Theoretical and structural analysis through the PM3 and DFT procedures were used to investigate the geometries, energies, vibrational frequencies and NMR spectra of derivatives of metal β-diketonate complexes, [M(β-dike)$_3$] and their mixed complexes.

The β-diketones studied are,Hacac, Htfac, Hhfac, Htbd, Htftbd, Hfbd, Htffbd, Hbzac, Htfbzac, Hfpa, Htpd, Hdbm and Hdhfpd; and their metal complexes with M = Al, Cr, Mn, Fe, and Co. Among the complexes studied, the symmetry point group D_3 was observed for acetylacetonate and hexafluoroacetylacetonate chelates and C_1 was observed for all other complexes. The region 3500 – 300cm^{-1} were studied for the IR vibrations. The carbonyl band assigned to asymmetric C = O (υ_{as}C = O) stretching mode appears at the 1869-1764cm^{-1} region for all the complexes except for the chromium complex which band fell below 1700cm^{-1}. The M – O frequencies for all the chelates are weak and fall below 600cm^{-1}.Qualitatively, the calculated frequencies agree with the expterimental results. However, on the quantitative aspects, the calculated frequencies differ by about 160 – 30cm^{-1} from the expterimental results. The NMR spectral analysis using the B3LYP/6-31G* basis set reveals that an increase in fluorine substitution deshields the attached protons and carbons thereby causing them to be shifted downfield. These findings are consistent with experimental results. The UV spectra of the cobalt derivatives of the complexes examined in the gaseous phase exhibited two broad bands with different λ_{max}values which are higher in energy than are found in the corresponding Aluminium compounds.

The general trend of the complexes in terms of stability with respect to the heat of formation irrespective of the central metal is M(hfac)$_3$> M(tfac)$_3$> M(Htffbd)$_3$> M(Htfbzac)$_3$ > M(Htftbd)$_3$> M(acac)$_3$> M(Hfbd)$_3$> M(Hbzac)$_3$> M(Hfpa)$_3$> M(Htbd)$_3$> M(Hftpd)$_3$> M(Hdbm)$_3$> M(Htpd)$_3$> M(Htbzac)$_3$> M(Dhfpd)$_3$. The order gives an indication of the electron withdrawing ability of CF3 groups relative to the positive mesomeric effects of the

aromatic substituents. It is also observed that increasing CF_3 substitution opens up the O…C…C bond angle and closes up that of C…C…C, C…O…M and O…M…O.

PM3 studies on β–diketonate, β-ketoiminate, β-diiminate, β-ketothiolate, β- dithiolate and β-imithiolate complexes of 4,4,4-trifluoro-1-(2-furyl)-1,3-butanedione (htffbd) reveals that the M-S bonds (2.306 Å average) are significantly longer than the M-O bonds (1.895 Å average) which are also longer than the M-N bonds (1.758 Å average).The C = C bonds on the keto (O) side of the ring is longer than the C = C bonds on the imine (N) side with the C = C bonds on the thio (S) side of the ring having the shortest bond distance (ie C = C(O) > C = C(N) > C = C(S) in bond length). Analysis of the HOMO and LUMO energy gap of these complexes gives the order; β–Diketonate< β–Ketothiolate< β–Ketoiminate< β– Diiminate< β–Thioiminate< β–Dithiolate.

Considering the calculated bond lengths for the N_6- tetradentatemacrocyclic complexes for cobalt, the two Co–Cl bonds were on the average 2.2245Å for trifluoro substituents, 2.2265Å for phenyl substituents and 2.2365Å for methyl substituents. The Co–N bond lengths on the average for the CF_3, phenyl and CH_3 substituents are respectively 2.040Å, 2.041Å and 1.989Å.

ACKNOWLEDGEMENT

Glory and honour be to ALLAH the most merciful for bringing me this far.

I am greatly indebted to Professor A. A. Adimado my supervisor for selecting the topic and supervising the work, his invaluable assistance, care and understanding made this work possible.

I am particularly grateful to Dr. Evans Adei and Dr. Richard Tia, the managers of the computational laboratory for their constructive criticisms, guidance and corrections. It has indeed been wonderful working in your laboratory.

DEDICATION

Dedicated to the entire Haruna family.

TABLE OF CONTENTS

CHAPTER ONE

CHAPTER FOUR

CHAPTER FIVE

LIST OF TABLES

LIST OF FIGURES

LIST OF ABBREVIATIONS

ABBREVIATION	TERM
AM1	Austin Model 1
B_1LYP	Exchange-correlation functionals of (Becke functional and Lee-Yang-Parr functional).
B_3LYP	Hybrid exchange-correlation functionals of (Becke-style three parameter functional and Lee-Yang-Parr functional).
Bipy	2,2'-bipyridine.
Bzac	Benzoylacetone.
CBS	Complete Basis set.
CFSE	Crystal Field Stabilization Energy.
CT	Charge transfer.
CVD	Chemical Vapour Deposition.
Dbm	Dibenzoylmethane.
DFT	Density Function Theorem.
Dhfpd	1,3-(2-furyl)-1,3-propanedione.
DMSO	Dimethylsulfoxide.
DNA	Deoxyribonucleic acid.
E	Energy.
FT-IR	Fourier Transform-Infrared Spectroscopy.
G_{96}LYP	Functional proposed by Gill and correlation has been included by Lee, Yang and Parr functional.
H	Hamiltonian operator.
Hacac	Acetylacetone.
Hbzac	1-phenyl-1,3-butanedione.
Hbztfac	4,4,4-trifluoro-1-phenyl-1,3-butanedione
HF	Hartree-Fock approximation.
Hfac	Hexafluoroacetylacetone.

Hfbd	1-(2-furyl)-1,3-butanedione.
Hfpa	1-(2-furyl)-3-phenyl-1,3-propanedione.
Hftpd	1-(2-furyl)-3-(2-thienyl)-1,3-propanedione.
HSAB	Hard Soft Acid Base.
Htbd	1-(2-thienyl)-1,3-butanedione.
Htbzac	1-phenyl-3-(2-thienyl)-1,3-propanedione
Htffbd (Htfa)	4,4,4-trifluoro-1-(2-furyl)-1,3-butanedione
Htfpybd	4,4,4-trifluoro-1-(3-pyridyl)-1,3-butanedione.
Htftbd(Htta)	4,4,4-trifluoro-1-(2-thienyl)-1,3-butanedione (2-thenoyltrifluoroacetone).
Htpd	1,3-(2-thienyl)-1,3-propanedione.
INDO	Intermediate Neglect of Differential Overlap
IR	Infrared Spectrum.
L	Ligand
M	Metal
MIA	Metal Ion Affinity.
MMFF	Molecular Mechanics Force Field.
MNDO	Modified Neglect of Differential Overlap.
MP2	Second-Order Møller-Plesset Perturbation Theory.
N	Nitrogen.
NDDO	Neglect of Diatomic Differential Overlap.
NLO	Second-Order Nonlinear Optical Responses.
NMR	Nuclear Magnetic Resonance.
NQR	Nuclear Quadrupole Resonance.
PDA	Polydiacetylene.
PDT	Photodynamic Cancer Treatment.
Phen	1,10-phenanthroline.

PM3	Parameterized Model 3.
S	Singlet
SCF	Self Consistent Field.
Tfac	4,4,4- Trifluoroacetylacetone (benzoyltrifluoroacetylacetone)
Tfnac	4,4,4- Trifluoro-1-(2-naphthyl)-1,3-diketonate
TGA	Thermogravimetric Analysis.
Tmhd	2,2,6,6-tetramethyl-3,5-heptanedionate.
TMS	Tetramethylsilane ($Si(CH_3)_4$)
T_{sub}	Temperature of sublimation.
UV	Ultraviolet Visible spectra.
VB	Valence bond.
XC	Exchange-Correlation.
ΔH_{sub}	Enthalpy of sublimation
$\Delta H^{\theta}f$	Enthalpy of formation.

LIST OF SYMBOLS

SYMBOL	TERM
Ψ	Wavefunction of Molecular System
ν	Stretching
νs	Symmetric stretching
νas	Asymmetric stretching
δ	Inplane bending
δs	Inplane bending scissoring
ρ	Inplane bending of rocking
τ	Out of plane bending twisting
ω	Out of plane bending wagging
γ	Out of plane bending
Δ ring	Inplane ring deformations
Γring	Out of plane ring deformations
v	Very
s	Strong
m	Medium
w	Weak

1.0 CHAPTER ONE

1.1 INTRODUCTION

Historically, most fundamental research in many of the physical sciences could be categorized as either theoretical or expterimental or a combination of both. Often the theoretician attempted to predict or exptlainexpterimental observations by constructing models and solving the resulting mathematical equations. However, in many instances the systems that the theoreticians could investigate and solve fully were much smaller or more "idealized" than the "real" chemical systems that the expterimentalist could observe.

As the science of theoretical chemistry has matured, its focus has shifted from analytically solvable problems, such as the atomic structure of hydrogen, to more complex problems for which analytical solutions are difficult or impossible to specify. The powerful, highly-parallel supercomputers that have evolved from recent advances in computing technology are ideally suited to the mathematical modeling of these complex chemical phenomena.

Computational chemistry methods encompass a variety of mathematical methods which fall into two broad categories: molecular mechanics and quantum mechanics. Many aspects of molecular structure and dynamics can be modeled using classical methods in the form of molecular mechanics and dynamics.

Ab initio, quantum chemistry is capable of calculating a wide range of chemical and physical phenomena of interest to a scientist. These methods can be used both to predict the results of future expteriments and to assist in the interpretation of existing observations. Quantum chemical calculations can also be a fast and inexptensive guide to the expterimental necessity. Although calculations will never exclude the need for expteriment, they can be a valuable

tool to provide insight into chemical and physical problems that may be unavailable to the expterimentalist. By starting from first-principle and treating the molecule as a collection of positive nuclei and negative electrons moving under the influence of coulumbic potentials, the computational ab initio Quantum Chemistry enables the structure, energy and other related properties of a molecule or molecular systems to be obtained by solving the Schrodinger equation:

$$H\Psi = E\Psi$$

Where H, E, and Ψ are the Hamiltonian operator, energy and wavefunction of the molecular system respectively.

While it is not possible to solve the Schrödinger equation for a many electron system, it may be assumed that where it is possible the resulting molecular properties would exactly reproduce the corresponding expterimental quantities.

Quantum Chemistry through mathematical equations has now made it possible to treat many-electron systems like transition metal compounds with accuracy that may be most challenging to the expterimentalists. Geometries, bond energies, vibrational frequencies and even NMR chemical shifts of transition metal compounds can be predicted reliably by Quantum chemical methods [Frenking*et al.*, 1996].

Qualitative electronic structural methods based on electron counting rules and theories of bonding have deepened our understanding of the properties of inorganic and organometallic transition metal complexes. This is justified by their ability to interpret expterimentally known physical and chemical properties [Asare, 1999].

A major attractiveness of various self consistent field (SCF) schemes based on the Kohn-Sham density functional method [Kohn and Sham, 1965, Ballhausen and Gray, 1962,

Driezler and da Providentia, 1984] in organometallic modeling [Salahub and Zerner, 1989, Sasa*et al.*, 1992] is its ability to handle larger systems of interest.

The computational effort of conventional ab initio methods increases as n^4 (and n^7 for post Hartree- Fock), compared to the n^3 for DFT methods of similar accuracy (n is the number of basis functions) [Ziegler and Tom, 1995]. The density functional approximation solves the electron exchange and correlation problem through a gradient correction. Results for organometallic [Ziegler and Tom, 1995] and cluster compounds [Salahub and Zerner, 1989] with DFT methods are generally in better agreement with expteriment compared to HF results for geometries, vibrational frequencies, photoelectron and spectra, and other properties that depend on the orbitals or on the density itself.

1.20 LIGAND AND METAL INTERACTIONS

For many years the search for new ligands has been a prevailing goal in coordination chemistry. Through the appropriate choice of ligands, it is possible generally to design and synthesize coordination compounds having particular specified properties. However, because of the intrinsic complexity of many of the bridging-group derivatized ligands, unexptected modes of coordination may sometimes occur, and reactions may follow undesired routes [Sylvester Burton, 2006].With the development of self-assembly supramolecular chemistry, the rational design and synthesis of supramolecular architectures based on covalent or supermolecular interactions have been an important content of coordination chemistry and have found applications in searching fornovel materials with catalytic, biological, and photophysical properties such as luminescent and nonlinear optical properties [Braga *et al.*, 2005]. Careful selection of a suitable, multifunctional, organic ligand with certain features, such as flexibility, versatile bonding modes, and the ability to undergo hydrogen bonding, is

helpful for constructing and tailoring the metal-organic supramolecular architectures. The properties, effectiveness and selectivity of transition metal catalysts are individual to each catalyst and determined by the inherent characteristics of the metal centre. The effect of the ligands and substituents bonded to the metal centre is profound and very near to limitless.

Weakly interacting systems remain a challenging class of materials to describe accurately within the DFT approaches in practice [Perdew*et al.*, 2005]. The difficulty has been attributed primarily to the dominant role of nonlocal correlation in describing weak interactions such as the van der Waals interaction, which is absent or incorrectly accounted for within many exchange-correlation (XC) approximations. Because the properties and stabilities of metal complexes are highly tunable through variation of the metal ion, the ligand set, and other molecular parameters, this makes the coordinate bond a remarkably versatile platform for macromolecular assembly.

Molecular manufacturing of advanced materials with specific properties and functions has become the major challenge that faces modern supramolecular nanotechnology. These properties and functions are determined by controlling the form, shape and distribution of each individual building block subunit and their precise placement within the supramolecule. Such intermolecular control imposes strict requirements on the nature, type and directionality of the bonding forces that operate within the entire aggregated structure. The chemical bonding of the subunits must be relatively weak, thermodynamically stable, and yet kinetically labile to allow the self arrangement of the subunits within the entire structure, thereby enabling the self-correction of possible defects. Another important requirement is the conformational rigidity of the building blocks in order to reduce entropic factors upon self-organization.

The more recently developed synthetic protocol, namely self-assembly, relies on critical information about the shape and properties of the target structures being preprogrammed into each individual building block, in order to construct nanoscopic assemblies from multiple building blocks in a single step. The rational design and construction of new polymeric compounds based upon assembly of metal ions and multifunctional organic ligands are an increasingly interesting research field due to their intriguing structural diversities and potential applications in functional materials [Lu *et al.*, 2003].

1.30 BETA-DIKETONE AS A LIGAND

1.31 COORDINATION CHEMISTRY

Coordination of organic molecules to metal ions frequently modifies the nature of the chemical reactions they can undergo.

The β-diketones or 1, 3-diketones bear two carbonyl groups that are separated by one carbon atom. This carbon atom is the α-carbon. In most β-diketones, the substituents on the α-carbon are hydrogen atoms. Only very few examples of rare-earth complexes of α-substituted β-diketonates are known. The substituent on the carbonyl function can be an alkyl group, a fluorinated alkyl group, an aromatic or a heteroaromatic group. Beta-diketonates form anions as a result of enolization and ionization after α-proton extraction by base [Maverick *et al.*, 1990]. These β -ketoenolate ions form very stable chelate complexes with most metal ions. The simplest β-diketone is acetylacetone (Hacac) (Scheme 1.1), where the substituents on both carbonyl groups are methyl groups. All other β-diketones can be considered as derived from acetylacetone by substitution of the CH_3 groups by other groups.

Scheme 1.1

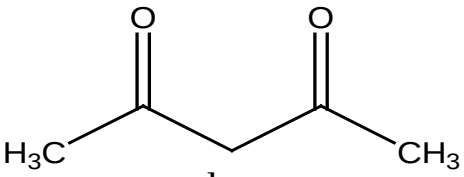

acetylacetone

1.32 METALLIC β-DIKETONATES

Metallic β-diketonates are amongst the most widely studied coordination compounds, and their chemistry has been investigated for most of the metals in the periodic table [Mehrotra *et al.*, 1978]. Metal acetylacetonates are used in chemical transformations such as oligomerization, polymerization, hydrogenation, isomerization of alkynes, coupling of organic halides and transesterification reactions, which require metal acetylacetonates as catalyst, as latent accelerators, which increase selectivity and formation of catalytically active sites [Sorokin *et al.*, 1986; Takimoto *et al.*, 2002, 2004].

β -diketones exist as equilibrium of keto-enol tautomers in solution with a higher percentage of the enol than the keto form [Eshraq, 2007]. The enolic hydrogen atom can be replaced by metal cation under appropriate conditions. The ligands normally form chelates with metals through two oxygen atoms and delocalize the negative charge over a six-membered metallocycle (Scheme 1.2a), while bonding to the *γ*-carbon (Scheme 1.2b) is also observed in some complexes [Garnovskii *et al.*, 1999] of soft Lewis acids, such as Pt^{2+}, Pd^{2+}, Hg^{2+}, Au^{+}, and Ag^{+}, in accord with the Hard Soft Acid Base(HSAB) principle. Metal β -diketonate chelate compounds are invaluable precursors for the chemical vapour deposition (CVD) of metal and non-metal thin films [Kodas and Hampdem- Smith, 1996; Rees, 1996]. In general, these compounds are favoured since they are relatively volatile, non-toxic and in the case of the parent acetylacetonate complexes, inexptensive [Samuels *et al.*, 1996].

Scheme 1.2

a b

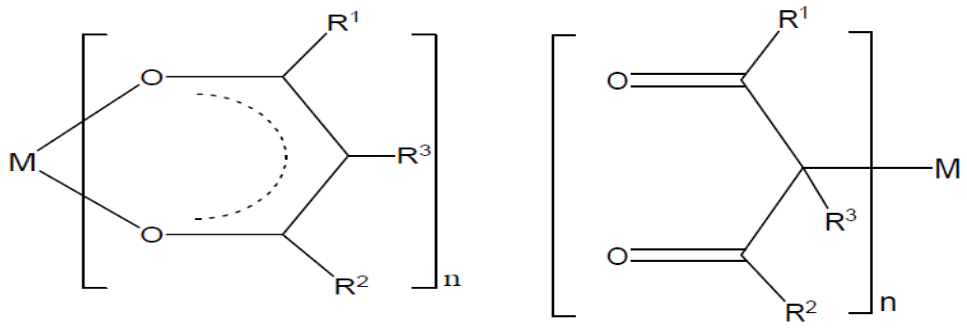

The properties of metallic β-diketonates, such as solubility, volatility, Lewis acidity, etc., can be tuned by changing R^1, R^2, and R^3 substituents. Replacing the substituent methyl groups of the parent derivative with other moieties has been demonstrated to influence the volatility of these complexes [Bradley and Andrew, 2000].

Apart from the bonding and structural aspects, research interests in metal β-diketonates include their applications in gas-liquid chromatographic techniques [Moshier and Sievers, 1975], contact shift reagents for the enhanced resolution of nuclear magnetic resonance spectra, laser technology, polymer industry [Mehrotra *et al.*, 1978], as well as fuels [Poonia and Bajaj, 1979]. More recently, a range of homometallic β-diketonates have been used to produce metal oxides upon thermal decomposition, and in most cases these species can function as precursors for CVD [Ozawa, 1991]. Specifically, Bi, Pb, and alkaline earth β-diketonates are widely used as CVD precursors for high-*Tc* superconductors [Ozawa, 1997]. Lanthanide β-diketonates are known as precursors for dopants and codopants in electroluminescent device thin films [Pasko *et al.*, 2004]. Some transition metal β-diketonates, such as Co [Pasko *et al.*, 2004], Cu [Wilson and Houl, 1985] Ni, Fe, and Zn [Itoh *et al.*, 1986] have been reported as oxide precursors for CVD as well. At the same time, many β-diketonates are also used as precursors to produce metal films or alloys [Igumenov, 1995]

and have been found to act as the most suitable precursors for deposition of noble metal films, including Pt, Rh, Ru, Pd, Ir, and Au.

In comparison with alkoxides, β-diketonates provide certain advantages for molecular precursors. Many metal diketonates have structures where the coordination number of the metal exceeds the valence of the metal. This makes the metal less accessible to nucleophilic attack, thus reducing the tendency of compounds to oligomerize and making the species more robust to hydrolysis [Otway *et al.*, 2000]. Metal β-diketonates can be dimeric, trimeric, tetrameric, or a higher complexity with various melting points. These organometallics have high vapor pressures and can be sublimed or volatilized under reduced pressure.

1.33 HETEROMETALLIC β-DIKETONATES

Most transition metals require octahedral coordination in their complexes. Therefore, the divalent transition metal unsolvated β -diketonates are capable of providing coordinatively unsaturated fragments M(β -dik)$_2$ (M = transition metal) in vapor phase, and thus are prospective starting materials for the preparation of heterometallic β -diketonates, which are built on Lewis acid-base interactions [Haitao Zhang, 2010]. Most of the unsolvated M(β -dik)$_2$ are found among the first row transition metal compounds. The second and third row transition metal species are relatively limited.

Bifunctional ligands based on acetylacetonates are attractive for use in construction of mixed-metal networks. The chelating nature of the bidentate O,O-donor ensures relatively low lability, and the negative charge on the ligand allows access to neutral complexes [Andrew *et al.*, 2010]in which the ligand is bonded to the metal through both oxygen atoms to form a six-membered ring as illustrated in scheme 1.2a.

β -diketonates are not generally considered as proper ligands for the formation of heterometallic species due to their chelating character. Only a few examples of heterometallic β -diketonate complexes have been reported to date. Cotton and co-workers were first to report [Bennett *et al.*, 1968] the synthesis of bimetallic β -diketonate, $CsY(hfac)_4$ from the reaction between Cs(hfac) and YCl_3 in aqueous ethanol. Structural study of this compound revealed an infinite motif in which Cs^+ cations are coordinated by the β -diketonate oxygen and fluorine atoms from $[Y(hfac)_4]^-$ anions. Shortly after that, two other similar β -diketonates, $CsM(hfac)_4$ (M = Eu, Am), were also isolated [Burns and Danford, 1969].

Research shows that polymeric $KMn(hfac)_3$ has been obtained [Troyanov *et al.*, 1999] from the reaction of K(hfac) with $Mn(NO_3)_2.6H_2O$ in aqueous ethanol. The latter heterometallic β -diketonate was shown to be volatile and, therefore, can hardly be regarded as an "ionic" compound. The other reported heterometallic β -diketonates include $Co(acac)_3Eu(fod)_3$ [Lindoy *et al.*, 1977] and a number of Pb-Cu compounds[Baidina *et al.*, 2006] such as $PbCu(hfac)_4$, $PbCu(hfac)_2(acac)_2$, $PbCu(hfac)_2(tfac)_2$, and $PbCu(hfac)_2(zis)_2$ (zis = 2-methoxy-2,6,6-trimethylheptan-3,5-dionato). These compounds were synthesized by the reactions of the corresponding homometallic β - diketonates in chloroform or toluene solutions.

Like metalloproteins, polymeric metal complexes feature site-isolated metal centers with responsive properties, and offer many opportunities for modification; they can form higher order assemblies, and function as soluble agents, films and coatings, or bulk materials. Beta-diketonates such as dibenzoylmethane for metals also serves as a UV absorber in sunscreens and has exhibited cancer preventive and therapeutic properties in model systems [Cassandra, 2006].

1.40 SPECTROSCOPIC ASPECTS OF β- DIKETONATES

1.41 INFRARED SPECTROSCOPY

A useful method for assigning the exact mode of bonding in metal-acetylacetonate complexes is based on infrared spectroscopy [Jackman, 1969]. The frequency of the stretching vibration of the C-O bond gives an idea of the strength and, therefore, the nature of that bond. Simple ketonic species, e.g., acetone, generally exhibit υ(C=O) at around 1700cm^{-1}, whereas esters show υ(C=O) at approximately 1300cm^{-1}. It is exptected that the nature of the ligand in the keto form and bonding through the γ- carbon would lead to higher υ(C=O) than in the enol form. Studies on many complexes shows that when acetylacetonate is bound in the enol form, υ(C=O) falls below 1600 cm^{-1}, whereas in the ketonic form and through the γ- carbon, υ(C=O) is found above 1600cm^{-1}.

1.42 UV-VIS SPECTROSCOPY

UV and visible absorption spectroscopy is a simple expterimental method for the investigation of the electronic structures of chemical compounds, although it provides little information on the state of occupation of electron levels. In the case of transition metal complexes with organic ligands containing a partially occupied d level, multiple intraligand π-π* and n- π* transitions, M - L and L - M charge transfer transitions, and d-d* transitions make the spectra in the UV and visible regions very complicated, such that their unambiguous interpretation becomes impossible. Additional information helpful in the assignment of absorption bands can be provided by quantum- chemical simulation depending on the approximation chosen.

1.43 NMR SPECTROSCOPY

The importance of NMR spectroscopy in chemistry is based on the fact that the resonance frequency is dependent on the chemical environment in which the nucleus is situated. The

dependence of magnetic resonance frequency on the chemical environment of the nucleus leads to a chemical shift. The theory of NMR chemical shift implies that all factors contributing to the electron density of the nucleus will influence its chemical shift [Weber and Thiele, 1998].

^{1}H-NMR spectrum of acetylacetone shows that the tautomeric interconversion of acetylacetone at room temperature is slow enough that the absorption peaks of both forms can be observed [Eshraq, 2007].

1.50 PHYSICAL AND CHEMICAL PROPERTIES OF METAL β -DIKETONATES

1.51 VOLATILITY

Transition metal β-diketonates have attracted considerable attention as CVD precursors to produce metal oxides or metal films due to their volatility and low temperature clean decomposition patterns [Pasko *et al.*, 2004]. A number of divalent transition metal β -diketonates have been reported as starting materials in the synthesis of supramolecular aggregates [Tabellion *et al.*, 2001], cubane-type metallic clusters [Ahmed *et al.*, 2007] and heterometallic complexes [Kessler *et al.*, 2003]. In addition, it has also been shown that these compounds may play an important role in catalysis [O'Neill *et al.*, 2003].

Much attention is given to the investigation of such an important property as volatility, which is necessary to optimize the parameters of coating deposition, to choose the precursors and to get the materials with adjusted properties.

β -diketonates have rigid structures, which make it easier to control the structures of precursors compared to coordinatively-versatile alkoxides. The enhanced observation in volatility may be rationalized either by an increased amount of intermolecular repulsion due to the additional lone pairs or that the reduced polarizability of fluorine (relative to hydrogen) causes fluorinated ligands to have less intermolecular attractive interactions [Reed, 1964].

Chemical vapour deposition (CVD) is the most versatile and promising technique for the deposition of oxide films and nanomaterials. A key requirement in this technology is the availability of precursors with adequate volatility [Jones, 2002] which allows achievement of acceptable oxide growth rates at moderate evaporation temperatures and a sufficiently large temperature ‘‘window’’ between evaporation and thermal decomposition. High volatility is also preferred for decreasing the nucleation of the precursor in the gas phase, as well as avoiding undesirable non-conformal granular coating. The low volatility or even nonvolatility of alkoxides has significantly limited their applications in this field.

1.52 AGGREGATION STATE AND MELTING POINT

Rare-earth β-diketonates are crystalline solids or viscous liquids. The compounds that are the easiest to obtain as crystalline solids are those of β-diketones with aromatic substituents. On the other hand, complexes of β-diketones with highly branched aliphatic groups have a strong tendency to form viscous oils. In general, the β-diketonate complexes are obtained as fine powders. Slow evaporation of a solution containing a complex can yield single crystals of a quality suitable for structure determination by X-ray diffraction.

For some complexes no melting point can be observed, because these complexes decompose before the melting point is reached. Typical examples of thermally unstable complexes are the acetylacetonate complexes and complexes of perfluorinated β-diketonates. Complexes of β-diketonates with long alkyl chains have lower melting points than complexes of β-diketonates with short alkyl chains [Koen, 2005].

1.53 COLOUR

Most solid rare-earth β-diketonates are white, yellow or brown, and in general their colour is determined by the colour of the β-diketonate ligands. Only in the case of white β-diketonate ligands, the typical colour of the lanthanide ion can be observed, for instance a greenish color for praseodymium (III) compounds and a blue-violet colour for neodymium (III) compounds.

Some europium (III) β-diketonates show a pink colour in daylight, because of the intense photoluminescence of these compounds [Koen, 2005].

1.60 MACROCYCLIC COMPLEXES

The field of macrocyclic chemistry of metals is developing very rapidly because of its variety of applications [Izan *et al.*, 1985] and importance in the areas of coordination chemistry. Efforts made in the last decades to the design and synthesis of macrocyclic or macroacyclic complexes and to study their physico-chemical properties [Fenton *et al.*, 1984] emphasized the great relevance of these systems in basic and applied chemistry. Many macrocyclic or macroacyclic systems containing an appropriate set of donor atoms and a suitable structural configuration are capable of producing new macromolecules which have been used in numerous chemical processes and technologies. Based on this concept many macrocyclic systems are available and are already applied in the fields of activation and catalysis, molecular materials, microelectronics, sensors, and so on [Lehn, 1978].

There has been a spectacular growth in the interest in metal complexes with tetraazamacrocyclic ligands followed by extensive work on the metal controlled template synthesis of macrocyclic species [Herlinger *et al.*, 1994]. Macrocyclic ligand systems often exhibit unusual properties and sometimes mimic related natural macrocyclic compounds because of their resemblance to many naturalmacrocycles, such as metalloproteins, porphyrins and cobalamine.

The complexes of polydentate macrocyclic ligands are at the fore front of bioinorganic chemistry due to their variety of geometrical forms available and the possible encapsulation of the metal ion [Adams *et al.*, 1987]. A number of nitrogen donor macrocyclic derivatives have long been used in analytical, industrial and medical applications. Macrocyclic compounds and their derivatives are interesting ligand systems because they are good hosts for metal ions, neutral molecules and organic guest ions. Template reactions have been

widely used for the synthesis ofmacrocyclic complexes, where, generally, transition metal ions areused as the templating agents.The metal ions direct the reactionpreferentially towards cyclic rather than oligomeric or polymericproducts.

Macrocyclic complexes have also received special attention because of their mixed soft–hard donor character and versatile coordination behaviour and their pharmacological properties, i.e., toxicity against bacterial growth (Collen *et al.*, 1997; Rosu *et al.*, 2006; Ritu *et al.*, 2010; Chandra et. al, 2009; Adimado *et al.*, 1991; Anant Prakash *et al.*, 2011).

1.61 PORPHYRIN AS A LIGAND

The synthesis of new structures of porphyrins hydrophilic / hydrophobic balance represents an important purpose in order to design new biomimetic substances. Porphyrins are molecules capable of drastically changing or adjusting their properties by reconfiguring the electron distribution of the aromatic ring due to the character and number of peripheral substitution groups.

In the realm of chemistry, it is fundamental that the shape of the molecules helps to determine their properties such as optical, coordination, host-guest behavior, etc. Porphyrin is a widely studied functional pigment that can coordinate a variety of metals with four pyrrolic nitrogens in a square-planar arrangement in the core. In the biotic system, porphyrin plays an essential role as a reaction center like chlorophyll, photosynthetic reaction center in the plants, and hemoglobin, oxygen carrier in a red hemocyte of vertebrates. It also acts as a useful biomimetic molecule in the artificial system [Maeda, 2005].

The porphyrins and metalloporphyrins have a huge potential number of applications like sensors, corrosion inhibitors and in catalysis. It is well-known the impact of porphyrins in the pharmaceutical domain, as colorimetric sensors and in medicine treatments in photodynamic cancer treatment (PDT), based on the fact that some porphyrins can fix in cancerous tissues,

and by their controlled light irradiation, photochemical changes occur, destroying the tumour, but leaving the healthy tissue unharmed.

The preparation and study of inorganic compounds containing biologically important ligands are made easier because certain metal ions are active in many biological processes. The fact that copper, together with magnesium, calcium, iron, zinc, chromium, vanadium and manganese are essential metallic elements and exhibit sufficient biological activity when associated with certain metal-protein complexes, participating in oxygen transport, electronic transfer reactions or the storage of ions [Albertin *et al.*, 1975], has created enormous interest in the study of systems containing these metals [Karlin and Zubieta, 1983].Thus, porphyrin-like molecules, structural variants of tetrapyrrolic macrocycles possessing $(4n + 2)\pi$electron delocalization, have been the favourite hunting ground for synthetic chemists in anticipation of their special properties. Therefore, there is a major thrust in designing and synthesizing structural variants of basic tetrapyrrole macrocycles in contemporary research [Furuta *et al.*, 2000].

1.70 APPLICATIONS OF SOME METALS

Metal ions, either alone or in complexes, have been used to disinfect fluids, solids and tissues for centuries. The potential antimicrobial activities of different metals and metal compounds have been under special interest during the recent years. For instance, copper is used today as a water purifier, algaecide, fungicide, nematocide, molluscide as well as antibacterial and anti-fouling agent.

In chrysotherapy, the Chinese used elemental gold for the treatment of diseases, 2500 BC [Merchant, 1998]. Recently, cisplatin has become the most well known of all metal based drugs leading to synthesis of its derivatives. Many more examples of metal- containing drugs have been reported in literature following the discovery of cisplatin by Rosenberg in 1969 [Rosenberg, 1998]. Gold containing complexes such as auranofin are commonly used to treat

rheumatoid arthritis [Sadler, 2010], radiopharmaceuticals based on metals such as technetium and rhenium are used in imaging and radiotherapy [Cowan, 1997], and ruthenium complexes have had some success as anticancer drugs [Clark, 1989]. Complexes containing gadolinium, cobalt, lithium, bismuth, iron, calcium, lanthanum, gallium, tin, arsenic, rhodium, copper, zinc, aluminium and lutetium have all been used in medicine [Bertini *et al.*, 2007].

1.71 COBALT AND COBALT COMPOUNDS

1.711 Co (III) IONS IN BIOLOGICAL SYSTEM

Cobalt is one of the most important trace elements in the world of animals and humans. The properties of cobalt oxides such as high catalytic activity at low cost, antiferromagnetism [Fischer *et al.*, 2001], electrochromism [Granquist, 1995] offer a great potential for their applications. In the form of vitamin B_{12} (cobalamin), this metal plays a number of crucial roles in many biological functions. Cobalamin is necessary for DNA synthesis, formation of red blood cells, and maintenance of the nervous system, growth and development of children. The Co^{3+} ion in vitamin B_{12} is stabilized by a chelating tetradentate macrocycle known as a corrin in which the four nitrogen atoms are located in equatorial positions in the octahedral geometry. The remaining ligands in the axial positions are a labile adenosyl residue in which the 5' carbon is directly bonded to cobalt and an *N*-bonded dimethylbenzimidazole ligand. Vitamin B_{12} is a cofactor for a number of enzymes, virtually all of which are isomerases, methyl transferases or dehalogenases. Other examples of cobalt containing enzymes in biology include nitrile hydratase, prolidase, glucose isomerase, methylmalonyl-CoA carboxytransferase, aldehyde decarbonylase, lysine-2,3-aminomutase,bromoperoxidase and methionine aminopeptidase but only nitrile hydratase possesses cobalt in oxidation state 3^+ [Kobayashi, 1999]. Co (III) is also found in certain cobalt-porphyrin containing proteins [Hatchikian, 1981].

1.712 ANTIVIRAL ACTIVITY OF COBALT (III) COMPLEXES

The simple Co^{3+} ion is unstable in water, but can be stabilized against reduction to Co^{2+} by coordination to ligands or chelators. By far the most common ligand type used to stabilize the Cobalt (III) ion in aqueous solution is the chelating N, O donor ligand. These cobalt (III) complexes derived from this ligand donor set have found application as antibacterial or antiviral agents [Eddie *et al.*, 2010]. In 1998, Epstein and coworkers reported that the cobalt complex CTC-96 was effective in the treatment of epithelial herpetic keratitis, one of the major causes of blindness in industrial nations [Epstein, 1998].

1.713 ANTIBACTERIAL ACTIVITY OF COBALT (III) COMPLEXES

Co (II) complexes are most studied on the antibacterial properties of cobalt complexes. This is presumably due to their aqueous stability, availability, and ease of synthesis agents [Eddie *et al.*, 2010]. However, a number of examples of stable Co (III) complexes have also been reported. Although polydentate ligands with N, O and S donor atoms in the coordination sphere of cobalt are the most common ligands used to stabilize Co^{3+} ion in aqueous solution, a striking exception to this rule is the homoleptic hexammine cobalt (III) complex which possesses high kinetic inertness in water. Reports on the antibacterial properties of cobalt (III) complexes frequently emphasize the increased effectiveness of cobalt ion coordination to a particular ligand when compared to the free ligand itself.

1.714 TOXICITY OF COBALT (III) COMPLEXES

The toxicity of metal-ion based therapeutics is a concern due to the intrinsic toxicity of some metal ions themselves. Cobalt is generally not considered to be a very toxic element. Most toxicity studies have been concerned with Co(II) metal ions, surgical implants, or cobalt metal dust [Keegan *et al.*, 2008], with one notable example of cobalt-induced mortality from drinking large quantities of beer that contained cobalt chloride or cobalt sulfate as a foam stabilizer [Barceloux, 1999]. There is much less known about toxicity of Co (III) complexes.

In general, it does not appear that Co (III) complexes are toxic at moderate levels of exposure, although some adverse effects on kidney function were reported [Eddie *et al.*, 2010].

1.720 CHROMIUM AND CHROMIUM COMPOUNDS

Chromium is probably the most controversial of the transition metal ions in terms of its toxicity and nutritional value [Katz and Salem, 1994] and so is the subject of growing interest in the public and scientific communities. The properties of cobalt oxides such as high catalytic activity at low cost, antiferromagnetism [Fischer *et al.*, 2001], electrochromism [Granquist, 1995] offer a great potential for their applications. Mammals need trivalent chromium to maintain balanced glucose metabolism [Mert, 1975], and thus chromium may facilitate insulin action [Nielsen *et al.*, 1993, Vincent, 1999]. This insulinogenic characteristic of chromium has prompted the hypothesis by Evans that chromium has an anabolic function [Evans, 1989].

1.80 OBJECTIVES

This study seeks to investigate the structural features(spectroscopic and bonding parameters) of the diketonates and macrocyclic systems through computational techniques. The objectives of the study are in three folds;

1) To determine the effect of different substituents on the structural and bonding parameters at different positions in some β-diketone metal complexes and their derivatives.
2) To determine the effect of changing the metal centre on the structural and bonding parameters in a β-diketone complex and its derivatives.
3) To study the changes in the spectroscopic properties and other bonding parameters of some macrocyclic complexes with varying central metals and substituents.

1.90 JUSTIFICATION

Density-functional theory (DFT) [Hohenberg *et al.*, 1964] and semi-empirical methods are promising methods for describing the electronic structure of realistic systems because of their applicability to a large class of materials ranging from molecules to solids, in terms of both accuracy and computational affordability. Since Chemistry which is a largely expterimental science, progresses by the development of models to exptlain expterimental observations, chemists have used molecular structural models as a foundation for understanding chemical and physical properties [Riddell and Robinson, 1974]. Since vibrational spectra supports the existence of a strong intramolecular bond of chelating nature of β-diketones, it leads to an enhancement of the resonance conjugation of the π-electrons, which causes a marked tendency for equalization of the bond orders of the valence bonds in the resulting chelated ring. It is exptected that any substituent or metal ion that affects the electron density ofthe chelated ring will also change the bond strength.Even though literature is extensive on the synthesis, structural characterization, and applications of metal complexes of derivatives of β-diketones [Krishnankutty and Rema, 1995; Krishnankutty *et al.*, 2008], scanty reports to the best of our knowledge are given on the computational aspects of the derivatives of these complexes. It is importanttherefore to explore a number of substituent's and metal ions and determine their effects on the spectroscopic and bonding parameters on β-diketones and macrocyclic complexes using computational techniques.

CHAPTER TWO

2.10 GENERAL LITERATURE REVIEW

2.11 β–DIKETONE METAL COMPLEXES AND THEIR DERIVATIVES

The spectroscopic and magnetic properties of trivalent metal complexes of 1-(2-thienyl)-1,3-butanedione (Htbd) and 4,4,4 - trifluoro - 1 - (2 - thienyl) - 1,3 - butanedione (Htftbd) (where M(III) = (Al, Cr, Mn, Fe, Co) have been examined [Patel and Adimado, 1980]. The IR band assignments suggested that substitution of a trifluoromethyl group in thenoylacetone for a methyl group increases the C = O and C = C bond strengths and decreases that of M---O bond of the chelate ring. The spectral and magnetic properties of these two series of complexes revealed that they are very similar to the corresponding tris-(2,4-pentanedionato) M(III) complexes [Pateland Adimado, 1980].

Wexler and Zink [Wexler and Zink, 1996] showed, when they studied luminescence and resonance of molecular distortions caused by ligand-centered transitions in metal acetylacetonate complexes, that the low temperature emission spectra of the β -diketonate complexes give direct support for the ligand-centered π to π * assignment of the emission band. The most important general supporting feature is that, for a given ligand, the energy of the emission is not very sensitive to the metal. In the case of the hexafluoroacetylacetone (hfac) complexes, no change in energy was observed when the metal was changed from gold to zinc. In the case of the acetylacetone (acac) complexes, changing the metal from gold to aluminium changes the value of energy by only 700cm^{-1}. The onset of the emission bands move only slightly in energy with changes in fluorine content in the acetylacetonate ligand. These small shifts are caused by the perturbations on the π orbital energies by the substitute CF_3 groups.

Do Couto *et al.*, performed a study on the enthalpy of formation of acetylacetone (acac) radical using a complete basis set approach [Do Couto *et al.*, 2006]. They found that, when the thermochemical properties of acetylacetone and its radical were investigated using DFT and ab- initio calculations, the most stable acac radical conformer is generated by a C-H bond homolysis. Their study was based on the complete basis set (CBS) extrapolation procedures, including CBS-QB3 and a modified CBS procedure that they named CBSQBS-tz. The enthalpy of formation of gaseous acac,$\Delta H^{\theta}f$ (acac,g) was estimated at -228.3 kJ/mol (CBS-QB3) and -226.7 kJ/mol (CBS-QB3-tz). Based on these results the $\Delta H^{\theta}f$ (acac,g)is -227 ± 8 KJ/mol.

In a study by Oluwatola [Oluwatola, 2011], some 2-substituted-1-phenyl-1,3-butanedionato nickel(II) complexes and their 2,2'-bipyridine (bipy) and 1,10-phenanthroline (phen) adducts were synthesized and characterized by elemental analyses, infrared, electronic spectral studies, conductance, and magnetic susceptibility measurements. The electronic spectral data were interpreted in terms of the $\pi_3 \rightarrow \pi_4^*$ and other transitions and the effect of the substituents at β-position on the different transitions determined. The infrared spectra of the nickel(II) complexes showed that the frequencies of the asymmetric C = O + C = C stretching vibrations were lowered from their ligand values.

The molecular geometries of various 3-substituted malondialdehyde and acetylacetone derivatives, in their chelate, open and H-centered conformations, have been optimized by Buemiand Felice [Buemiand Felice, 1997]. They evaluated the hydrogen bond energies, in order to estimate the effect of 3-substitution steric hindrance on the hydrogen bond strength. Calculations were performed at the *abinitio*3–21G and 6–31G** level, with and without correlation energy inclusion, using the Møller–Plesset approach (where possible) and the

B3LYP functional. The frequencies of the O–H stretching mode were evaluated too. The resultsobtained indicate that the Cs chelate conformations are the most stable structures. The O---O distances are rather longer than the values typical of the H-centered conformers, at least in gas phase. The strengthening of the hydrogen bridge, on passing from the parent to the 3-substituted derivatives, is not so relevant as exptected on the ground of literature data, the maximum increase being about 21 KJ mol^{-1} (in 3-t-butyl-acetylacetone). An increase of the steric effect to stress the O---O distance caused the breaking of the hydrogen bridge instead of strengthening, so indicating that the literature X-ray geometries (in particular the O---O distances) are governed, at least partially, by crystalline forces.

In a work done by the group of Natalia [Natalia *et al.*, 2001],tris-(acetylacetonato) chromium (III), $Cr(acac)_3$, was chosing as the object of investigation for study of kinetic features of mass transfer. On the basis of expterimental data the dependences of mass transfer rate versus carrier gas flow rate (0.5–40 $l{\cdot}h^{-1}$), temperature (162–242°C), aggregated condition of precursor (powder, crystal, melt) and size of evaporation surface were obtained. The processes of sublimation of film samples of tris-(acetylacetonato) chromium (III) were analyzed in detail. The features of sublimation of films were exptlained by nature of rate profile of gas flow in the expterimental reactor. Activation parameters of sublimation/evaporation processes were estimated (the enthalpy of sublimation process of Cr $(acac)_3$ was equal to 133.8 ± 4.2 $KJmol^{-1}$ and the enthalpy of evaporation process is equal to 79.4 ± 4.2 $KJmol^{-1}$).

DFT B3LYP method was employed to calculate the second-order nonlinear optical (NLO) responses of the derivatives of disubstituted seven-vertex cobaltacarborane metallocenyl. The results showed that cobaltacarborane metallocenyl plays a pushing/pulling role and a bridge

role to transfer electron in these molecules. The five-membered ring of cyclopentadiene is more beneficial to increase second-order NLO response than the five-membered ring composed of two C atoms and three B atoms in cobaltacarborane. Moreover, the second-order NLO response is more powerful when one substituent containing electron donor group and one substituent containing electron acceptor group are located at meta position [Liu *et al.*, 2009].

Camerman and co-workers [Camerman *et al.*, 1983] found from an X-ray crystal structure on a drug complex crystallized from acetylacetone (2,4-pentanedione) that the drug contains one molecule of acetylacetone per asymmetric unit in the crystal lattice. The acetylacetone does not interact with the other molecules in the crystal but displays a keto-enol configuration stabilized by an intramolecular hydrogen bond. Comparison of bond lengths for acetylacetone in the solid state, together with that postulated for the molecule from the electron diffraction radial distribution curves, and which were obtained in substituted β-diketones, suggested that the apparent acetylacetone keto-enol ratio in liquid and gas phase may be in error if they include an assumption of symmetry of bond lengths for the enol form.

Liang and his group [Liang *et al.*, 2009] performed systematic and extensive conformational search of neutral aspartic acid in gas phase. Possible 1296 structures were optimized at the B3LYP/6-311++G** level and a total of 122 stable conformers were determined. Single-point energy computations were done at the MP2/aug-cc-pvdz level. The discussion shed light on the influences of the arrangements of α- and β-carboxyls, intramolecular hydrogen bond interactions and the intramolecular ring tension on the molecular stabilities.

Özgur and Cemal have studied the possible stable conformers of 1-pentylamine (1-pa) molecule expterimentally and theoretically by FT-IR and Raman spectroscopy in the region

of 4000–400 cm^{-1}. The optimized geometric structures concerning the minimum on the potential energy surface were investigated by Becke-3–Lee –Yang–Parr (B3LYP) density functional method together with 6-31G (d) basis set. Optimized energies of the possible conformers were obtained in the gas phase and within the chloroform, carbon tetrachloride, methanol and water solvent environments with different polarities. Comparison between the expterimental and theoretical results indicates that density functional B3LYP method is able to provide satisfactory results for predicting vibrational wavenumbers [Özgur and Cemal, 2010].

Work done by Raissi [Raissi *et al.*, 2006] has investigated the molecular structure and vibrational assignment of trifluoroacetylacetone (tfac) using density functional theory calculations and vibrational spectroscopy. Both theoretical and expterimental methods showed that tfac has an asymmetric double minimum potential energy surface with a low barrier, about 11.0 KJ/mol. The geometrical equilibrium parameters in the most stable structure at different levels of density functional theorem was compared to the corresponding non-fluorinated acetylacetone and showed that hydrogen bond strength of chelated ring was about 66 KJ/mol less than its value in acetylacetone.

The geometry, frequency and intensity of the vibrational bands of aluminium(III) tris–acetylacetone $Al(acac)_3$ and its 1, 3, 5-^{13}C derivative were obtained by the Hartree-Fock (HF) and Density Functional Theory (DFT) with the B3LYP, B1LYP, and G96LYP functional and using the 6-31G* basis set [Tayyari *et al.*, 2002]. The calculated frequencies were compared with the solid IR and Raman spectra. All of the measured IR and Raman bands were interpreted in terms of the calculated vibrational modes. Most of the computed bands were predicted to be at higher wavenumbers than the expterimental bands. The calculated bond lengths and bond angles were in good agreement with the expterimental results. Analysis of

the vibrational spectra indicated a strong coupling between the chelated ring modes. Four bands in the 500–390cm^{-1} frequency range were assigned to the vibrations of metal---ligand bonds.

In another study, [Tayyari *et al.*, 2002] investigated the molecular and vibrational structure of 1,1,1,6,6,6-hexafluoropentane-2,4-dione (hexafluoro-acetylacetone) by means of density functional theory (DFT) calculations and compared them with those of acetylacetone, the parent molecule. According to the theoretical calculations hfac has an asymmetric structure with hydrogen bond strength of about 12 Kcalmol^{-1}, about 6 Kcalmol^{-1} less than that of acetylacetone. The weakening of hydrogen bond was consistent with frequency shifts for OH/OD stretching, OH/OD out of plane bends and O...O stretching modes upon substitution of methyl hydrogen atoms with fluorine atoms. The symmetric structure based on electron diffraction data is interpreted as superposition of two asymmetric structures.

Téllezs and co-workers [Téllezs *et al.*, 2001]tried to understand the metal-ligand regain spectra of bis(acetylacetonato) tin(IV) by employing density functional theorem B3LYP/6-31+G* calculations and Fourier transform infrared and Raman spectra. The percentage of deviation of the bond lengths and bond angles gave a good picture of the normal modes.

Work done by Bradley and Andrew [Bradley and Andrew, 2000] established the volatile trends for a series of M (β-diketonate)$_n$ complexes, where M = Cu (n = 2); Al, Sc, Cr, Fe, Co, Ga (n = 3); Zr (n = 4) and β-diketonate = acetylacetonate (acac), trifluoroacetylacetonate (tfac), hexafluoroacetylacetonate (hfac) and 2,2,6,6-tetramethyl-3,5-heptanedionate (tmhd). From the sublimation enthalpies (ΔH_{sub}) calculated from thermogravimetric analysis (TGA) data, it was shown that the dependence of ΔH_{sub} on the number and type of intermolecular

interactions appears to be more substantial than molecular mass effects. The relationship between the ΔH_{sub} and T_{sub} of the substituted β-diketonate derivatives as compared with the values for parent M(acac)n may be used to predict either quantity for a range of M(β-diketonate)n complexes where the values for M(acac)n are known.

The molecular structure of bis (acetylacetonato) beryllium using gas electron diffraction technique has been determined [Shibata *et al.*, 1980]. This study showed that the complex has a D_2d symmetry in which oxygen atoms are arranged tetrahedrally around the central beryllium atom, and C_{methyl}-H bond is eclipsed with C-O bond.

Optimized geometries and vibrational frequencies of polydiacetylenes (PDAs) and their derivatives were studied by density functional calculations at the B3LYP/6-31G* level by Bin *et al.*[Bin *et al.*, 2008]. They used time-dependent density functional theory to determine the vertical transition energies and corresponding oscillator strengths. Calculations showed that different side groups in these linear carbon chains can significantly modify their structural and electronic properties, whereas the effect of terminal substitution is negligible.

Density functional theory (DFT) calculations were performed by Maryam and co-workers at the B3LYP/6-311++G(d, p) level to determine coordination geometries, absolute metal ion affinities, and free energies for all possible complexation stable products formed by monovalent metal cations including Li^+, Na^+, K^+ with the nucleoside 2′-deoxyguanosine. All computations indicate that the metal ion affinity (MIA) decreases on going from Li^+ to Na^+ and K^+ for 2′-deoxyguanosine. It was found that metal binding significantly change the values of the phase angle of pseudorotation (P) in the sugar unit of these nucleosides but, O_6-

protonation do not significantly change the values of the torsion angles and angle of pseudorotation (P) [Maryam *et al.*, 2010].

Brittain studied magnesium acetylacetonate in chloroform-d using proton magnetic resonance spectroscopy [Brittain, 1975]. The spectra gave evidence for conformational equilibrium.

The ^{1}H NMR chemical shifts of $Mg(acac)_2$, $Be(acac)_2$, $Zn(acac)_2$, $Ca(acac)_2$ and $Ba(acac)_2$ in various solvents showed that the shifts tend to cluster in two groups: one occurring from 1.70 ppm to 1.83 ppm downfield from TMS and other from 1.93 ppm to 2.02 ppm up field. All bis complexes exhibit one methyl resonance in one group or the other, but only $Mg(acac)_2$ in $CDCl_3$ shows resonances in both groups.

Acetylacetonato ion can form other types of complexes in which the metal is bonded to the γ -carbon atom of acetylacetonato ion [Macklin *et al.*, 1976]. Macklin found, when he studied mercury β-diketonato complexes, that the metal to ligand ratios is 1:1, 1:2 and 2:3 from the result of elemental analysis. The vibrational spectra show that mercury is always bound to the γ -carbon of acetylacetone and is not chelated through the oxygen atoms in any of the compounds. The generation of compounds with various ligands to metal ratios depends on replacing one or both hydrogen atoms on the γ -carbon of acetylacetone by mercury.

Afsharidescribed [Afshari *et al..*, 2010] a theoretical investigation of the geometrical parameters and the ^{17}O and ^{33}S nuclear quadrupole resonance (NQR), parameters of phenacyl phenyl sulfide derivatives. The calculations were carried out using Gaussian 98 package by applying the Hartree–Fock method (HF), the second-order Møller–Plesset perturbation theory (MP2), and the density functional theory (DFT) and by employing the 3-21G, 6-31G, and 6-311G basis sets in the Townes–Daily approximation. It was shown that all of the methods can be used to predict the NQR parameters.

2.12 MACROCYCLIC METAL COMPLEXES AND THEIR DERIVATIVES

Theoretical research on porphyrins, like other aspects of porphyrin chemistry, is driven by considerations of great biological importance of these molecules, their extensive coordination chemistry, and growing number of applications [Lecomte *et al.*, 2000].

Wu [Wu *et al.*, 1997] carried out density functional calculations using both the BLYP/3-21G and BLYP/6-31G** methods on free-base porphyrins and their possible isomers with an N_4-metal coordination core. Ghosh and Jynge reported BLYP/6-31G** calculations on cis and trans- porphyrin isomers having [3:0:1:0], [3:1:0:0] and [4:0:0:0] connectivity [Ghosh and Jynge, 1997]. Core modification in the skeleton by replacing one or two pyrrole nitrogens by other heteroatoms such as O and S alters the electronic structure and results in the formation of modified porphyrins. Introducing other heteroatoms yields new classes of compounds containing novel chelating properties.

Adimado and co-workers [Adimado *et al.*, 1991] studied two series of metal complexes obtained by reacting $CoCl_2{\cdot}6H_2O$, $NiCl_2{\cdot}6H_2O$, $CuCl_2{\cdot}2H_2O$ with 2,6-diaminopyridine (Dapy) and, either acetylacetone (Hacac) or benzoylacetone (HBzac), which yielded the $HADMCl_2$ and $HBDMCl_2$ (M = Co^{II}, Ni^{II} and Cu^{II}) complexes. Each of the HAD and HBD moieties in the complexes contained a 16-member N_6-tetradentate macrocyclic ligand derived from acac: Dapy (1:1) or HBzac: Dapy(1:1) respectively. The ligands were found to coordinate through all the four azomethine nitrogen atoms which are bridged by the 1,3-diketone moieties.

The antimicrobial efficiencies of $HADMCl_2$ and $HBDMCl_2$ and of their precursors, with special reference to Staphylococcus *aureus, Escherichia coli, Salmonella typhi*and*Pseudomonas aeruginosa*have been evaluated. *P. aeruginosa* was found to be the most resistant, while *S. aureus* appeared to be the most susceptible to the test compounds.

Ashu *et al.* [Ashu *et al.*, 2002] have studied some antifertility inhibitors of 18 to 24-membered tetraazamacrocyclic complexes of iron(II) and manganese(II). The complexes were synthesized by template condensation using 1,3 phenylenediamine with malonic acid, succinic acid, glutaric acid and adipic acid. The complexes were characterized by elemental analyses, molecular weight determinations, infrared, electronic, magnetic moment, Mossbauer and mass spectral studies. The elemental analyses were consistent with the formation of the complexes $[M(N_4Ln)Cl_2]$ (M = Fe(II) or Mn(ll)). The spectral studies confirm the octahedral geometry around the central metal atom. The complexes were screened in vitro against a number of fungi and bacteria to assess their growth inhibiting potential.

Raman and his group [Raman *et al.*, 2006] prepared four copper(II) complexes using macrocyclic ligands which were synthesized by the condensation reaction of diethyl phthalate with Schiff bases derived from o-phenylene diamine and Knoevenagel condensed β-ketoanilides (obtained by the condensation of acetoacetanilide and substituted benzaldehydes). On the basis of spectral studies, a square-planar geometry for the copper complexes was proposed.

The in vitro antifungal activities of the compounds were tested against fungi such as *Aspergillus niger, Rhizopus stolonifer,Aspergillus flavus, Rhizoctonia bataicola* and *Candida albicans*. All the synthesized copper complexes showed stronger antifungal activities than free ligands. The minimum inhibitory concentrations (MIC) of the copper complexes were found in the range of 8~28 μg/ml.

A phenol-based novel macrocyclic binucleating compartmental ligand *N,N*-bis(2,6-diiminomethyl-4-methyl-1-hydroxyphenyl) malonoyldicarboxamide has been prepared

[Mruthyunjayaswamy *et al.*, 2005] by template method by reacting 2,6-diformyl-4-methylphenol, malonoyl dihydrazide and the metal chlorides of Cu(II), Ni(II), Co(II), Cd(II), Zn(II) and Hg(II) in methanol to get a series of dinuclear complexes. The complexes were characterized by elemental analyses, conductivity measurements, magnetic susceptibility data, IR, UV-Vis, ESR, NMR and FAB mass spectral data. The compounds were tested for their antibacterial and antifungal properties against *Escherichia coli, Staphyloccocusaureus, Aspergillus niger and Fusarium oxysporum*. Magnetic susceptibility measurements of Cu(II), Ni(II) and Co(II) complexes reveal that these complexes exhibit antiferromagnetic coupling behavior due to the presence of two metal ions in close proximity. FAB mass spectrum of the Cu(II) complex gave a clear evidence for the dinuclear nature. The ligand and the complexes were found to be less active against the tested bacteria, but the ligand alone was found active against the fungus *Fusarium oxysporum*.

Tetraaza Macrocyclic complexes of transition metals of Ni(II), Cu(II), Cr(III), Fe(III), Mn(II) have been synthesized and characterized by elemental analysis using, UV-Vis, Infrared spectroscopy by Ritu *et al.* [Ritu *et al.*, 2010]. In vitro antibacterial activity of macrocyclic complexes against five bacteria i.e. Streptococcus mutans, Escherichia coli, Staphylococcus aureus, Streptococcus pyogenes, Streptococcus pneumoniae were tested to assess their inhibiting activities and compared with standard ampicilline.

The macrocyclic complexes of Co(II) and Ni(II) having chloride or thiocyanate ions in the axial position have been synthesized and characterized by Gaber *et al.* [Gaber *et al.*, 2008]. The complexes were synthesized by the template condensation of o-phenylenediamine or 2, 3-butanedionedihydrazone with the appropriate aldehydes in NH_4OH solution in the presence

of the metal ions, Co(II) and Ni(II). Spectral studies indicated that the complexes have an octahedral structure.

The metal chelates inhibit the growth of microorganisms. It is assumed that production of the enzymes is being affected as the microorganisms are unable to utilize food for themselves or intake of nutrient decreases and consequently growth ceases. The greater toxicity of metal complexes than the starting ligand can also be exptlained on the basis of the chelation theory [Lehninger, 1975; Srivastava, 1981]. Chelation reduces the polarity of metal ion mainly because of partial sharing of its positive charge with the donor group and possible electron-delocalization over the whole chelate ring. This increases the lipophilic character of the metal complex, which subsequently favours its permeation through the lipid layers of the organism cell membrane and the normal cell process being impaired.

CHAPTER THREE

3.0 METHODOLOGY

Derivatives of acetylacetonate complexes were constructed from the parent structure and subjected to computational calculations. Examples of other substituted betadiketonates are shown in scheme 1.3 below;

Scheme 1.3

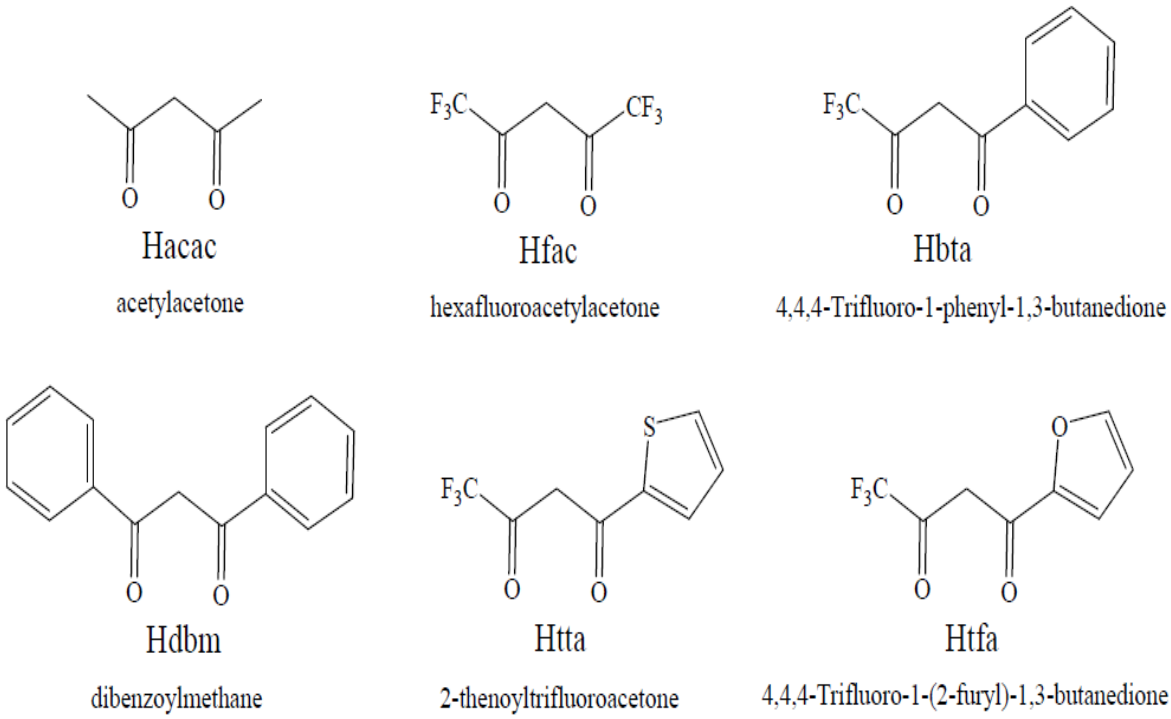

The metal ions considered in this study included Al, Co, Cr, Fe, and Mn.

3.1 COMPUTATIONAL DETAILS

All theoretical calculations of the complexes were performed using SPARTAN' 08[*SPARTAN, 2008*] 132V4 Molecular Modeling Package. Due to size considerations, single point energy calculations at DFT B3LYP/6-31G* level of theory were performed on PM3

optimized geometries (B3LYP/6-31G* //PM3). The relative energies of all the isomers were computed considering the parent structures and the corresponding analogues.

- In view of the open-shell system and the electron configuration of the metals (+III states), spin unrestricted calculations were carried out.
- The charge assignments of the geometry-optimized structures and dipole moments were derived from the Mulliken population analysis [Mulliken, 1955].
- The starting geometries of the molecular systems were constructed using SPARTAN'S graphical model builder and minimized interactively using the Sybyl [Clark *et al.*, 1989] force field.

All geometries were fully optimized without any symmetry constraints and then subjected to full frequency calculations to verify the nature of stationary points

CHAPTER FOUR

4.10 SEMI-EMPIRICAL PM3 AND DENSITY FUNCTIONAL THEORY (DFT) STUDIES OF METAL BETADIKETONE AND ITS STEPWISE FLUORINATED DERIVATIVES.

4.11 RESULTS AND DISCUSSION

Semi-empirical PM3 and density functional theorem (DFT) methods were used to investigate the geometries, energies, vibrational frequencies and NMR spectra of acetylacetone and its complexes with some metals. The molecular vibrational modes can be classified based on their behavior under the effect of symmetry operations. The symmetry point group D3 was observed for acetylacetonate and hexafluoroacetylacetonate chelates as C1 was observed for the other stepwise fluorinated complexes. Vibrational frequency assignments reported in this work using the Semi-empirical PM3 and density functional theorem (DFT) methods were not based only on the band wave numbers, but also on the frequency intensities. There are several vibrational modes for chelates of acetylacetone corresponding to their internal vibrations. These vibrational modes are calculated for the lowest minima of the chelates at the PM3 and the B3LYP levels of theory using the standard 6-31G* basis set. The calculated frequencies which were computed with these methods were not scaled. The recommended scale factor for B3LYP frequency calculations however is 0.9614 [Jeffrey *et al.*, 2007]. Figure 4.10 below shows a sample of the optimized β-diketonates complex displaying the atomic numbering.

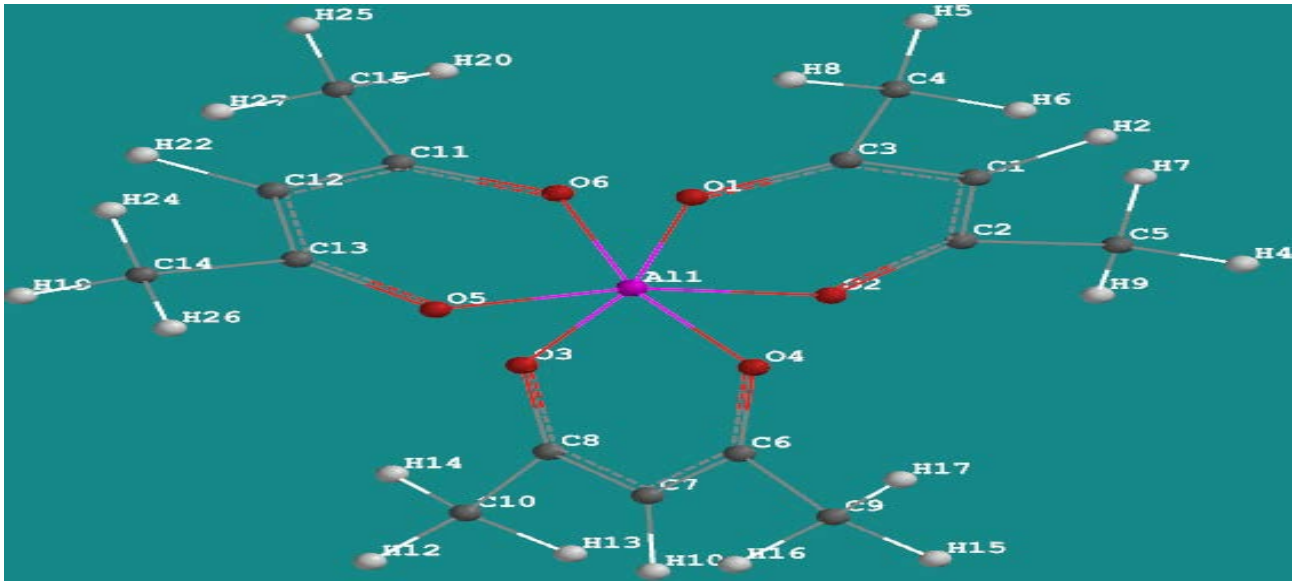

Figure4.10 DFT optimized structure of [Al(acac)$_3$] as derivative of the other metal β-diketonates showing atom numbering.

Table 4.10 Calculated Bond lengths (Å) and Bond angles (degrees) of Aluminium trisacetylacetonate [Al(acac)$_3$] at the B3LYP/6-31G* level of theory.

Bond lengths (Å)		Bond angles (degree)	
Al1 - O1	1.854	O2 - Al1-O1	104.60
O1 - C3	1.266	O3- Al1- O4	104.60
O3 - C8	1.266	O5- Al1- O6	104.60
C1 = C2	1.401	O1 – C3 – C1	126.14
C7 = C8	1.401	C2 – C1 – C3	127.01
C3 – C4	1.501		
C6 – C9	1.510		

Table 4.11 Calculated Bond lengths (Å) and Bond angles (degrees) of Aluminium tris-1-fluoro- 2,4-pentanedione [Al(fpd)$_3$] at the B3LYP/6-31G* level of theory.

Bond lengths (Å)		Bond angles (degree)	
Al1 - O1	1.882		
O1 - C3	1.166	O2 - Al1-O1	91.89
O3 - C8	1.189	O3- Al1- O4	91.76
C1 = C2	1.402	O3 – C3 – C1	123.32
C7 = C8	1.403	O3 – C8 – C7	123.63
C3 - C9	1.502	C2 – C1 – C3	128.70
C4 - C6	1.498	C6 – C7 – C8	128.75
C4 - F1	1.362		

Table 4.12 Calculated Bond lengths (Å) and Bond angles (degrees) of Aluminium tris-1,5-difluoro-2,4-pentanedione [Al(dfpd)$_3$] at the B3LYP/6-31G* level of theory.

Bond lengths (Å)		Bond angles (degree)	
Al1 - O1	1.982	O1-Al1-O2	91.89
O1 = C3	1.189	O1-C3=C1	123.32
C1 = C2	1.402	C2=C1=C3	128.75
C2 - C5	1.498	Al1-O1=C3	117.58
C5 - F5	1.383		

Table 4.13 Calculated Bond lengths (Å) and Bond angles (degrees) of Aluminium tris-1,1,1,5,5-pentafluoro-2,4-pentanedione [Al(pfpd)$_3$] at the B3LYP/6-31G* level of theory.

Bond lengths (Å)		Bond angles (degree)	
Al1-O1	1.978	O1-Al1-O2	91.16
Al1-O2	1.985	Al1-O1-C3	116.88
O1=C3	1.191	O7=C1=C17	125.96
C3=C1	1.410	O1=C3=C1	122.80
C1=C2	1.405	C3=C1=C2	128.57
C2-C5	1.504		
C5-F5	1.363		

Table 4.14 Calculated Bond lengths (Å) and Bond angles (degrees) of mixed Aluminium bisacetylacetonate and 1-fluoro-2,4-pentanedione [Al(acac)$_2$(fpd)] at the B3LYP/6-31G* level of theory.

Bond lengths (Å)		Bond angles (degree)	
Al1 - O1	1.915	O4 – Al1- O3	91.07
O1 - C3	1.275	O2 – Al1- O1	90.25
O3 - C8	1.271	O3 – C3 – C1	124.41
C1 = C2	1.406	O2 – C2 – C1	125.78
C7 = C8	1.402	C8 – C7 – C6	122.57
C3 - C9	1.510	C6 – C7 – C8	125.45
C4 - C6	1.510		
C2 - O2	1.271		
C5 - F8	1.381		

Table 4.15 Calculated Bond lengths (Å) and Bond angles (degrees) of mixed Aluminium acetylacetonate, 1-fluoro-2,4-pentanedione and1,5-difluoro-2,4-pentanedione [Al(acac)(fpd)(dfpd)] at the B3LYP/6-31G* level of theory.

Bond lengths (Å)		Bond angles (degrees)	
Al1 - O1	1.849	O2- Al1-O1	104.85
O1 - C3	1.268	O3- Al1- O4	102.77
O3 - C8	1.264	O3 – C3 – C1	126.10
C1 = C2	1.402	O3 – C8 – C7	126.63
C7 = C8	1.398	C2 – C1 – C3	127.13
C3 - C9	1.510	C6 – C7 – C8	125.45
C4 - C6	1.539		
C2 - O2	1.266		
C4 - F1	1.358		

Table 4.16 Calculated Bond lengths (Å) and Bond angles (degrees) of Aluminium bisacetylacetonate and 1,1,5,5-tetrafluoro-2,4-pentanedione [$Al(acac)_2(ttfpd)$] at the B3LYP/6-31G* level of theory.

Bond lengths (Å)		Bond angles (degree)	
Al1 - O1	1.848	O2 - Al_1-O1	104.95
O1 - C3	1.268	O3- Al_1- O4	103.04
O3 - C8	1.264	O3 = C3 = C1	125.99
O2 - C2	1.268	O3 = C8 = C7	126.78
C1 = C2	1.402	C2 = C1 = C3	127.20
C7 = C8	1.398	C6 = C7 = C8	126.60
C3 - C9	1.510		
C4 - C6	1.539		
C4 - F1	1.358		

Table 4.17 Calculated Bond lengths (Å) and Bond angles (degrees) of Aluminium tris(1-fluoro- 2,4-pentanedione) [$Al(tfpd)_3$] at the B3LYP/6-31G* level of theory.

Bond lengths (Å)		Bond angles (degrees)	
Al1 - O1	1.982	O2 - Al1- O1	91.89
O1 - C3	1.188	O3- Al1- O4	91.76
O3 - C8	1.189	O3 – C3 – C1	123.32
C1 = C2	1.404	O3 – C8 – C7	123.63
C7 = C8	1.403	C2 – C1 – C3	128.70
C3 - C9	1.502	C6 – C7 – C8	128.75
C4 - F1	1.364		

4.12 INFRARED SPECTROSCOPIC ANALYSIS

The IR spectra of $M(acac)_3$, $M(fpd)_3$, $M(dfac)_3$, $M(dfpd)_3$, $M(tfpd)_3$, $M(ttfpd)_3$, $M(tfac)_3$, $M(ttfac)_3$, $M(pfpd)_3$ and $M(hfac)_3$ (M = Al or Co)together with their mixedligandcomplexes have been computed at the B3LYP level of theory on PM3 optimized structures between 300-3500cm^{-1} region. Vibrational assignments were carried out with the aid of the density functional theory (DFT) [Becke, 1993: Parr and Yang, 1989] calculations with B3LYP/6-31G* basis sets.

From calculations, symmetric and asymmetric stretching band frequencies of methyne and methyl groups are exptected to be observed. The IR spectra of all the chelates are characterized by the presence of weak bands in the range 2992-3232cm^{-1} which indicates the various symmetric CH vibrations (υ_sC-H).

The region 1550-1750cm^{-1} is characterized by the presence of two strong bands assignable to the symmetric C = O and C = C stretching vibrations for all the chelates except for $M(fpd)_3$, $M(dfpd)_3$ and$M(pfpd)_3$ which appearedbeyond 1900cm^{-1}. These carbonyl bands observed are all lower than are recorded in the free ligands indicating the involvement of the carbonyl groups in bonding. The C = O stretching frequency of $Al(fpd)_3$ and $Co(fpd)_3$ are much stronger than are found in the other complexes and appears respectively at 1965 cm^{-1}and 2012cm^{-1}.

The medium intensity bands observed between 1496-1536cm^{-1}in all the chelates are assignable to the in plane and out of plane combination bands due to CH and CH_3 groups. The CH_2-F stretching vibrations are observed at 1203-1441cm^{-1} for all the complexes. The weak vibrational bands at 1037-1073cm^{-1}are due to the deformations of the C-O and CH_3 groups.

The characteristic out of plane bending and deformation vibrations of the CH_2F groups are observed at 784-893cm^{-1} region. The υ_sM – O vibrational frequencies are very weak and are observed below 600cm^{-1} region of the spectrum. The observed infrared bands are displayed in tables 4.18 - 4.22 below.

Table 4.18 Calculated vibrational frequencies (cm^{-1}) of Aluminium tris-1,1- difluoro-2,4-pentanedione [Al(dfac)$_3$] at the B3LYP/6-31G* level of theory.

IR(cm^{-1})	assignment	IR(cm^{-1})	assignment
3112w	υ_sC-H	1303s	δC – O + C-C
2967m	υ_{as} CF_2-H	1260s	δCH
1744vs	υ_sC=O	1185s	ωCH-F_2
1620vs	υ_sC=C	1066w	τC-CH_3
1585m	$\upsilon_{as}$$CH_2$-F + CH_3	992w	τC-O + C-C
1518w	δsCH_3	751w	δO - C=C
1498w	δCH_3	688m	υ_sM – O + CH_3
1421s	υ_{as}C - F	489w	υ_sM – O

υ_s = symmetric stretch, υ_{as} = asymmetric stretch, δ = in plane bending, ω = out of plane bending (wagging), τ = out of plane bending (twisting), δs = in plane scissoring, Γring = Out of plane ring deformations, Δ ring = in plane ring deformations.

Table 4.19 Calculated vibrational frequencies (cm^{-1}) of Aluminium tris(1-fluoro- 2,4-pentanedione) [Al(fpd)$_3$] at the B3LYP/6-31G* level of theory.

IR(cm^{-1})	assignment	IR(cm^{-1})	assignment
3145w	υ_sC-H	1053w	Δ ring
2987w	$\upsilon_s$$CH_2$-F	884m	τCH
1965vs	υ_sC=O	664w	ωC-O + C-C
1610vs	υ_sC=C	624w	ωM-O + C=C
1516w	υ_{as}CH+CH_3	563m	δM-O + C=C
1495m	δCH_2-F + CH_3	483m	υM – O
1319w	υC=C- CH_3	432w	υM – O
1191m	υ_{as}C - F		
1073w	τC – O + CH_3		

υ_s = symmetric stretch, υ_{as} = asymmetric stretch, δ = in plane bending, ω = out of plane bending (wagging), τ = out of plane bending (twisting), δs = in plane scissoring, Γring = Out of plane ring deformations, Δ ring = in plane ring deformation.

Table 4.20 Calculated vibrational frequencies (cm^{-1}) of Aluminium bisacetylacetonate and 1-fluoro-2,4-pentanedione [$Al(acac)_2(fpd)$] at the B3LYP/6-31G* level of theory.

IR(cm^{-1})	Assignment	IR(cm^{-1})	Assignment
3039w	υ_sC-H + CH_3	1113m	δCH_2-F
2067vs	$\upsilon_s CH_2$-F	1062w	ωCH_3
1651vs	υ_sC=O	796w	τCH
1574w	υ_sC=C	630w	τC-C-C
1527w	υ_sC-CH_3	499m	υ_sM-O
1497m	υ_sO-C-CH_3	397m	υ_sM-O
1427vw	$\delta s CH_3$		
1309w	υ_{as}C-C-C		

υ_s = symmetric stretch, υ_{as} = asymmetric stretch, δ = in plane bending, ω = out of plane bending (wagging), τ = out of plane bending (twisting), δs = in plane scissoring, Γring = Out of plane ring deformations, Δ ring = in plane ring deformations.

Table 4.21 Calculated vibrational frequencies (cm^{-1}) of Aluminium acetylacetonate,1-fluoro-2,4-pentanedione and1,5-difluoro-2,4-pentanedione [Al(acac)(fpd)(dfpd)] at the B3LYP/6-31G* level of theory.

IR(cm^{-1})	assignment	IR(cm^{-1})	assignment
3108w	υ_sC-H	1323m	δCH_3
1706vs	υ_sC=O	1293w	ωCH_2-F
1608vs	υ_sC=C	1266m	τ CH
1532m	υ_{as}C-CH_3	1067w	ωCH_3
1520m	υ_sO-C-CH_3	977w	υM-O
1497w	$\upsilon_s CH_3$	889w	τCH
1441w	$\delta s CH_2$-F	731m	υ_{as}M – O + CH_3
1429w	ωCH_3	412w	υ_sM – O

Table 4.22 Calculated vibrational frequencies (cm^{-1}) of Aluminium bisacetylacetonate and 1,1,5,5-tetrafluoro-2,4-pentanedione [$Al(acac)_2(ttfpd)$] at the B3LYP/6-31G* level of theory.

IR(cm^{-1})	Assignment	IR(cm^{-1})	Assignment
3110w	υ_sC-H + CH_3	980w	Δch
2992s	$\upsilon_s CF_2$-H	865w	Ωch
1732vs	υ_sC=O	738m	υ_{as}M – O + CH_3
1534vs	υ_sC=C	699w	δC-O + C-C
1519m	δ C-CH_3	521w	δM-O
1445m	$\delta_s CF_2$-H	405w	υ_sM – O
1322m	δCH_3		
1249w	τCH_2-F		
1051w	$\upsilon_{as}CH_3$		

υ_s = symmetric stretch, υ_{as} = asymmetric stretch, δ = in plane bending, ω = out of plane bending (wagging), τ = out of plane bending (twisting), δs = in plane scissoring, Γring = Out of plane ring deformations, Δ ring = in plane ring deformations.

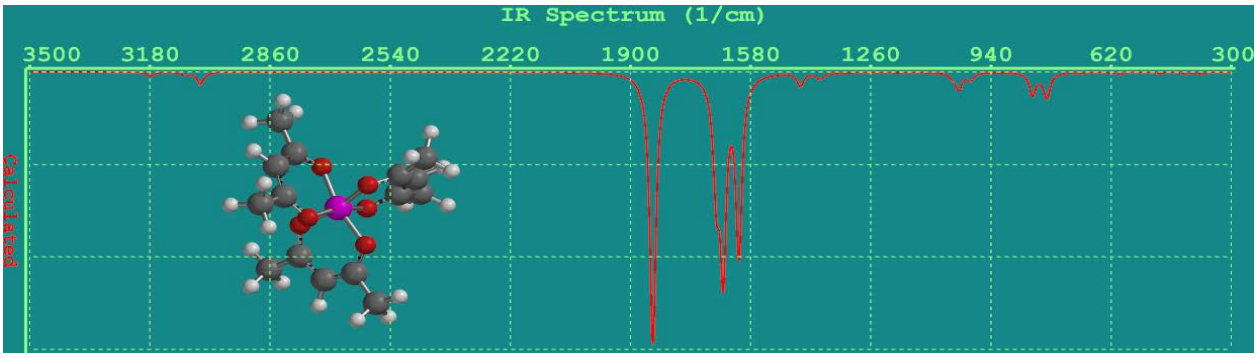

Figure4.11 Infrared spectrum of [$Al(acac)_3$] in the gas phase showing the ball and spoke module computed at the B3LYP/6-31G* level of theory.

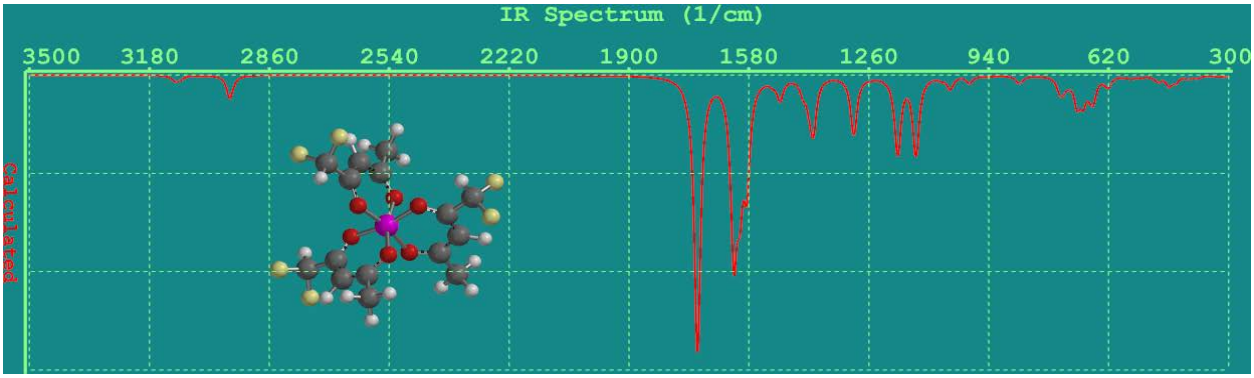

Figure4.12 Infrared spectrum of [Al(dfac)$_3$] in the gas phase computed at the B3LYP/6-31G* level of theory.

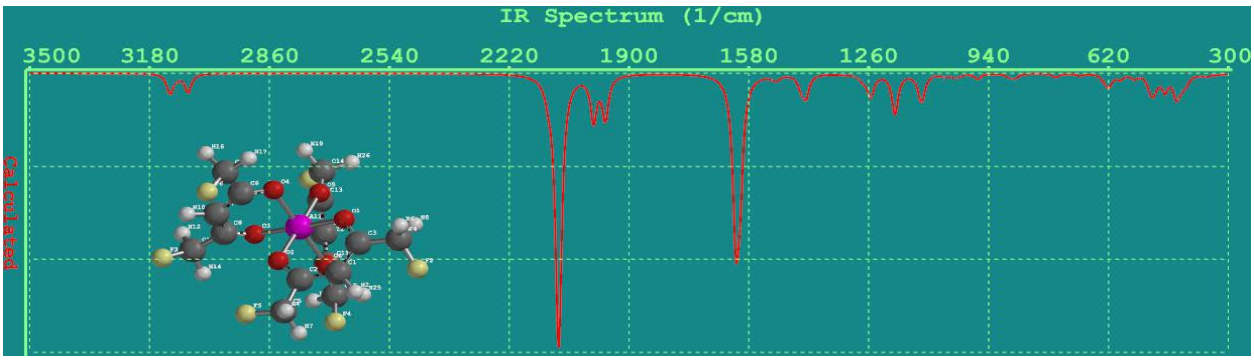

Figure4.13 Infrared spectrum of [Al(dfpd)$_3$] in the gas phase computed at the B3LYP/6-31G* level of theory.

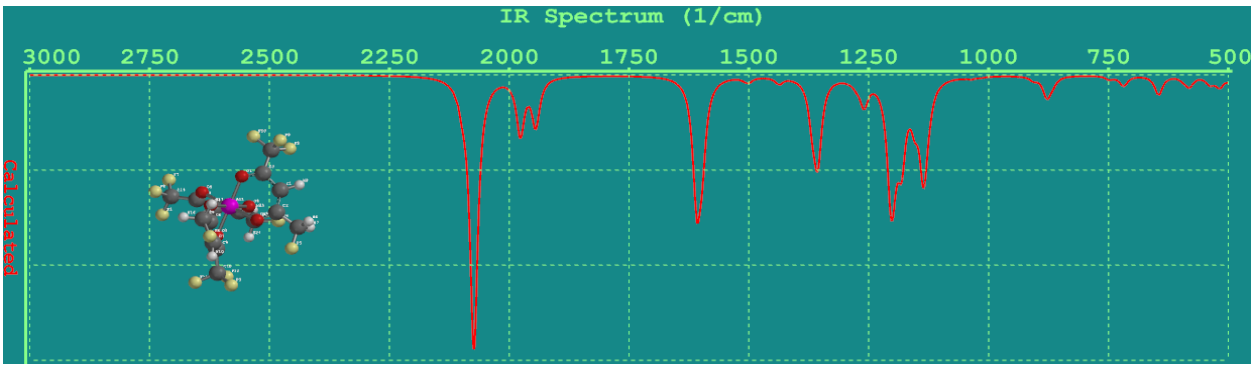

Figure4.14 Infrared spectrum of [Al(pfpd)$_3$] in the gas phase computed at the B3LYP/6-31G* level of theory.

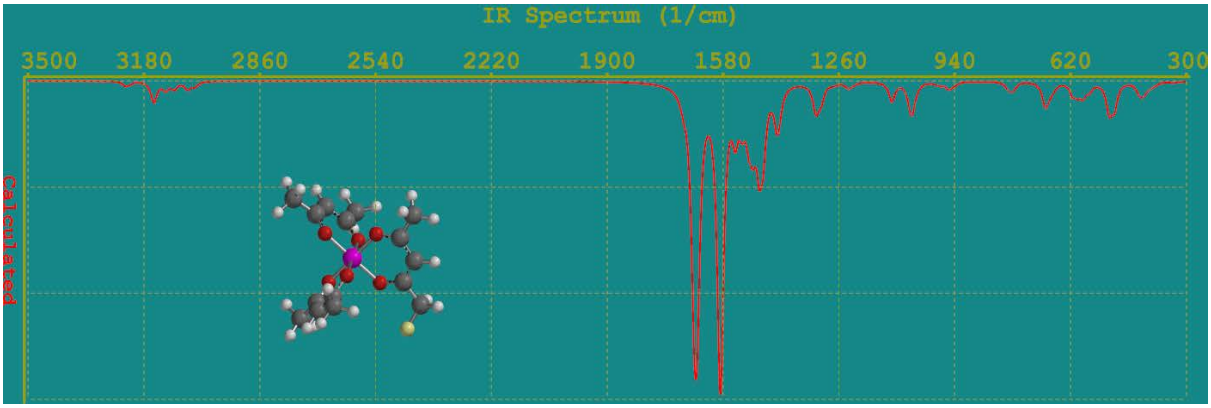

Figure4.15 Infrared spectrum of [Al(acac)$_2$(fpd)] in the gas computed at the B3LYP/6-31G* level of theory.

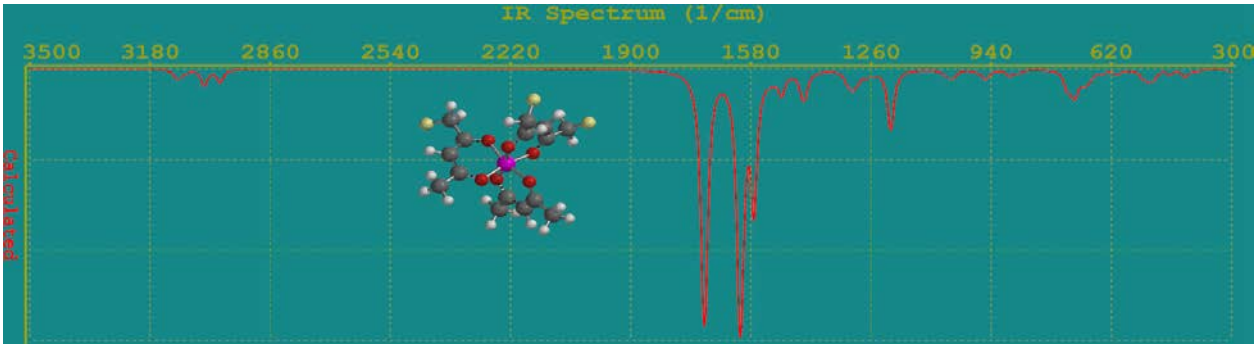

Figure4.16 Infrared spectrum of [Al(acac)(fpd)(dfpd)] in the gas phase module computed at the B3LYP/6-31G* level of theory.

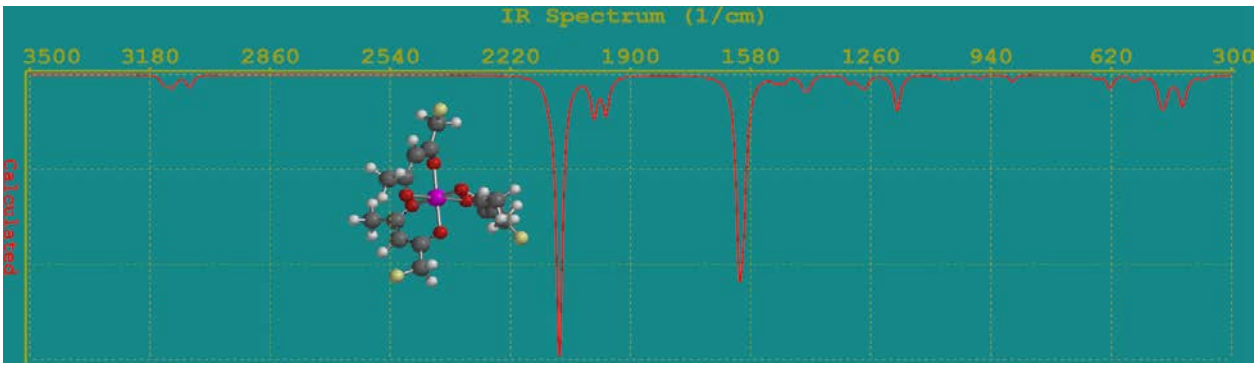

Figure4.17 Infrared spectrum of [Al(fpd)$_3$] in the gas phase showing computed at the B3LYP/6-31G* level of theory.

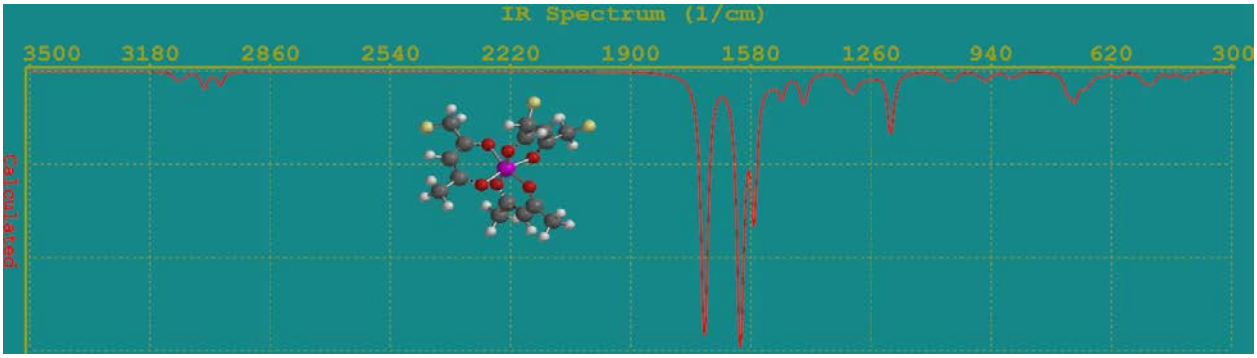

Figure4.18 Infrared spectrum of [Al(acac)(fpd)(dfpd)] in the gas phase module computed at the B3LYP/6-31G* level of theory.

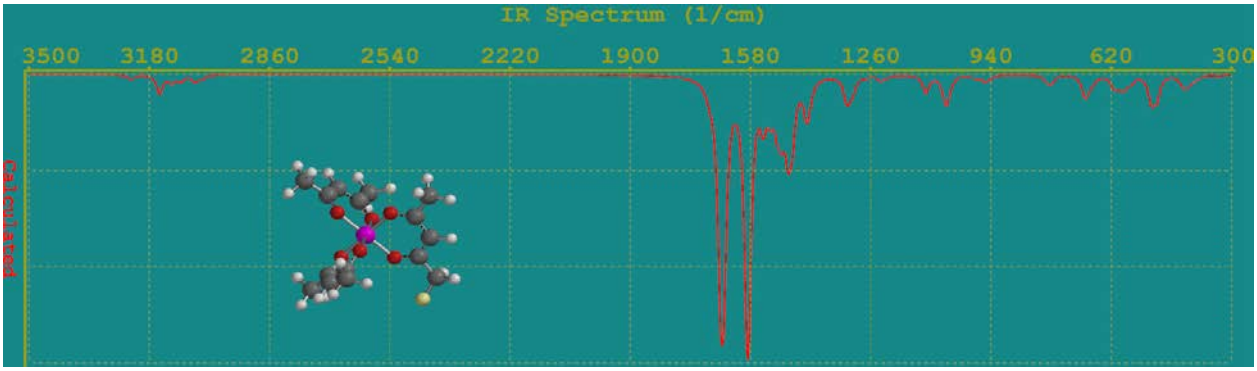

Figure4.19 Infrared spectrum of [Al(acac)$_2$(fpd)] in the gas phase computed at the B3LYP/6-31G* level of theory.

4.13 NMR SPECTROSCOPIC ANALYSIS

4.131 ^{1}H-NMR SPECTRA

When the ^{1}H-NMR spectra of the ligands in the gas phase were examined, peaks corresponding to $CH_3C\underline{H}CH_3$ were observed at 5.10 to 5.04ppm (s, 1H) for Al(acac)$_2$(fpd) complex and 5.53-5.13ppm(s, 1H) for Al(acac)(fpd)(dfpd). Al(ttfpd)(acac)$_2$ and Al(fpd)$_3$ had their peaks at 4.70-4.79ppm(s,1H) and 4.53-4.54ppm(s,1H) respectively. The deshielded $CH_2FCC\underline{H}CCH_2F$ proton of Al(ttfpd)(acac)$_2$ is observed at 5.56ppm(s, 1H). The peak of $CH_3C\underline{H}CH_2F$ proton of the ligand appears at 4.83ppm (s,1H) for Al(acac)$_2$(fpd), 4.71-4.80ppm(s,1H) for Al(acac)(fpd)(dfpd), 4.64-4.68ppm(s, 1H) for Al(acac)$_2$(ttfpd) and 4.45-4.48ppm(s, 1H) for Al(fpd)$_3$. The signals observed at 4.53-4.67ppm(s, 2H) for

Al(acac)(fpd)(dfpd), 4.53ppm(s, 2H) for Al(ttfpd)(acac)$_2$ and 4.06-4.13ppm(s,2H) for Al(fpd)$_3$ are assigned respectively to C$\underline{H}_2$F protons. The peak of CH protons neighbouring to fluoro groups were observed between 4.76 and 4.42ppm (s, 1H) for Al(acac)$_2$(fpd). The appearance of two peaks is an indication that the two protons are stereochemically inequivalent. The peak corresponding to the terminal C$\underline{H}_3$ groups in Al(acac)$_3$, Al(acac)$_2$(fpd) and the other analogues are very intensive and are observed at 1.39ppm to 2.00ppm (s, 15H). The intensity of the peak is as a result of the overlap of the spectra of the several protons at the same position in the spectrum. That of Al(acac)(fpd)(dfpd), Al(ttfpd)(acac)$_2$ and Al(fpd)$_3$ protons appear at 1.19-1.91ppm(s, 9H), 1.13-1.82ppm(s, H) and 0.93-1.92ppm(s, 12H) respectively. These primary protons are well shielded by the more electronegative atoms and hence they are shifted upfield.

The observation is that an increase in fluorine substitution deshields the attached protons thereby causing them to be shifted downfield.

Similar results of these complexes recorded for cobalt derivatives were observed rather at higher frequencies. The unusual shifts of these protons and the inability of Cr, Fe and Mn complexes to converge might be as a result of the introduction of the d^n- electrons in the transition series which perturbs the electronic distribution and interaction.

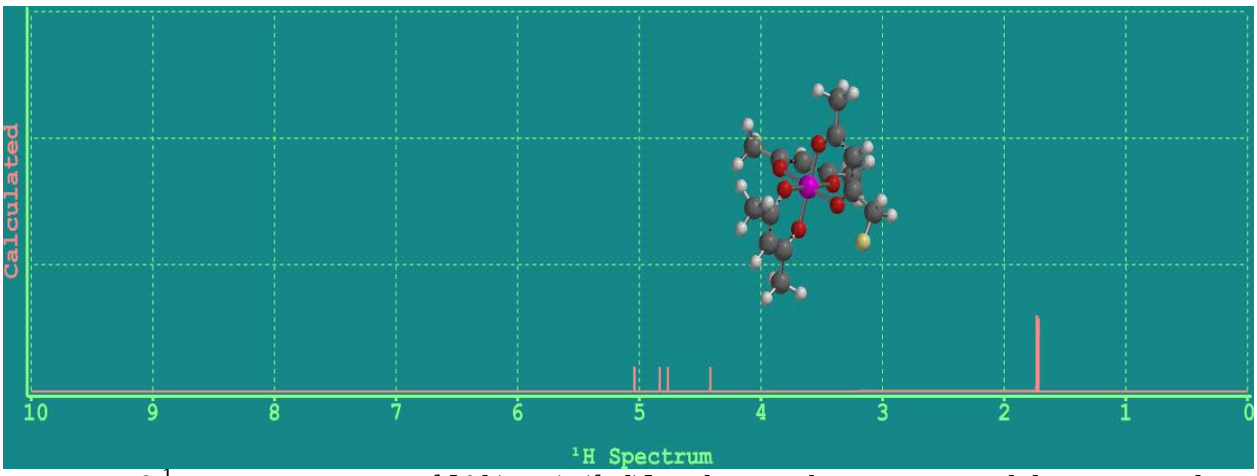

Figure 4.20 ^{1}H-NMR spectrum of [Al(acac)$_2$(fpd)] in the gas phase module computed at the B3LYP/6-31G* level of theory.

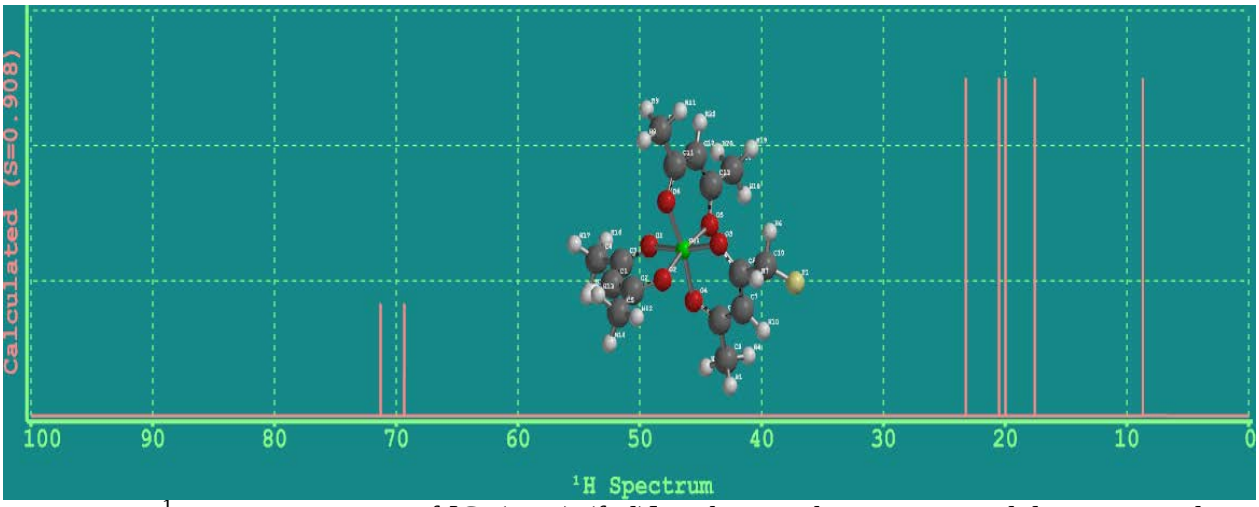

Figure 4.21 ^{1}H-NMR spectrum of [Co(acac)$_2$(fpd)] in the gas phase module computed at the B3LYP/6-31G* level of theory.

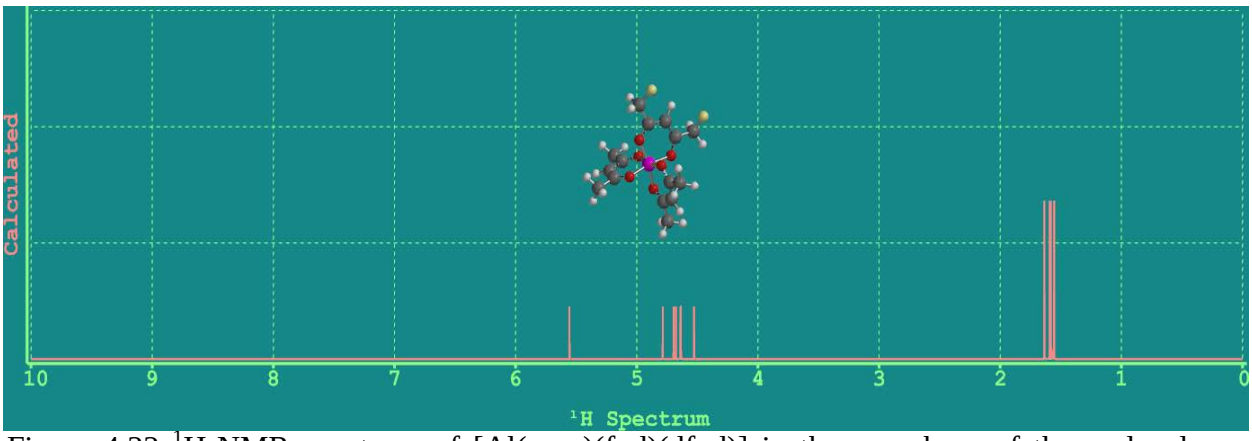

Figure 4.22 ^{1}H-NMR spectrum of [Al(acac)(fpd)(dfpd)] in the gas phase of the molecule computed at the B3LYP/6-31G* level of theory.

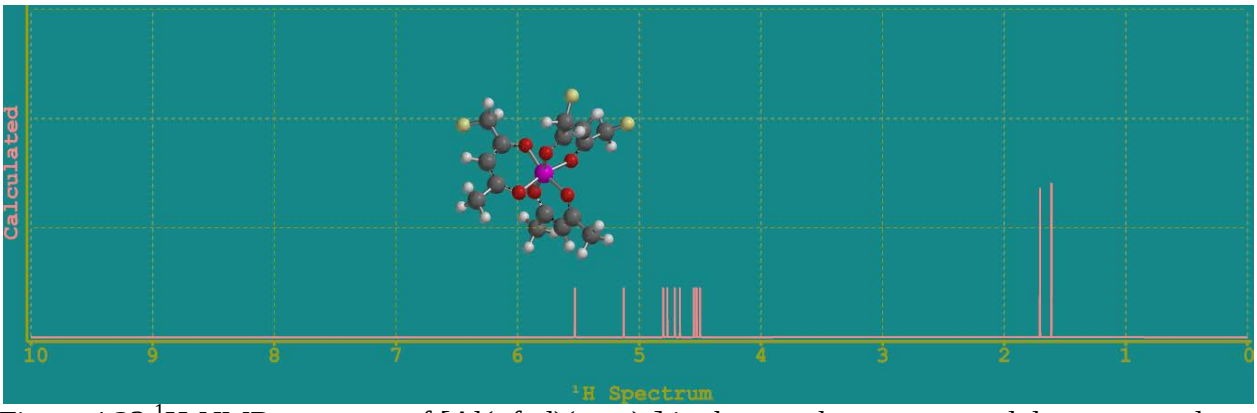

Figure 4.23 ^{1}H-NMR spectrum of [Al(ttfpd)(acac)$_2$] in the gas phase module computed at the B3LYP/6-31G* level of theory.

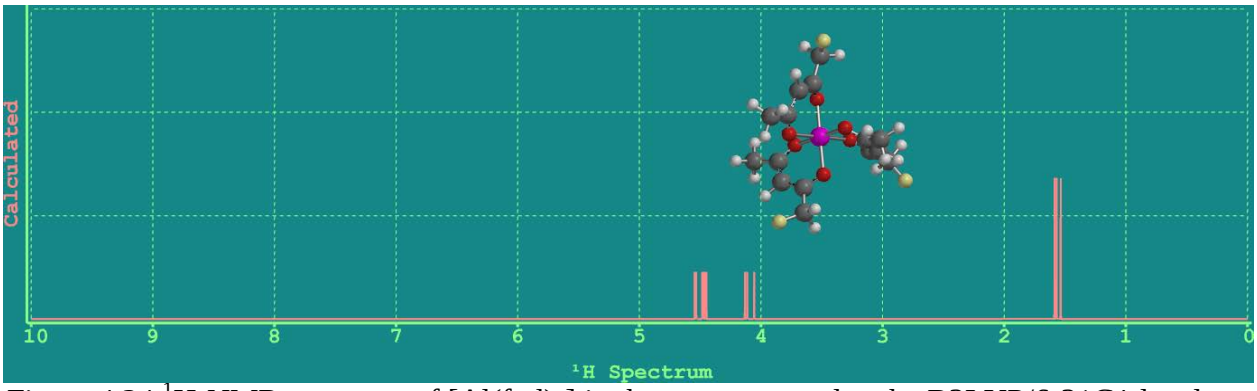

Figure 4.24 ^{1}H-NMR spectrum of [Al(fpd)$_3$] in the gas computed at the B3LYP/6-31G* level of theory.

4.132 ^{13}C-NMR SPECTRA

In the ^{13}C-NMR spectra of chelates, seven different peaks were observed for Al(acac)$_2$(fpd), eleven for Al(acac)(fpd)(dfpd), six for Al(ttfpd)(acac)$_2$ and five for Al(fpd)$_3$ complexes. There is variation in the spectra of the complexes because the substituted fluorine groups alter the electronic distribution of neighbouring atoms. The peak found between 26.62 to 26.71ppm is assigned to the methyl carbons (<u>C</u>H$_3$) in Al(acac)$_2$(fpd). These peaks are shifted downfield to 20.92-21.65ppm, 20.86-20.94ppm and 20.87-20.88ppm for Al(acac)(fpd)(dfpd), Al(ttfpd)(acac)$_2$ and Al(fpd)$_3$ respectively upon fluorine substitutions. The peak of <u>C</u>H$_2$F appears at 80.94ppm, 76.17-77.21ppm, 76.26-77.18ppm and 72.94-73.05ppm for Al(acac)$_2$(fpd), Al(acac)(fpd)(dfpd), Al(ttfpd)(acac)$_2$ and Al(fpd)$_3$ in that order. The <u>C</u>H carbon peaks are observed at 93.87-97.52ppm for Al(acac)$_2$(fpd), 83.61-87.83ppm for Al(acac)(fpd)(dfpd), 83.45-87.73ppm for Al (ttfpd)(acac)$_2$ and 81.08-81.43ppm for Al(fpd)$_3$. The peak corresponding to the <u>C</u>CH$_2$F carbon appears at 176.57ppm and that of the O<u>C</u>CH$_3$ carbons are observed at 179.40-181.10ppm for Al(acac)$_2$(fpd), 168.18ppm and 170.14-173.54ppm for Al(acac)(fpd)(dfpd), 169.76-169.79ppm and 170.04-172.02ppm for

$Al(ttfpd)(acac)_2$ and 161.14-163.48ppm for $Al(fpd)_3$. The proximity of the carbonyl carbon peaks in the complexes is an indication that the electronic environments of these groups are not very different. The most intense spectra are observed for $Al(ttfpd)(acac)_2$.

It is worth noting that the ^{13}C-NMR spectra of the cobalt derivatives of these complexes had most of the peaks going beyond 225ppm and in some cases below 0ppm which is the range usually found and reported. Again attempts made to compute the ^{13}C-NMR for Cr, Fe and Mn at the B3LYP/6-31G* level of theory failed to converge.

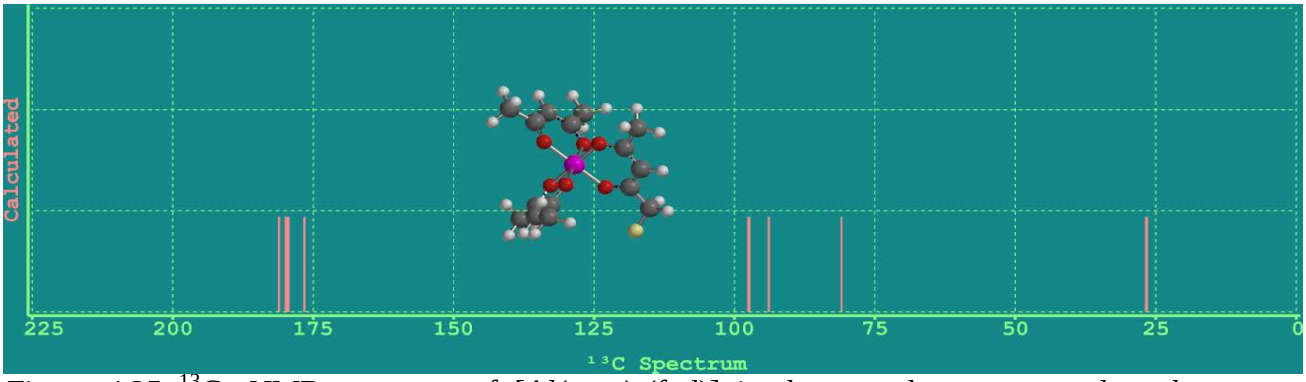

Figure 4.25 ^{13}C -NMR spectrum of $[Al(acac)_2(fpd)]$ in the gas phase computed at the B3LYP/6-31G* level of theory.

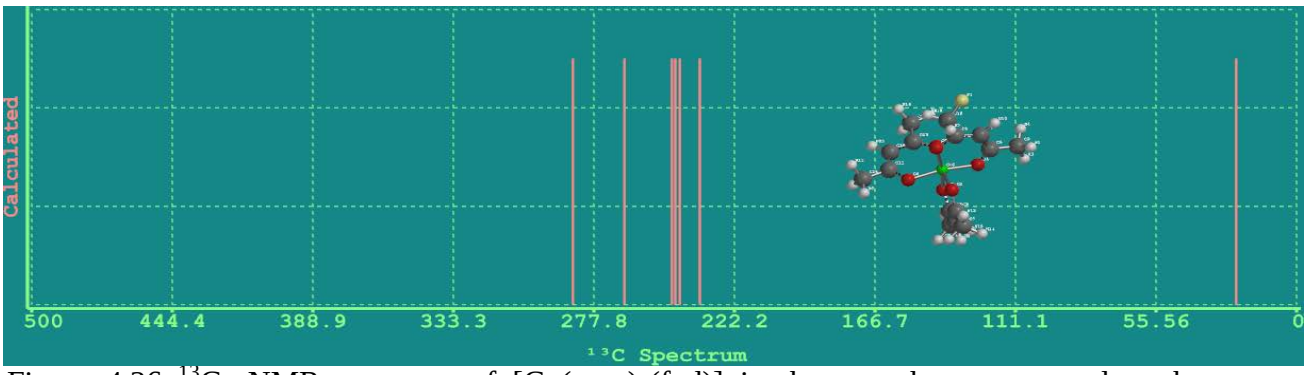

Figure 4.26 ^{13}C -NMR spectrum of $[Co(acac)_2(fpd)]$ in the gas phase computed at the B3LYP/6-31G* level of theory.

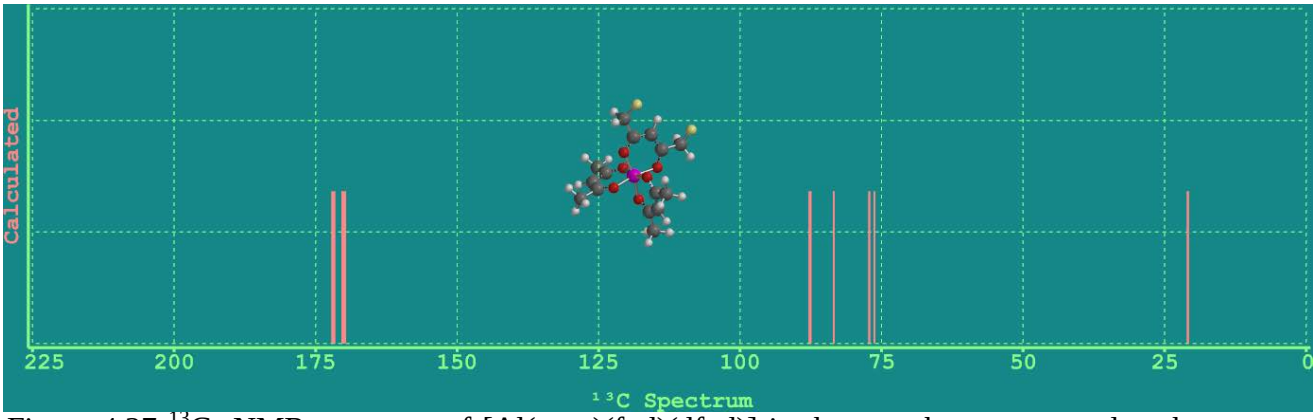

Figure 4.27 ^{13}C -NMR spectrum of [Al(acac)(fpd)(dfpd)] in the gas phase computed at the B3LYP/6-31G* level of theory.

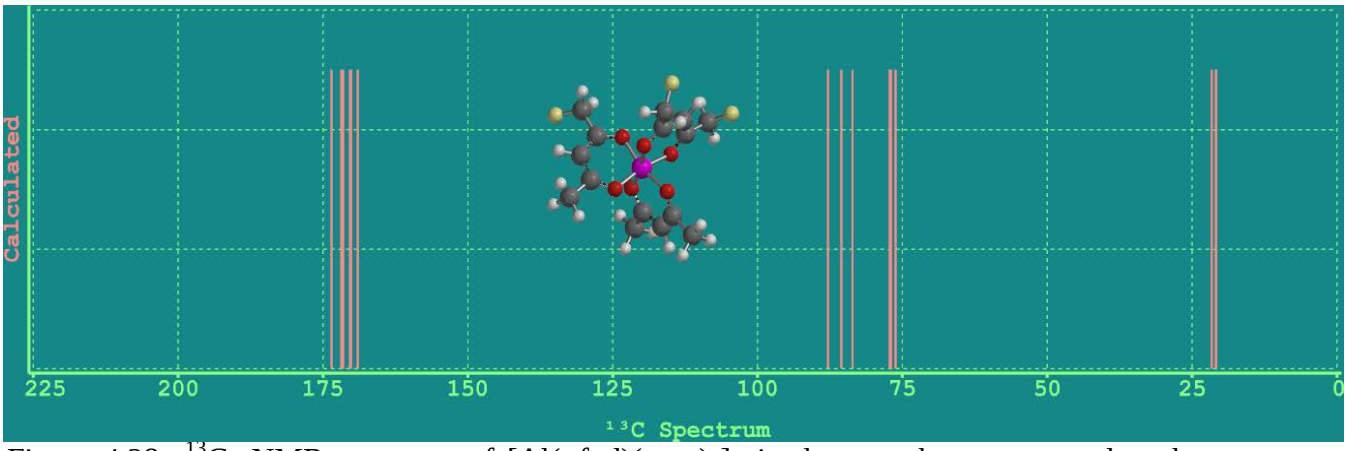

Figure 4.28 ^{13}C -NMR spectrum of [Al(ttfpd)(acac)$_2$] in the gas phase computed at the B3LYP/6-31G* level of theory.

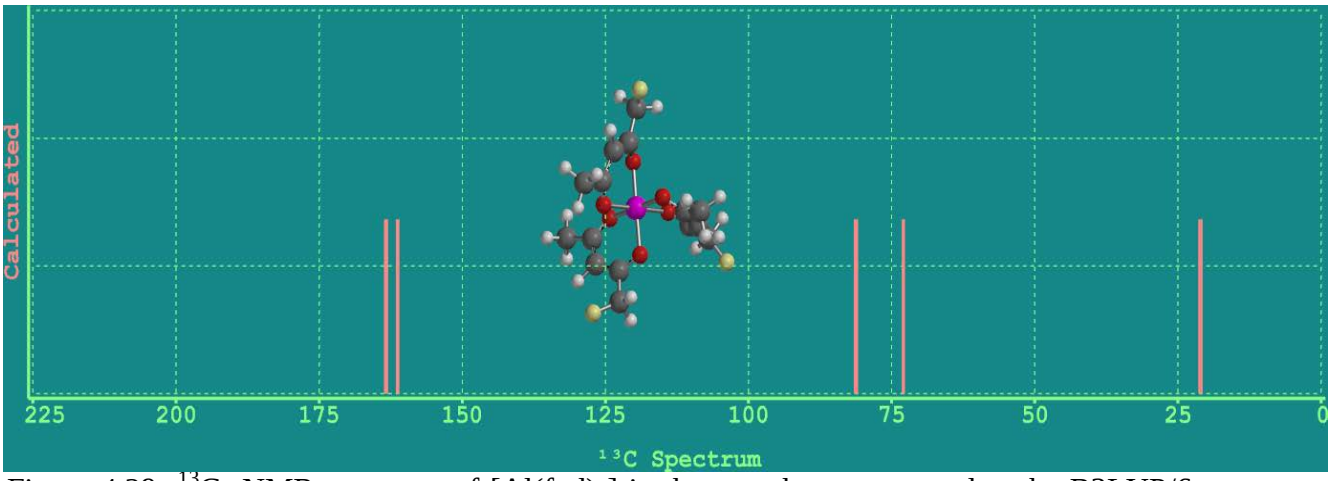

Figure 4.29 ^{13}C -NMR spectrum of [Al(fpd)$_3$] in the gas phase computed at the B3LYP/6-31G* level of theory.

4.133 ^{19}F-NMR SPECTRA

The ^{19}F-NMR output of $Al(acac)_2(fpd)$ shows the fluorine resonance signal at δ-244.42ppm and δ-700.75 for $Co(acac)_2(fpd)$. The three fluorine atoms in Al(acac)(fpd)(dfpd) are observed at δ-269.93ppm, δ-270.22ppm and δ-270.70ppm displaying the similitude in their chemical environment. $Al(ttfpd)(acac)_2$ signals appear at δ-269.00ppm and δ-270.08ppm which are virtually the same as found in the complex Al(acac)(fpd)(dfpd). The peaks corresponding to $Al(fpd)_3$ complex were observed between δ-275.77 and δ-275.85ppm.

4.140 UV SPECTRA

The electronic spectra of the stepwise fluorinated aluminium betadiketonates examined in vacuum using the B3LYP method exhibited a single broad band with different λ_{max} values. The spectral bands ranged between 276.63 and 303.59nm for $Al(acac)_2(fpd)$, 266.08 and 321.00nm for Al(acac)(fpd)(dfpd), 268.90 and 323.54nm for $Al(ttfpd)(acac)_2$ and 274.25 and 282.22nm for $Al(fpd)_3$. The λ_{max} for $Al(acac)_2(fpd)$, Al(acac)(fpd)(dfpd), $Al(ttfpd)(acac)_2$ and $Al(fpd)_3$ are found respectively at 276.63nm, 289.13nm, 294.92nm and 276.03nm. These bands can be assigned to the charge transfer transitions from the metal to anti-bonding orbitals of the ligand.

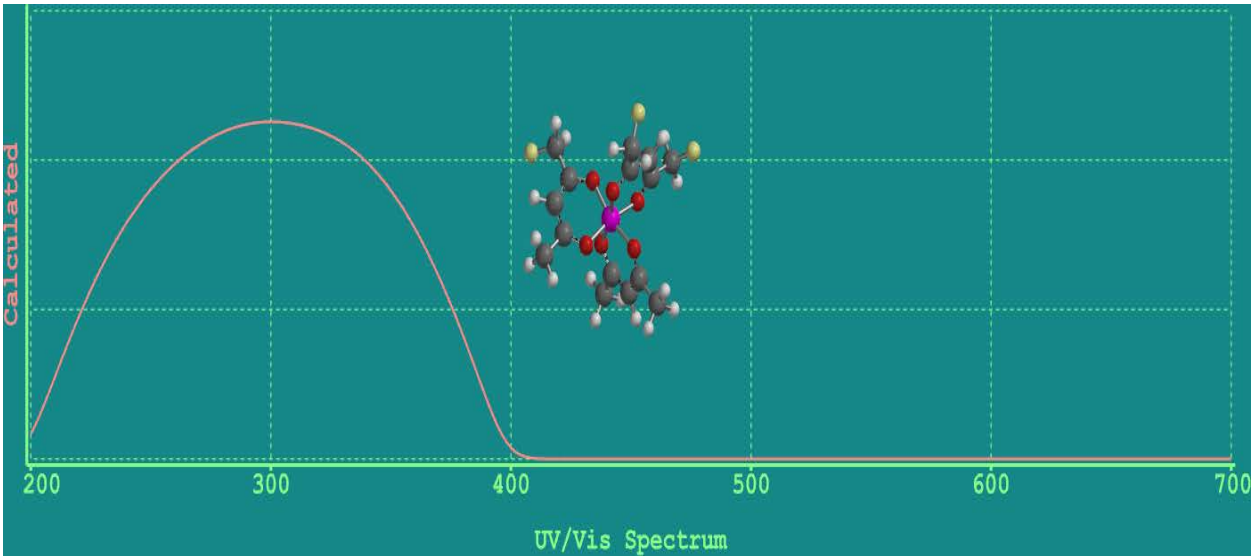

Figure 4.30. UV spectrum of [Al(ttfpd)(acac)$_2$] in the gas phase as representative of the other Al stepwise fluorinated complexes computed at the B3LYP/6-31G* level of theory.

The UV spectra of the cobalt derivatives of the complexes examined in the gas phase exhibited two broad bands with different λ_{max} values which are higher than are found in the corresponding Aluminium compounds. The spectra ranged between 361.38 and 508.05nm for Co(acac)$_2$(fpd), 361.66 and 510.15nm for Co(acac)(fpd)(dfpd), 361.38 and 508.05nm for Co(ttfpd)(acac)$_2$ and 364.02 and 511.49nm for Co(fpd)$_3$. The λ_{max} for Co(acac)$_2$(fpd), Co(acac)(fpd)(dfpd), Co(ttfpd)(acac)$_2$ and Co(fpd)$_3$ are situated respectively at 362.78 and 494.57 nm, 362.78 and 494.57nm, 361.66 and 490.77nm, and 370.05 and 495.08nm.

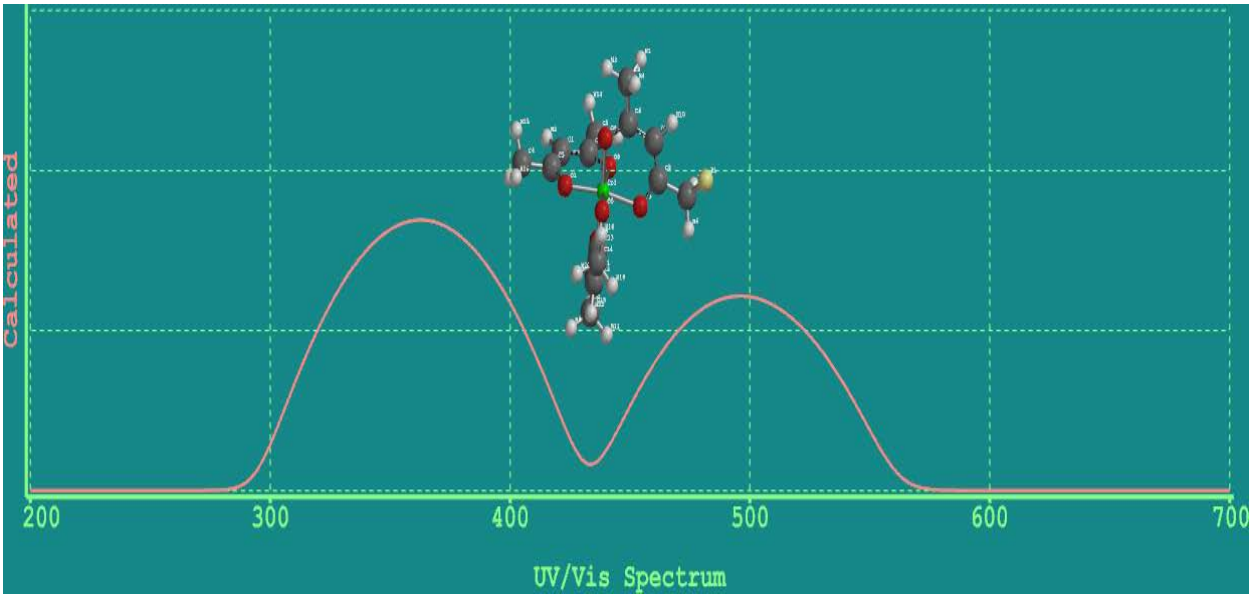

Figure 4.31 UV spectrum of $[Co(acac)_2(fpd)]$ in the gas phase as representative of the other stepwise fluorinated cobalt (III) complexes computed at the B3LYP/6-31G* level of theory.

SEMI-EMPIRICAL PM3 AND DENSITY FUNCTIONAL THEORY (DFT) STUDIES OF METAL BETADIKETONE, ITS FLUORINATED AND AROMATIC DERIVATIVES.

4.20 RESULTS AND DISCUSSION

4.21 1-(2-Thienyl)-1,3-butanedione (Htbd), 1-(2-furyl)-1,3-butanedione (Hfbd) and 1-phenyl-1,3-butanedione (Hbzac) Metal Complexes.

4.211 IR vibrational frequencies (cm^{-1})

The IR spectra of the complexes of thienyl, furyl and phenyl substituted betadiketonates with some trivalent metals were studied in the range 3500- 300cm^{-1}. From the calculations in this work and the expterimental vibrational frequencies reported by other workers [Hancock and Thornton, 1969; Patel and Adimado, 1980], principal infrared spectra of tris(acetylacetonato) metal complexes are presented in Table 3.23 below. Infrared studies on diketones have shown that electron releasing substituents give rise to low $\upsilon_{as}(C = O) + \upsilon_{as}(C = C)$ [Hancock and Thornton, 1969; Patel and Adimado, 1980].

Comparing the IR spectra of the metal chelates with those of organic ligands themselves, Table 4.23 would elucidate the structure of bonding between the ligands and metal ions. There exist some quantitative variations in the calculated and expterimental vibrational frequencies in the infrared spectra of Htbd, Hfbd and Hbzac complexes. The theoretical results of the different metal complexes however appear around similar characteristic frequency range for all the chelates.

The carbonyl band which is assigned to asymmetric C = O (υ_{as}C = O) stretching mode appears at the 1869-1764cm^{-1} region for all the complexes except for the chromium complex which had its vibrational frequency band falling below 1700cm^{-1}. The asymmetric C = C (υ_{as}C = C) stretch appears in the 1680-1581cm^{-1} region of the spectra of the complexes. The asymmetric stretches of C = O shows considerable shifts of about 128 - 68cm^{-1} to lower frequencies on complexation with the intensity of the bands also becoming stronger on complexation. The weakening or lower frequency shifts in the chelates is an indication that the carbonyl groups (C = O) of the ligand moieties participate in chelate formation.

The asymmetric C = C stretching frequencies in the free ligands spectra were either weakened or shifted to lower frequencies in all the chelates. These frequencies show much of a shift on complexation in all the metals to about 47- 40cm^{-1}. The expterimental results [Adimado, 1980, 1981] however, could not observe the bands beyond 1650cm^{-1}. The peaks that were found between 3180-2860cm^{-1} theoretically and are assigned to the CH_3 + CH vibrations were not found expterimentally and this may be accounted for due to impurities and the medium in which the expteriment was carried out.

For most part of the spectrum, it is safe to assume that the expterimental and theoretical separations in the observed vibrational spectra are in fact minimal and do coincide on many observed fundamental bands. The absorption bands in the 1570-1390cm^{-1} region are assigned to the aromatic rings stretching modes. The coupled vibrations of the asymmetric C = O and CH bands of Htbd, Hfbd and Hbzac are observed at 1389-1351cm^{-1} on complex formation.

The symmetric C = O stretching vibrations appear at a higher frequency in the complexes of all the metals. The calculated values were however, quite higher than the expterimental results. The symmetric C = C = C bands are observed between 1233-1211cm^{-1} which are below the expterimental values of 1242-1230cm^{-1}.

The 1200cm^{-1} band assigned to the coupled υC = C + υC-R modes shift to a higher frequency by about 47-21cm^{-1} on complexation.

The chelate ring deformation bands are observed at 1205-1075cm^{-1} on complexation.

The IR spectra of all the chelates exhibited a band in the range 818-706cm^{-1}, assigned to the metal-ligand stretches (combination bands). The chelate ring deformation bands coupled with the metal –oxygen bands are observed at 650-535cm^{-1}. The weak M-O vibrational bands observed below 600cm^{-1} region are poorly resolved in all the complexes.

Our results correlate well with the findings by Tayyari and co-workers [Tayyari *et al.*, 2002]. They used HF and DFT methods with the B3LYP, B1LYP, and G96LYP functionals and using the 6-31G* basis set to investigate the geometry, frequency and intensity of vibrational bands of $Al(acac)_3$ and its derivatives. The calculated frequencies were compared with the solid IR and Raman spectra. All of the measured IR and Raman bands were interpreted in terms of the calculated vibrational modes. Most of the computed bands were predicted to be at higher wavenumbers than the expterimental bands. The calculated bond lengths and bond angles were in good agreement with the expterimental results.

Table 4.23 Assignment of the observed vibrational frequencies (cm^{-1}) of 1-(2- thienyl) – 1,3-butanedione (Htbd) and its metal complexes at the PM3 level of theory.

Ligand		Al		Cr		Mn		Fe		Co	
Cal.	Expt.	Cal.	Expt.	Cal.	Expt.	Cal.	Expt.	Cal.	Expt	Cal.	Expt.
1764vs	1620vs	1832vs	1600s	1636s	1598s	1841vs	1600m	1727vs	1600m	1769vs	1595s
1635s	1615vs	1642vs	1575s	1594s	1570s	1619vs	1572m	1582vs	1570m	1568s	1568m
1541vs	1525sh	1536 s	1535s	1561m	1535s	1506s	1530s	1543s	1535s	1522s	1530s
1485s	1465s	1461s	1500s	1502m	1500s	1501s	1505s	1505m	1510s	1463s	1508s
1456s	1418s	1452m	1450sh	1443w	1422sh	1487s	1420m	1444m	1422m	1413m	1420sh
1408m	1382w	1398s	1400s	1393w	1390s	1425s	1395s	1406s	1395s	1405m	1390s
1378m	1360m	1363s	1352s	1351w	1350s	1392s	1350s	1389s	1350s	1387s	1354s
1322m	1280s	1354m	1315m	1331w	1309m	1353m	1286m	1358m	1302m	1372w	1290vs
1206m	1240m	1213m	1238m	1233w	1242s	1214w	1230m	1333m	1240m	1211w	1240s
1179w	1210w	1200w	1200w	1226m	1202w	1208w	1200w	1220m	1200w	1205m	1205w
1140w	1090m	1092m	1098s	1205w	1100s	1098m	1098s	1186m	-	1175s	1100m
1095m	1075s	1078m	1080sh	1106w	1080w	1077w	1080w	1100m	1100s	1100m	1078w
1072m	1035m	1040m	1042sh	1085w	1042w	1039w	1044w	1079s	1080w	1078w	1045w
1001s	998s	1004s	1005vs	1042w	1005s	1009s	1005m	1047m	1042w	980m	1005m
997m	945s	981s	980s	1008w	964s	918m	958m	1005s	1004m	958m	965m
962m	868s	865s	865s	981m	868s	863m	868m	967m	965m	896s	865s
884m	-	825m	825m	873w	834m	820s	830m	874m	868m	-	812m
843s	800s	806s	804vs	802w	804vs	800m	800s	823s	818m	784m	800m
803s	780s	776s	775vs	785w	778vs	777w	780s	803s	800s	770m	764s
786s	720vs	712s	730vs	718w	-	725w	730s	780m	780s	706w	724s
754m	665w	690m	684m	687w	682m	681m	678m	730m	730s	664m	670w
692w	-	651w	650w	628w	650w	639w	645w	688w	678m	650m	650w
620m	605w	-	610w	616w	618s	614w	610w	650w	645w	-	625w

595m	-	602m	600s	602w	600s	583m	580m	603w	608w	593w	585w
-	-	-	-	551w	555m	535w	-	583w	580vs	558w	560w
-	-	536w	532sh	475w	470m	456w	468w	539w	535m	465w	460w
-	-	456s	452vs	445w	444vs	449w	438s	462w	468w	448w	454s
-	-	418w	420s	379w	374s	397w	370w	438w	430vs	421w	428w

All experimental results are from [Adimado *et al*]

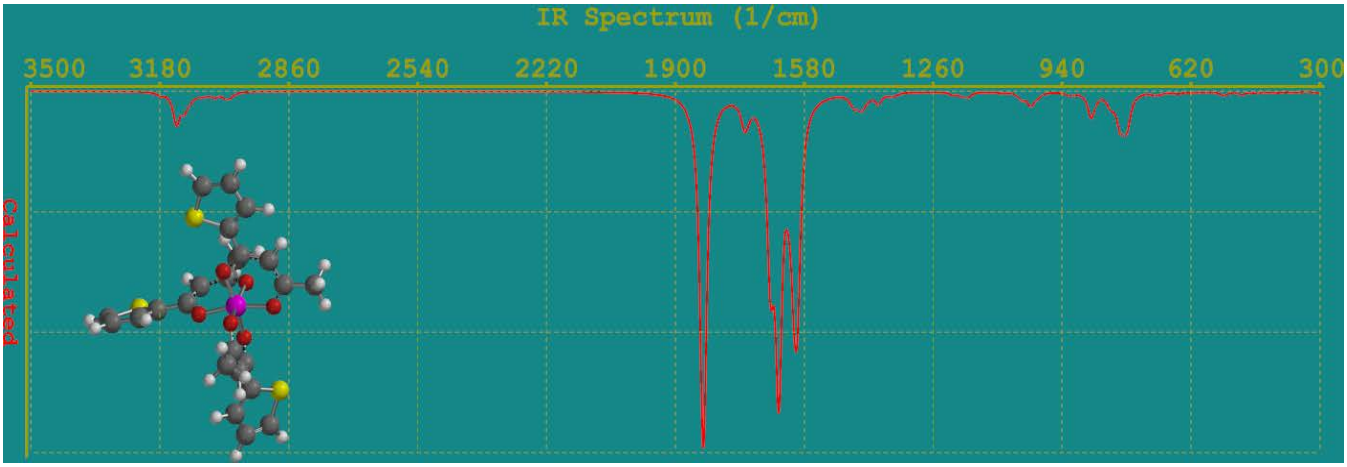

Figure 4.32 Infrared spectrum of $[Al(Htbd)_3]$in the gas as representative of $M(Htbd)_3$ computed at the B3LYP/6-31G* level of theory.

Table4.24 Assignment of the observed vibrational frequencies (cm^{-1}) of 4,4,4 – trifluoro - 1-(2-furyl)-1,3-butanedione (Htftbd) and its metal complexes at the PM3 level of theory.

		Al		Cr		Mn		Fe		Co	
Cal.	Expt.	Cal.	Expt.	Cal.	expt.	Cal.	Expt.	Cal.	Expt.	Cal.	Expt.
1765vs	-	1746s	-	1746s	-	1673vs	1604s	1678vs	-	1635vs	1598vs
1694vs	1655s	1658vs	1600s	1658vs	1600s	1631vs	1595s	1647vs	1603vs	-	1580vs
-	1620s	1630s	1595s	1630s	1575s	1605s	1540s	1574s	1575vs	1544vs	1540s
1551s	1525m	1587vs	-	1587vs	1542s	1567m	-	1565m	1548m	1542s	1518w
1534s	-	1507s	1550s	1507s	1515w	1545m	1460m	1548m	1520w	1522s	-
1526s	1450w	1481m	1515w	1581s	1444m	1481s	1410vs	1493w	1435w	1450m	1435w
1461vs	1420s	1437w	1450m	1464vs	1410vs	1457s	-	1413m	1410vs	1413m	1420vs
1439m	-	1400s	1412vs	1421s	1390sh	-	1358m	1408m	1390w	1405m	1390w
1385m	1365m	1371s	1390m	1379m	1360m	1396 m	1300m	1398s	1360s	1387m	1355s
1315m	1350w	1360s	1365m	1355s	1320s	1356m	-	1370s	1310vs	1383s	1315vs
-	1282w	1329s	1330m	1333m	1264m	-	1260m	1356s	1260m	1372s	1260m
1182m	1260w	1268m	1263s	1260m	1240s	-	1240s	-	1240m	-	1240m
1177w	1200m	1190m	1200s	1247w	1205s	1202m	1200m	1145m	1204m	1211w	-
-	1130w	1151m	1150s	1150w	1140s	1144m	1140m	1114s	1145s	1205w	1202s
1108s	1100m	1095m	1090w	1088m	1090w	1091w	1090w	1086m	1088w	1200w	1145s
1074m	1070w	1073m	1072s	1101s	1072s	1085s	1060s	1079w	1072s	1166w	1088w
1054w	-	1034w	1045w	1079m	1045w	1076m	-	1008w	1045w	1078w	1072s
-	-	1029w	1028w	1001w	1022w	-	1005m	1005w	1020m	1076m	1045w
-	984s	934s	950vs	989s	944vs	936s	938vs	-	-	1016w	1022w
885m	940m	928s	-	-	-	927s	-	948m	942vs	958s	950vs
860vs	862vs	858s	867s	864s	868s	892m	868s	851s	865s	881s	865s
830m	805m	797w	798vs	796s	795vs	822m	800vs	818m	800vs	843m	795vs
796m	765sh	781w	780m	786m	780m	800m	778m	778w	778m	784w	785vs
775s	740s	756s	758m	767m	758w	779m	758w	-	758w	770m	758w

-	-	730m	730m	749m	732m	706m	735s	733w	735vs	706s	728vs
692s	680m	691m	695m	697m	695m	697m	690m	694m	692m	703m	700m
670m	635s	637s	660s	672s	668s	658m	655s	650m	650vs	650m	630w
565m	610w	607s	604s	604s	604vs	599s	600vs	597w	598vs	603m	605s
-	580w	559m	565w	559s	552m	546s	542s	551m	540m	549w	550w
-	-	473m	465w	469w	468vw	466w	465vw	461 w	465vw	464w	-
-	-	429w	428vs	444w	-	-	-	-	-	465m	465vw
-	-	415w	-	-	410s	408w	392m	379m	382m	421m	435m
-	-	375w	375s	374w	350m	340w	340m	340w	342m	348w	352m

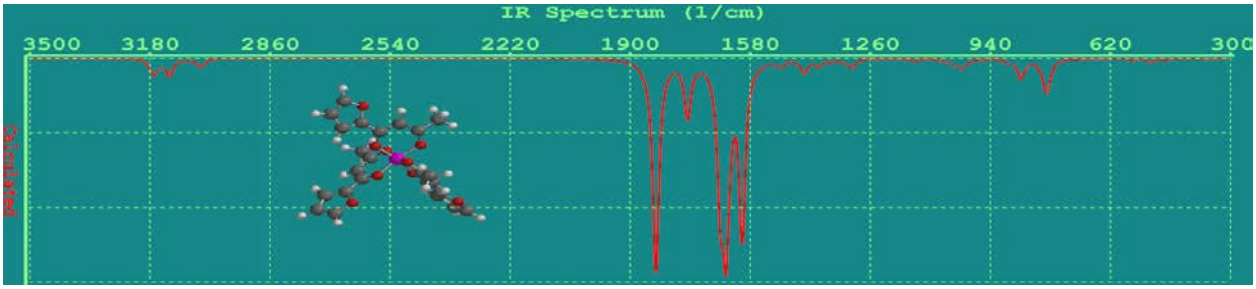

Figure 4.33 Infrared spectrum of [Al(Htftbd)$_3$] in the gas phase as representative of M(Htftbd)$_3$computed at the PM3 level of theory.

4.30 Acetylacetonate (acac), trifluoroacetylacetonate (tfac) and hexafluoroacetylacetonate (hfac) metal complexes.

One of the most powerful ways of dealing with normal modes, especially of complex molecules, is to classify them according to their symmetries. For the above complexes studied, acetylacetonate (acac) and hexafluoroacetylacetonate (hfac) chelates had D_3 symmetry whilst trifluoroacetylacetonate (tfac) chelate had a symmetry point group of C_1. There exists only a slight change in energy with changes in fluorine content in the acetylacetonate ligand. Wexler and Zink [Wexler and Zink, 1996] explained these small shifts to be caused by the perturbations on the π orbital energies by the substitutes CF_3 groups.

4.31 Relevant IR vibrational frequencies (cm^{-1})

Table4.25 Assignment of the observed vibrational frequencies (cm^{-1}) of Hexafluoroacetylacetone (hfac) and its metal complexes.

Ligand	Al	Cr	Mn	Fe	Co
1978s	1870vs	1712s	1815vs	1740w	1809vs
1864vs	1653vs	1632s	1655s	1686vs	1634vs
-	1606s	1586s	1617m	1588s	1575s
1565m	1572w	1571w	1575m	1574m	1573m
1537s	1569w	1569w	1567m	1568m	1554m
1535w	1548w	-	1555w	1566w	1552w
1517m	1545w	-	1501w	1491w	1524w
-	-	-	1487w	1486w	1490w
-	1392m	1395m	1423m	1466m	1409m
-	1375w	1391m	1380w	1382w	1380w
1389w	-	1348m	1364m	1371w	1377w
1386s	1318w	1324w	1303m	1320w	1320w
1286m	-	1249s	1255m	1295m	1311w
1212s	-	-	1248m	1278m	-
-	1196w	1128w	1197w	1181w	1168w
-	-	1104w	1176w	1173w	1008w
-	-	1000w	-	1024w	994w
-	-	986w	978w	984w	978w
-	960w	949w	960w	977w	908w
-	868m	901w	898w	900w	898w
-	861w	888w	877w	888w	875w
837m	778m	833w	827w	878w	-
769m	738w	703w	757w	797w	697w
721w	704w	696w	702w	702w	693w
697w	699w	691w	699w	695w	613w
658m	657w	625w	661w	676w	609w
620w	630w	578w	643w	631w	561w
549w	589w	553w	604w	613w	553w
-	512w	511w	579w	574w	529w
-	477w	468w	547w	486w	472w
-	405w	427w	426w	465w	414w
-	340w	342w	353w	365w	355w

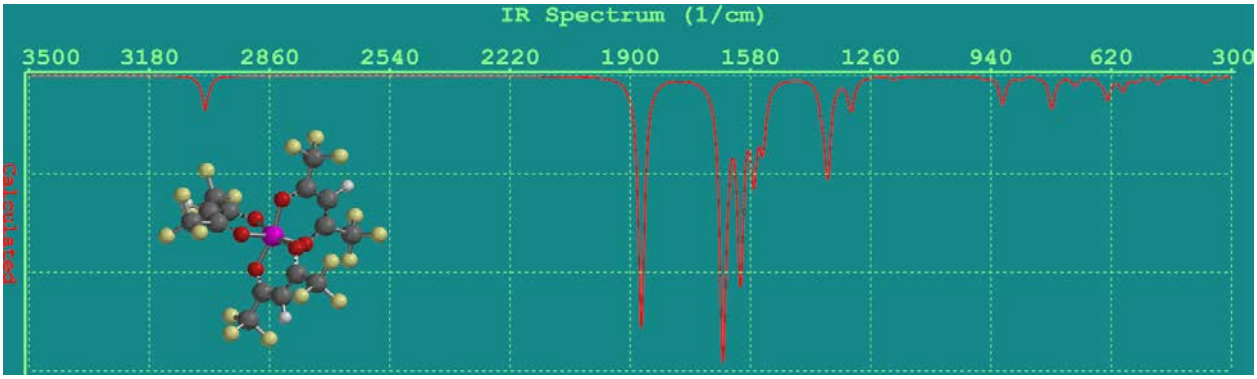

Figure 4.34. Infrared spectrum of $Al(hfac)_3$ in the gas phase as representative of $M(hfac)_3$ computed at the B3LYP/6-31G* level of theory.

4.32 UV SPECTRA

The UV spectrum of the Hexafluoroacetylacetone ligand show two broad bands with maxima at 175.35 and 267.51nm due to the various n → π* and π → π* transitions. Trifluoroacetylacetone (tfac) has its maxima at 222.36 and a shoulder around 310nm. These absorption maxima on complexation shifted appreciably to higher wavenumbers. Trifluoroacetylacetone on complexation showed two distinct bands that had shifted both bathochromically and hypochromically with their absorption maxima at 365.95nm and 371.89nm.

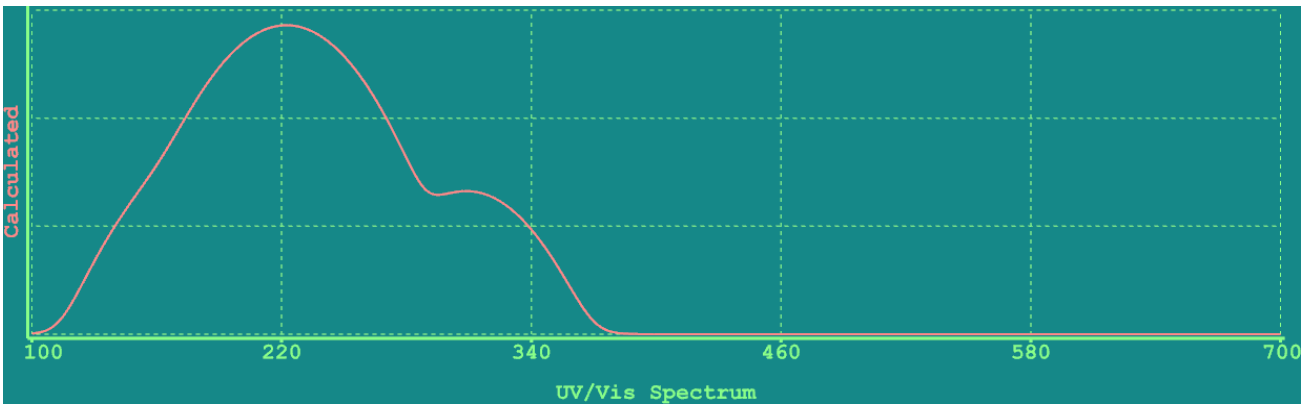

Figure 4.35 UV spectrum of free tfac in the gas phase computed at the B3LYP/6-31G* level of theory.

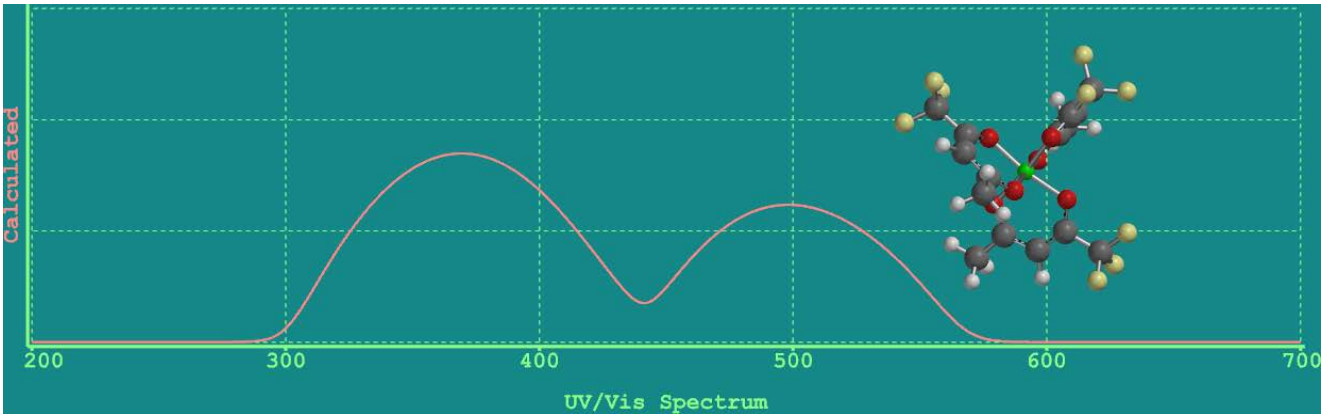

Figure 4.36 UV spectrum of $Co(hfac)_3$ in the gas phase computed at the B3LYP/6-31G* level of theory.

4.40 4,4,4-trifluoro -1- (2-thienyl)-1,3-butanedione (Htftbd), 4,4,4 - trifluoro-1-(2-furyl)-1,3-butanedione (Htffbd), 4,4,4-trifluoro-1-phenyl-1,3-butanedione (Hbztfac) and 4,4,4 - trifluoro –1-(3-pyridyl) -1,3 - butanedione (tfpybd) metal complexes.

4.41 Relevant IR vibrational frequencies (cm^{-1})

The IR spectra of the complexes in the region 1850-1500cm^{-1} is characterized by the presence of three strong bands at ≈ 1720, 1654 and 1587cm^{-1} assignable respectively to the asymmetric stretching modes of C = O, C = C = C and that from the aromatic rings. Eshraq found that the calculated vibrational modes at 1601cm^{-1} and 1581cm^{-1} at the HF and the B3LYP levels of theory, respectively, can be attributed to the stretching mode of the C = C and the C = O groups, υ(C = C), υ(C = O), in the enolic form [Eshraq, 2007].The coupled vibrations of C = O and C = C are observed between 1581-1540cm^{-1} for all the complexes. The weak bands that appeared between 1377-1340cm^{-1} and 1333-1324cm^{-1} are assigned to the symmetric stretches of the C = O and C = C = C respectively.

Between 1322-1236cm^{-1} and 1222-1216cm^{-1} are assigned respectively to the coupled vibrations from the in-plane and out-of- plane C-CF_3 and C-C + C-R. The in-plane pyridine stretching modes of vibrations are observed at 1109-1021cm^{-1} region of the spectrum.

The CH out-of-plane, CF_3 in-plane and C-R stretching vibrations respectively appear at 940-827 cm^{-1}, 807-791cm^{-1} and 786-691cm^{-1}. Deformations of the chelate ring and M - O bands are observed at 682-589$cm^{-1}$and the vibrations of the chelate ring appear at 539-510cm^{-1}.

The M-O stretching vibrations are weak and are observed between 476-321cm^{-1} regions of the spectra. For comparison, the fundamental expterimental frequencies and corresponding calculated vibrational frequencies at the PM3 level of theory are given in Table 4.26.

Table 4.26 Assignment of the observed vibrational frequencies (cm^{-1}) of 4, 4, 4 - trifluoro –1-(3-pyridyl) -1,3 - butanedione (tfpybd) and its metal complexes.

Ligand		Al		Cr		Mn		Fe		Co	
Cal.	Expt	Cal.	Expt	Cal.	Expt	Cal.	Expt	Cal.	Expt	Cal	Expt
1654s	1645s	1618s	1620m	1587vs	1600s	1639vs	1620s	1618s	1615s	1647s	1618s
1615vs	1615s	1570vs	1580m	1556s	1570s	1580vs	1580m	1581vs	1575m	1581vs	1580m
1570vs	1540m	1539s	1550m	1535m	1545m	1545s	1542s	1542m	1542m	1543s	1542m
1532vs	1524s	1516vs	1515w	1488m	1485m	1487m	1480s	-	1485w	1495m	1480m
1461s	1444s	1422vs	1475s	1428m	1446vs	1465m	1425m	1447s	1450s	1413s	1428m
1430s	1390w	1396s	1390w	1390s	1390w	1397s	1390w	1392m	1390w	1391m	1390w
1372m	1322m	-	1320s	1315s	1315vs	-	1305vs	1359m	1310s	-	1305vs
1334s	1300vs	1264vs	1265s	1234vs	1265s	1245m	1265m	1271s	1260m	1266m	1262m
1204vs	1230s	1215vs	1205s	1220s	1210s	1195s	1205s	1209s	1200s	1219m	1210s
1183s	1185m	1159s	1150s	1157m	1155s	1147vs	1148vs	1150vs	1150s	1146s	1145s
1142m	1140s	1100m	1100m	1142m	1130w	1102m	1105w	-	1125sh	-	-
1095m	1068m	1080m	1080m	1093m	1085m	1078s	1082s	1094m	1090w	1079m	1082m
1005m	1010w	1053s	962s	1037s	1028m	-	1048s	-	1025w	1045w	1050m
943m	948m	965w	940w	955m	955s	1039s	1038s	949m	950m	1040m	1035sh
891m	925m	943w	830sh	850m	818sh	953m	950m	845m	840m	956m	950m
831w	835m	825m	815m	813w	-	810m	810m	817m	812m	824w	835w
799m	790m	790m	790m	788s	795vs	807s	795s	777s	788s	819s	790vs
735s	775vs	743w	760m	747m	740m	736m	740m	749m	736m	-	740sh
710vs	730s	722m	728m	730m	724m	725m	730m	-	724m	-	725m
674m	720vs	700m	702m	707m	700m	668s	705s	705s	700m	707m	705s
653m	670m	664s	664s	670s	670s	-	658vs	660s	656s	690s	660s
637m	645vs	632s	608m	605m	605vs	643s	642m	619m	620w	643m	645m
598s	620vs	587m	570sh	587m	570m	594vs	585vs	615s	594m	605m	590m
-	575s	530w	530w	533m	530w	519m	525m	528m	535m	548m	530m
498m	485m	428w	425m	451w	460w	476m	480w	472m	480w	484m	450m
-	-	394w	398m	420m	420m	427w	442m	443w	405w	410w	415m
-	-	376w	375m	371w	365m	385w	380m	333w	330w	404w	405w
-	-	347w	350m	347w	342m	341w	340m	-	310w	348w	350m

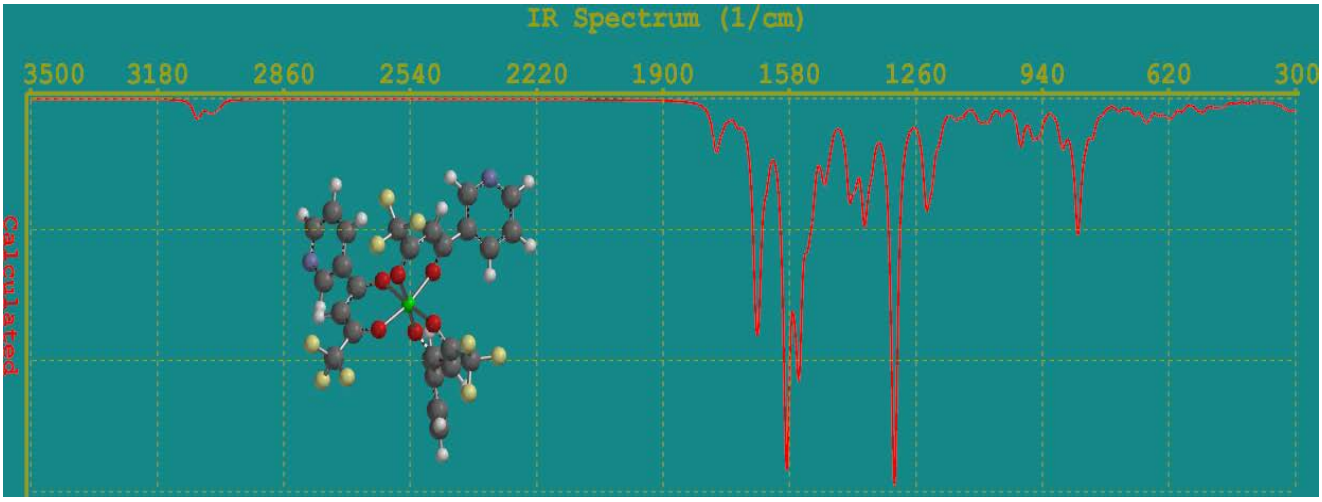

Figure 4.37.Infrared spectrum of $Cr(tfpybd)_3$ in the gas phase as representative of $M(tfpybd)_3$ computed at the PM3 level of theory.

4.50 1-phenyl-3-(2-thienyl)-1,3-propanedione (Htbzac), 1-(2-furyl)-3-phenyl-1,3-propanedione (Hfpa) and dibenzoylmethane (Hdbm) metal complexes.

4.51 Relevant IR vibrational frequencies (cm^{-1})

These compounds have aromatic substituents with one arm having either O or S as a heteroatom in the ring and the other side been a phenyl group. The calculated frequencies at the PM3 level of theory show the C = O and C = C stretching modes, ν(C = O) and ν(C = C) at 1678cm^{-1} in the IR spectrum. The movement of the stretching mode of the C = O group appears at 1635 for asymmetric stretching mode and at 1536cm^{-1} for symmetric stretching mode for the aluminium complexes. The vibrational mode at 1322cm^{-1} is assigned to the in plane bending of the methyne group, δ (CH). The band at 986cm^{-1} is assigned to the inplane bending of the C = CH - C group, δ (C = CH - C). The vibrational mode at 645cm^{-1} is assigned to the inplane deformation of the ring, Δring. The M – O frequencies are weak and observed at 399cm^{-1}.

Table4.27 Assignment of the observed vibrational frequencies (cm^{-1}) of dibenzoylmethane (Hdbm) and its metal complexes.

Ligand	Al	Cr	Mn	Fe	Co
1689vs	1678vs	1662vs	1660vs	1680vs	1665vs
1586vs	1635vs	1647vs	1614vs	1641s	1621vs
1573vs	1605vs	1604vs	1609s	1605vs	1579s
1536vs	1595vs	1578s	1597s	1580vs	1575m
1351m	1581vs	1572s	1541s	1552m	1544m
1336w	1538s	1539vs	1538m	1538m	1538m
1312w	1533m	1485s	1534m	1512m	-
1300w	1455m	1442m	1452m	1453m	1470m
1228vw	1373w	1340m	1377m	1345m	1344w
1166vw	1330w	1332m	1333m	1324m	1332w
1156w	1322m	1320m	1320m	1320m	1323w
1127w	1255vw	1237m	1237w	1251w	1255w
1113w	1227vw	1224m	1227w	1227w	1229w
1032w	1224vw	1217w	1225w	1216w	1222w
1007w	1107vw	1101w	1106w	1104w	1109w
940m	1044vw	1043w	1041w	1043w	1044w
928m	1029vw	1021w	1030w	1022w	1029w
842m	986w	984w	988w	985w	986w
828m	872m	864m	869m	870m	877m
751m	830m	829m	827m	854m	830m
648m	803m	807s	801m	791m	800m
636m	763s	774m	786m	781m	785m
611m	709s	722m	706m	705m	709m
-	700m	691m	701m	700m	703m
-	678s	676m	668m	678m	673m
-	646m	645m	65m	655m	650m
-	617m	589w	618w	595w	610w
-	539m	520w	536w	526w	537w
-	509w	509w	501w	516w	510w
-	437w	456w	440w	476w	446w
-	399w	401w	391w	321w	394w

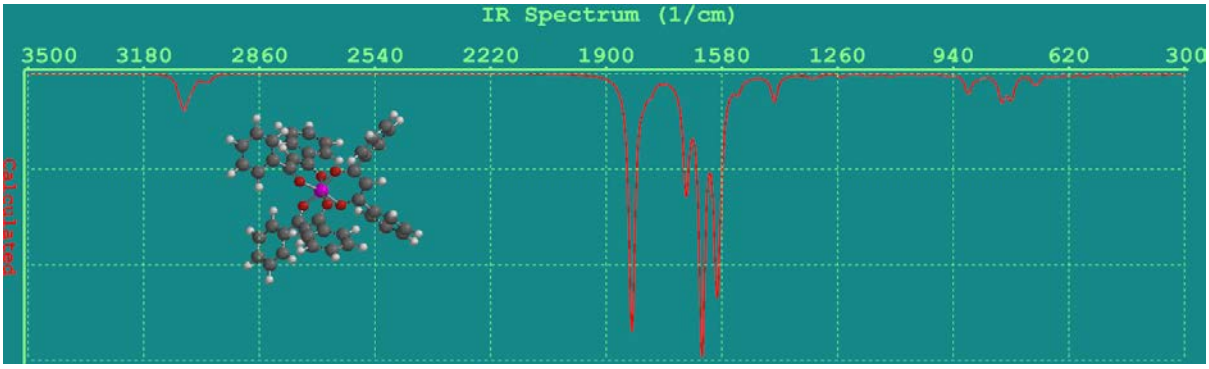

Figure 4.38.Infrared spectrum of $Al(Hdbm)_3$ in the gas phase as representative of $M(Hdbm)_3$computed at the PM3 level of theory.

4.60 COMPARISON BETWEEN PM3 AND DFT OPTIMIZED ENERGIES OF SOME COMPLEXES.

The enthalpy of formation values can reveal information about the stability of a compound. In general, compounds having high energy content tend to be unstable due to increased motion of constituent particles. Such systems tend to lose energy in order to attain stability.

Tables 4.28(a and b) below presents the relative formation energies and dipole moments for the structures studied in kJ/mol. On CF_3 substitution, the transitions occur at lower energies [Patel and Adimado, 1981].The results from the tables show that the lowest energy structures are the $M(hfac)_3$. As can be seen from table 4.28a and table 4.28b, the PM3 and B3LYP results are substantially different. It is known [Jalbout *et al.*, 2004] that PM3 and B3LYP methods give similar geometries, but rather different energies, as is apparent from the tables 4.28(a and b).It is logical since the DFT method has electron correlation which exceeds PM3 in energetic computations. Therefore, it can be expected that differences should exist which are observed as such. The general trend of the complexes in terms of stability with respect to the heat of formation irrespective of the central metal is $M(hfac)_3$> $M(tfac)_3$> $M(Htffbd)_3$> $M(Htfbzac)_3$ > $M(Htftbd)_3$> $M(acac)_3$> $M(Hfbd)_3$> $M(Hbzac)_3$> $M(Hfpa)_3$> $M(Htbd)_3$> $M(Hftpd)_3$> $M(Hdbm)_3$> $M(Htpd)_3$> $M(Htbzac)_3$> $M(Dhfpd)_3$. The order clearly shows that the fluorinated derivatives of the betadiketonates studied form the most stable complexes.

For the aromatic substituents, the furyl groups form more stable compounds than the phenyl groups which are also more stable than the thienyl ring complexes. This could probably be attributed to a more electronegative oxygen atom in the furyl ring than sulphur in the thienyl ring.It was exptected that an increase in the dipole moment of the compounds should lead to the formation of a less stable structure but the observed moments and the associated energies do not exhibit a regular trend for some of the complexes.

Table 4.28a Calculated Enthalpy of formation ($kJmol^{-1}$) and dipole moment (Debye, D) of Aluminium, Iron and Manganese complexes at the PM3 and B3LYP/6-31G* level of theory.

	ΔH^0f				ΔH^0f			ΔH^0f	
Comp.	PM3	B3LYP	μ(D)	Comp.	PM3	μ(D)	Comp.	PM3	μ(D)
$Al(acac)_3$	-1560	-3355559	0.00	$Fe(acac)_3$	-1740	0.72	$Mn(acac)_3$	-1396	0.01
$Al(tfac)_3$	-3377	-5673302	4.35	$Fe(tfac)_3$	-3433	3.90	$Mn(tfac)_3$	-3116	3.65
$Al(Htbd)_3$	-983	-	1.04	$Fe(Htbd)_3$	-1266	3.86	$Mn(Htbd)_3$	-724	1.07
$Al(Hfbd)_3$	-3243	-4821760	9.23	$Fe(Hfbd)_3$	-1702	5.17	$Mn(Hfbd)_3$	-1173	1.06
$Al(Hbzac)_3$	-1104	-4838103	0.11	Fe $(Hbzac)_3$	-1394	3.62	$Mn(Hbzac)_3$	-850	0.92
$Al(hfac)_3$	-5133	-8008691	0.00	$Fe(hfac)_3$	-5098	0.63	$Mn(hfac)_3$	-4840	0.64
$Al(Htftbd)_3$	-2794	-9696984	5.15	$Fe(Htftbd)_3$	-2995	9.34	$Mn(Htftbd)_3$	-2549	4.52
$Al(Htffbd)_3$	-3243	-	9.23	$Fe(Htffbd)_3$	-3444	10.92	$Mn(Htffbd)_3$	-2995	9.63
$Al(Htfbzac)_3$	-1104	-4838103	0.11	$Fe(Htfbzac)_3$	-3106	7.44	$Mn(Htfbzac)_3$	-2678	4.83
$Al(Hftpd)_3$	-856	-	1.13	$Fe(Hftbd)_3$	-1143	5.57	$Mn(Hftpd)_3$	-615	1.74
$Al(Htbzac)_3$	-511	-	2.20	$Fe(Htbzac)_3$	128	14.44	$Mn(Htbzac)_3$	-290	2.17
$Al(Hfpa)_3$	-976	-	0.60	$Fe(Hfpa)_3$	-1266	6.27	$Mn(Hfpa)_3$	-736	1.29
$Al(Htpd)_3$	-3	-	0.36	$Fe(Htba)_3$	460	6.45	$Mn(Htpd)_3$	-197	2.24
$Al(Dhfpd)_3$	-1304	-6305667	0.58	$Fe(DHfbd)_3$	466	3.40	$Mn(Dhfpd)_3$	-1058	1.54
$Al(Hdbm)_3$	-649	-	0.36	$Fe(Hdbm)_3$	-965	5.23	$Mn(Hdbm)_3$	-414	1.38

Table 4.28b Calculated Enthalpy of formation ($kJmol^{-1}$) and dipole moment (Debye, D) of the complexes at the PM3 and B3LYP/6-31G* level of theory.

	$\Delta H^{\theta}f$				$\Delta H^{\theta}f$	
Comp.	PM3	B3LYP	μ(D)	Comp.	PM3	μ(D)
$Co(acac)_3$	-7975	-3080613	0.00	$Cr(acac)_3$	-347	0.00
$Co(tfac)_3$	-9786	-	4.28	$Cr(tfac)_3$	-2070	5.00
$Co(Htbd)_3$	-7405	-	1.42	$Cr(Htbd)_3$	186	1.29
$Co(Hfbd)_3$	-7856	-	0.75	$Cr(Hfbd)_3$	-270	0.94
$Co(Hbzac)_3$	-7531	-	0.11	Cr $(Hbzac)_3$	63	1.32
$Co(hfac)_3$	-11537	-	0.00	$Cr(hfac)_3$	-3686	0.00
$Co(Htftbd)_3$	-9213	-	5.62	$Cr(Htftbd)_3$	-1530	4.23
$Co(Htffbd)_3$	-9663	-	10.07	$Cr(Htffbd)_3$	-1984	10.49
$Co(Htfbzac)_3$	-9341	-	4.80	$Cr(Htfbzac)_3$	-1656	2.31
$Co(Hftpd)_3$	-7289	-	0.83	$Cr(Hftbd)_3$	289	1.24
$Co(Htbzac)_3$	-6204	-	18.31	$Cr(Htbzac)_3$	276	7.92
$Co(Hfpa)_3$	-7411	-	0.55	$Cr(Hfpa)_3$	-170	2.79
$Co(Htpd)_3$	-6840	-	0.90	$Cr(Htba)_3$	753	1.00
$Co(Dhfpd)_3$	-6065	-	9.08	$Cr(DHfbd)_3$	-161	0.68
$Co(Hdbm)_3$	-7089	-	0.03	$Cr(Hdbm)_3$	503	0.65

4.70 A Plot Of Molecular Weight Against ΔH^{θ}_{f} forM(Betadiketonate)$_3$ Complexes With Different Metal Centers

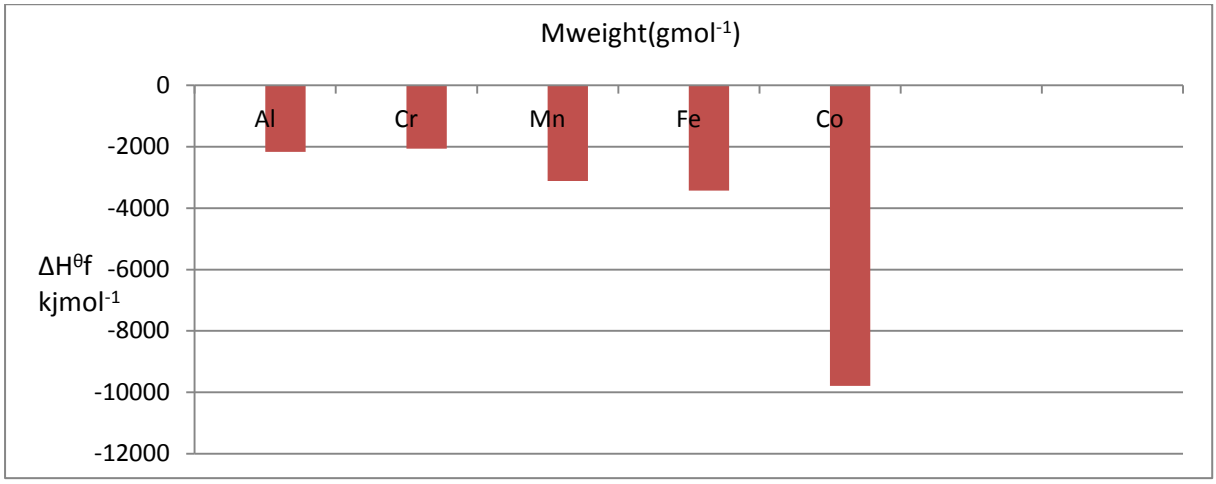

Figure 4.39 M(Hbd)$_3$.

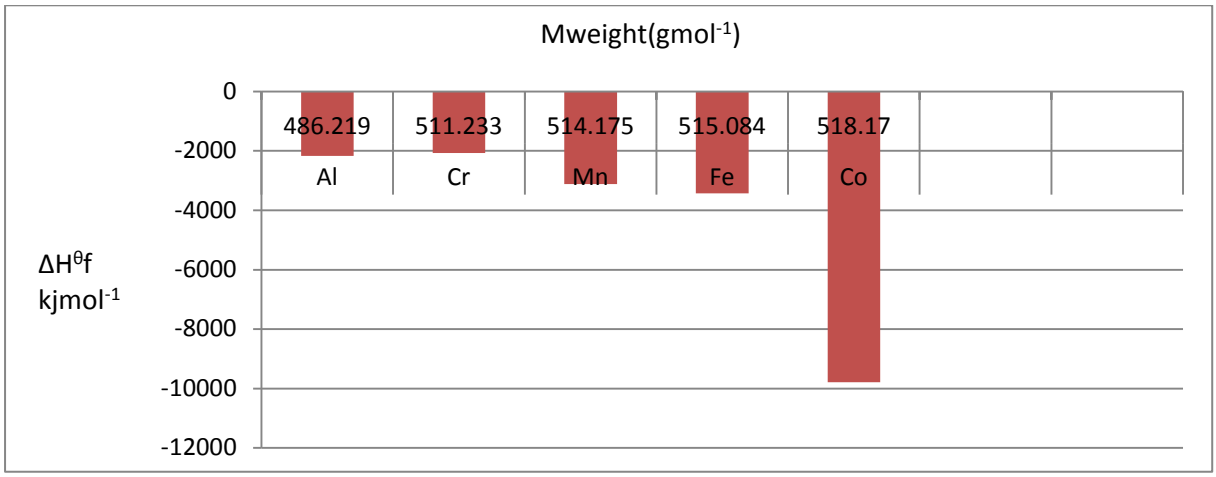

Figure 4.40 M(Hfac)$_3$

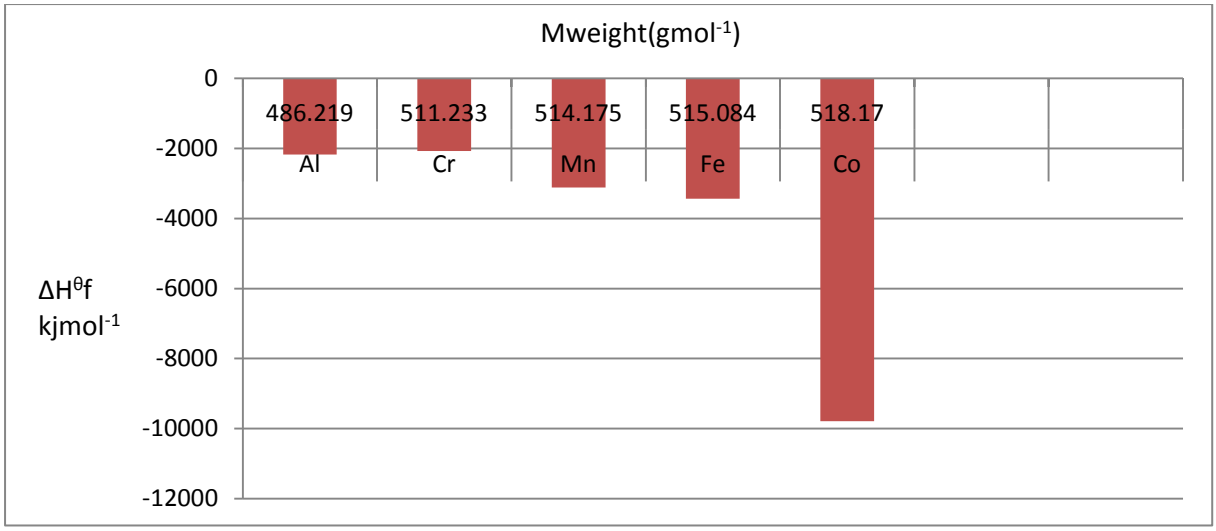

Figure 4.41 $M(Hdbm)_3$

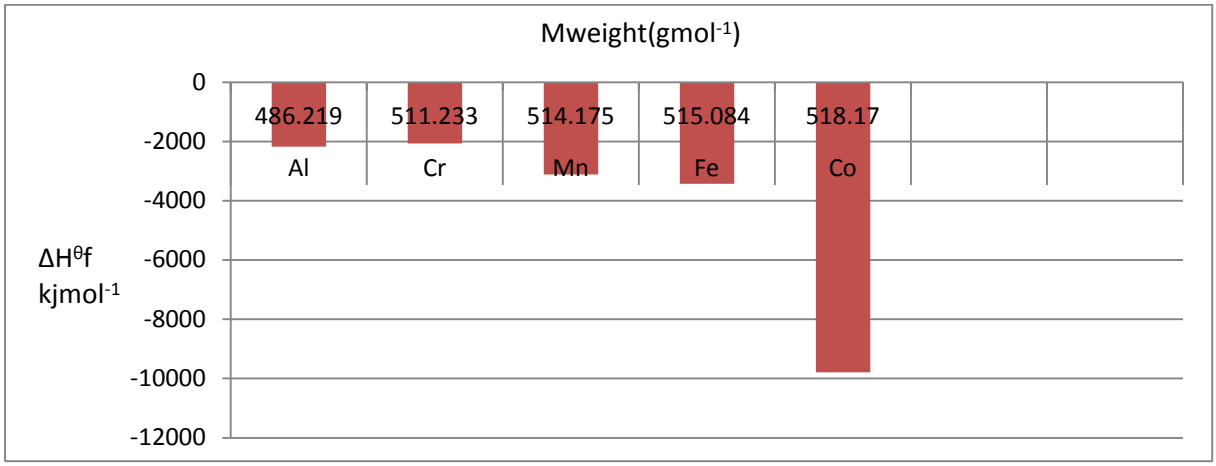

Figure 4.42 M $(Dhtbd)_3$

4.80 A Plot of Molecular Weight of Metal Complexes against $\Delta H^{\theta}f$ for Different Substituents with the Same Metal Centre.

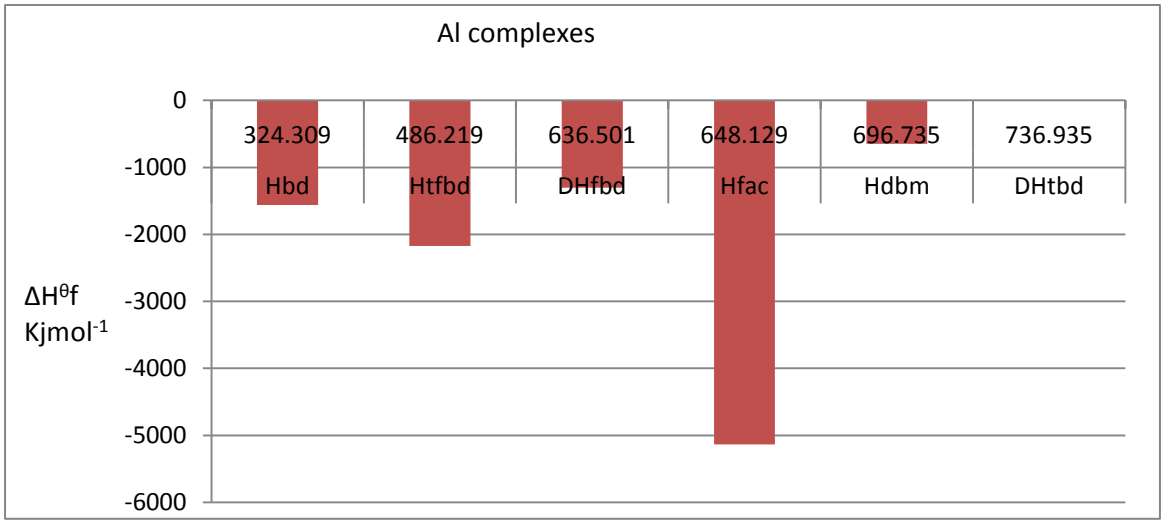

Figure 4.43 Al complexes

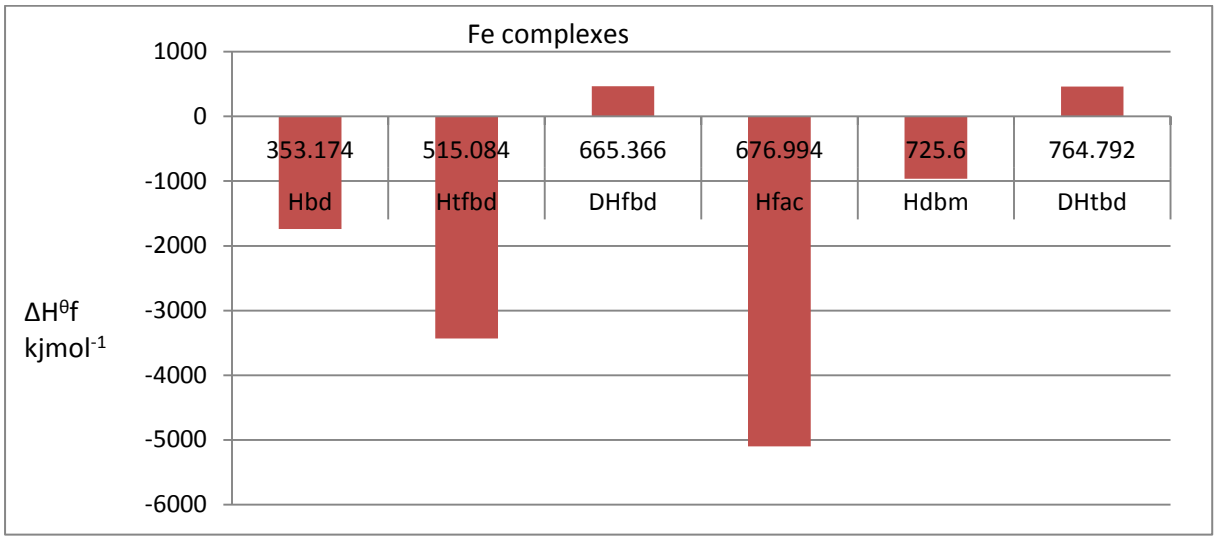

Figure 4. 44 Fe complexes

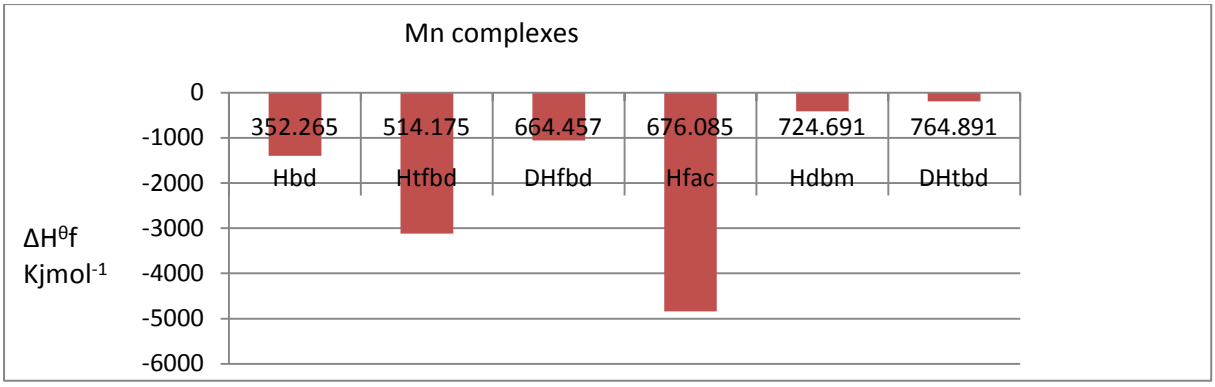

Figure 4.45 Mn complexes

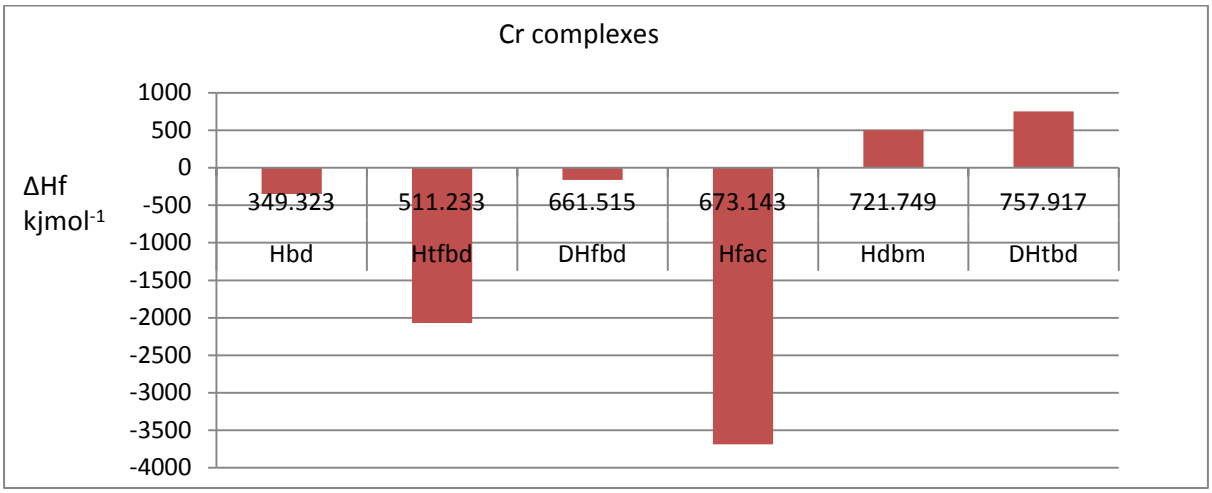

Figure 4.46 Cr complexes

4.81 STRUCTURAL CORRELATION BETWEEN CALCULATED ΔH^{θ}_{f} VALUES.

One major problem in modeling these complicated metal organic systems is calculation of metal contribution in intermolecular interactions. With the transition metals, availability of empty d- orbitals and the trend of Crystal Field Stabilization Energy (CFSE) [Hancock and Thornton, 1970] aids in the formation of covalent bonds.

From the tables of reported results, it can be seen that acac, tfac, hfac group of ligands provide a measure of the effect of the enthalpy of formation with fluorine substitution. An increase in the fluorine content leads to the release of a higher amount of energy (ie.

ΔH^{θ}_{f} is more negative). In table 4.28b, it is seen that the ΔH^{θ}_{f} for the acac, tfac and hfac complexes are -7975 kjmol^{-1},-9785 kjmol^{-1}and -11537 kjmol^{-1} respectively at the PM3 level of theory. Thus hfac > tfac > acac in volatility [Bradley and Andrew, 2000]. The number of d-electrons for the transition metals studied are d^3, d^4, d^5 and d^6 for Cr(III), Mn(III), Fe(III) and Co(III) respectively. The complexes with aromatic substituent's furyl, thienyl, and phenyl rather have a lower ΔH^{θ}_{f} values (less exothermic) when compared to the fluorinated substituent's. This could be explained based on the electron withdrawing ability of fluorine and the resonance effect by the aromatic rings. Replacement of one CH_3 (per ligand) with CF_3 results in an increase in ΔH^{θ}_{f} by an appreciable amount irrespective of the metal at the centre. There is a further increase in ΔH^{θ}_{f} upon substitution of the second CH_3 group. It may be seen clearly that the oxidation state of the metal determines the quantum of decrease in ΔH^{θ}_{f}.

The Tables4.24-4.30below containing the results of intramolecular distances and bond angles reveal that for the fluorinated complexes, the bond distance increases with increasing fluorine content and this causes a decrease in the bond angles of the complexes. Increasing CF_3 substitution opens up the O…C…C bond angle and closes up that of C…C…C, C…O…M and O…M…O. However, the extent of closure is not as appreciable as the angle opening. ΔH^{θ}f values for the M(β - dike)$_3$ complexes indicates that Co(acac)$_3$ should have the greatest intramolecular interactions. For the Co(acac)$_3$complex, the closest interaction is the C…O = 1.310 Å and an O…C…C bond angle of 124.04°. For the Fe(acac)$_3$ complex, the closest C…O distance is 1.307Å with an O…C…C angle of 122.60°.

The large inductive effect created by CF_3 groups should give rise to a significantly different charge distribution in the chelate ring and a correspondingly different co-ordination sphere in fluorinated derivatives relative to acac complexes [Watkins, 1978].

Since the structures of the Al, Fe, Mn, Cr, and Co acetylacetonate complexes are isomorphous, it would be exptected that their behavior should be related to the molecular weight of the complex [Bradley and Andrew, 2000]. The trend of the molecular weight and ΔH^{θ}_{f} displayed in figures 4.8- 4.20 above shows that the d^n transition metal complexes exhibit a non-linear correlation. Since similar molecular weights give very different ΔH^{θ}_{f} values, it indicates that molecular weight is relatively unimportant, but the nature and degree of the intermolecular interactions are likely to be predominant factors in the ΔH^{θ}_{f} for these complexes. Because the properties and stabilities of metal complexes are highly tunable through variation of the metal ion, the ligand set, and other molecular parameters [Felipe *et al*., 2008], it makes the coordinate bond a remarkably versatile platform for macromolecular assembly.

Table 4.29 Calculated Average bond distances (Å) and molecular weight of Aluminium (III) and Manganese (III) complexes.

Complex	C=O	C=C	M-O	Mweight	Complex	C=O	C=C	M-O	Mweight
$Al(acac)_3$	1.266	1.401	1.854	324.309	$Mn(acac)_3$	1.282	1.401	1.974	352.265
$Al(tfac)_3$	1.262	1.414	1.854	648.129	$Mn(tfac)_3$	1.283	1.398	1.975	514.175
$Al(Htbd)_3$	1.267	1.403	1.560	486.219	$Mn(Htbd)_3$	1.293	1.406	1.978	556.562
$Al(Hfbd)_3$	1.264	1.387	1.854	480.405	$Mn(Hfbd)_3$	1.291	1.400	1.924	508.361
$Al(Hbzac)_3$	1.267	1.402	1.852	510.522	$Mn(Hbzac)_3$	1.294	1.406	1.979	538.478
$Al(hfac)_3$	1.258	1.396	1.858	648.129	$Mn(hfac)_3$	1.274	1.394	1.955	676.085
$Al(Htftbd)_3$	1.262	1.384	1.856	691.524	$Mn(Htftbd)_3$	1.286	1.400	1.924	718.472
$Al(Htffbd)_3$	1.264	1.387	1.854	642.315	$Mn(Htffbd)_3$	1.289	1.400	1.975	670.271
$Al(Htfbzac)_3$	1.267	1.402	1.852	672.432	$Mn(Htfbzac)_3$	1.286	1.398	1.924	700.388
$Al(Hftpd)_3$	1.267	1.267	1.850	734.919	$Mn(Hftpd)_3$	1.291	1.401	1.921	712.658
$Al(Htbzac)_3$	1.266	1.403	1.852	715.827	$Mn(Htbzac)_3$	1.293	1.405	1.953	743.783
$Al(Hfpa)_3$	1.268	1.405	1.851	666.618	$Mn(Hfpa)_3$	1.293	1.401	1.922	694.574
$Al(Htpd)_3$	1.275	1.402	1.844	736.935	$Mn(Htpd)_3$	1.281	1.402	1.970	764.891
$Al(Dhfpd)_3$	1.266	1.404	1.854	636.501	$Mn(Dhfpd)_3$	1.298	1.406	1.976	664.457
$Al(Hdbm)_3$	1.266	1.401	1.853	696.735	$Mn(Hdbm)_3$	1.289	1.400	1.923	724.691

Table 4.30 Calculated Average bond distances (Å) and molecular weight of Cobalt (III) and Chromium (III) complexes.

Complex	C=O	C=C	M-O	Mweight	Complex	C=O	C=C	M-O	Mweight
$Co(acac)_3$	1.310	1.396	1.871	356.260	$Cr(acac)_3$	1.310	1.396	1.871	349.323
$Co(tfac)_3$	1.559	1.400	1.894	518.170	$Cr(tfac)_3$	1.309	1.400	1.873	511.233
$Co(Htbd)_3$	1.284	1.402	1.894	560.557	$Cr(Htbd)_3$	1.325	1.400	1.876	553.620
$Co(Hfbd)_3$	1.287	1.402	1.893	512.356	$Cr(Hfbd)_3$	1.326	1.400	1.876	505.419
$Co(Hbzac)_3$	1.285	1.402	1.893	542.473	$Cr(Hbzac)_3$	1.322	1.400	1.878	535.536
$Co(hfac)_3$	1.277	1.396	1.894	680.080	$Cr(hfac)_3$	1.301	1.393	1.871	673.143
$Co(Htftbd)_3$	1.283	1.401	1.894	722.467	$Cr(Htftbd)_3$	1.323	1.402	1.874	715.530
$Co(Htffbd)_3$	1.284	1.400	1.893	674.266	$Cr(Htffbd)_3$	1.325	1.400	1.877	667.329
$Co(Htfbzac)_3$	1.281	1.400	1.895	704.383	$Cr(Htfbzac)_3$	1.320	1.403	1.880	697.446
$Co(Hftbd)_3$	1.289	1.403	1.891	716.653	$Cr(Hftbd)_3$	1.329	1.401	1.875	709.716
$Co(Htbzac)_3$	1.291	1.402	1.888	747.778	$Cr(Htbzac)_3$	1.301	1.403	1.894	740.841
$Co(Hfpa)_3$	1.285	1.403	1.892	698.569	$Cr(Hfpa)_3$	1.324	1.401	1.879	691.632
$Co(Htpd)_3$	1.287	1.404	1.892	764.854	$Cr(Htpd)_3$	1.325	1.402	1.876	757.917
$Co(Dhfpd)_3$	1.271	1.401	1.887	668.452	$Cr(Dhfpd)_3$	1.325	1.402	1.879	661.515
$Co(Hdbm)_3$	1.286	1.401	1.893	728.686	$Cr(Hdbm)_3$	1.324	1.400	1.873	721.749

Table 4.31 Calculated Average bond distance (Å) and molecular weight of Iron (III) complexes.

Complex	C=O	C=C	M-O	Mweight
$Fe(acac)_3$	1.307	1.399	1.853	353.174
$Fe(tfac)_3$	1.304	1.400	1.850	515.084
$Fe(Htbd)_3$	1.263	1.500	1.974	557.471
$Fe(Hfbd)_3$	1.307	1.404	1.878	509.270
$Fe(Hbzac)_3$	1.261	1.500	1.979	539.387
$Fe(hfac)_3$	1.287	2.674	1.856	676.994
$Fe(Htftbd)_3$	1.308	1.407	1.878	719.381
$Fe(Htffbd)_3$	1.305	1.400	1.868	671.180
$Fe(Htfbzac)_3$	1.291	1.390	1.862	701.297
$Fe(Hftbd)_3$	1.290	1.471	1.943	713.567
$Fe(Htbzac)_3$	1.274	1.500	1.950	744.692
$Fe(Hfpa)_3$	1.289	1.464	1.941	695.483
$Fe(Htpd)_3$	1.273	1.406	1.887	764.792
$Fe(Dhfpd)_3$	1.306	1.502	1.911	665.366
$Fe(Hdbm)_3$	1.289	1.395	1.874	725.600

Table 4.32 Calculated Average Bond Angles (°) of Aluminium (III) and Manganese (III) complexes.

Comp.	O=C=C	C=C=C	C=O-M	O-M-O	Comp.	O=C=C	C=C=C	C=O-M	O-M-O
$Al(acac)_3$	126.93	125.04	119.06	97.66	$Mn(acac)_3$	128.98	128.87	114.18	104.63
$Al(tfac)_3$	119.03	109.42	109.47	87.94	$Mn(tfac)_3$	127.85	123.75	117.39	95.02
$Al(Htbd)_3$	125.75	127.31	118.40	92.07	$Mn(Htbd)_3$	125.40	122.88	116.01	91.56
$Al(Hfbd)_3$	127.67	124.02	119.24	91.73	$Mn(Hfbd)_3$	128.64	127.60	114.68	96.96
$Al(Hbzac)_3$	126.99	125.19	118.85	93.33	$Mn(Hbzac)_3$	125.33	122.86	115.60	97.12
$Al(hfac)_3$	125.72	127.31	118.40	92.79,	$Mn(hfac)_3$	128.87	124.13	114.06	99.82
$Al(Htftbd)_3$	126.14	127.01	117.98	92.23	$Mn(Htftbd)_3$	129.59	126.72	113.98	96.73
$Al(Htffbd)_3$	129.91	126.65	118.85	92.71	$Mn(Htffbd)_3$	127.29	123.05	116.19	97.01
$Al(Htfbzac)_3$	125.75	126.66	119.17	92.56	$Mn(Htfbzac)_3$	129.53	126.72	114.08	96.53
$Al(Hftbd)_3$	126.37	127.11	119.07	86.51	$Mn(Hftbd)_3$	128.65	127.54	114.46	95.92
$Al(Htbzac)_3$	125.00	126.96	118.23	92.15,	$Mn(Htbzac)_3$	126.55	125.71	110.05	100.89
$Al(Hfpa)_3$	126.21	126.49	118.41	92.61	$Mn(Hfpa)_3$	127.08	124.66	117.18	96.22
$Al(Htpd)_3$	126.25	126.93	118.24	91.65	$Mn(Htpd)_3$	128.92	128.51	114.75	104.76
$Al(Dhfpd)_3$	126.21	126.30	118.74	86.65,	$Mn(Dhfpd)_3$	125.25	122.28	115.37	96.34
$Al(Hdbm)_3$	125.39	125.56	119.63	92.09,	$Mn(Hdbm)_3$	128.71	127.36	114.17	95.44

Table 4.33 Calculated Average Bond Angles (°) of Cobalt (III) and Chromium (III) complexes.

Complex	O=C=C	C=C=C	C=O-M	O-M-O	Complex	O=C=C	C=C=C	C=O-M	O-M-O
$Co(acac)_3$	124.04	120.93	130.26	101.42	$Cr(acac)_3$	122.54	119.77	127.33	89.80
$Co(tfac)_3$	128.65	123.61	118.68	101.54	$Cr(tfac)_3$	124.49	120.76	128.80	90.43
$Co(Htbd)_3$	127.91	124.48	119.05	101.57	$Cr(Htbd)_3$	124.01	122.43	124.22	91.89
$Co(Hfbd)_3$	128.81	124.35	119.22	101.41	$Cr(Hfbd)_3$	124.20	122.10	124.10	91.72
$Co(Hbzac)_3$	127.80	124.44	119.02	101.49	$Cr(Hbzac)_3$	124.09	122.29	124.38	91.58
$Co(hfac)_3$	129.52	122.65	118.49	101.33	$Cr(hfac)_3$	125.40	119.33	130.02	89.59
$Co(Htftbd)_3$	129.52	123.62	118.68	101.60	$Cr(Htftbd)_3$	124.58	121.58	124.25	91.93
$Co\ (Htffbd)_3$	128.76	123.39	118.76	101.52	$Cr(Htffbd)_3$	124.80	121.08	124.08	91.32
$Co(Htfbzac)_3$	128.69	123.63	118.69	101.58	$Cr(Htfbzac)_3$	124.87	121.47	125.03	92.43
$Co(Hftbd)_3$	127.78	124.23	119.16	101.46	$Cr(Hftbd)_3$	124.05	122.25	124.19	91.80
$Co(Htbzac)_3$	127.46	124.70	119.18	101.66	$Cr(Htbzac)_3$	124.29	121.25	130.18	92.04
$Co(Hfpa)_3$	127.95	124.37	119.03	101.63	$Cr(Hfpa)_3$	124.24	122.27	123.87	91.92
$Co(Htpd)_3$	127.56	124.44	119.22	101.67	$Cr(Htpd)_3$	123.93	122.42	124.17	91.83
$Co(Dhfpd)_3$	126.13	124.74	120.38	101.70	$Cr(Dhfpd)_3$	124.09	122.19	124.07	92.02
$Co(Hdbm)_3$	127.71	124.19	118.66	101.54	$Cr(Hdbm)_3$	123.98	122.39	124.48	91.72

Table 4.34 Calculated Average Bond Angles (°) of Iron (III) complexes.

Complex	O=C=C	C=C=C	C=O-M	O-M-O
$Fe(acac)_3$	122.60	123.42	114.87	98.54
$Fe(tfac)_3$	122.92	122.12	115.44	98.94
$Fe(Htbd)_3$	125.22	129.37	108.82	107.30
$Fe(Hfbd)_3$	121.48	121.10	108.83	95.97
$Fe(Hbzac)_3$	107.6	121.40	96.25	107.47
$Fe(hfac)_3$	127.2	126.60	116.34	98.28
$Fe(Htftbd)_3$	114.17	121.33	90.71	97.65
Fe $(Htffbd)_3$	123.17	120.77	111.57	95.28
$Fe(Htfbzac)_3$	126.09	126.17	119.78	97.34
$Fe(Hftbd)_3$	111.96	119.54	91.07	95.51
$Fe(Htbzac)_3$	248.42	126.53	117.69	107.49
$Fe(Hfpa)_3$	112.57	120.43	90.67	95.92
$Fe(Htpd)_3$	120.415	112.64	91.69	102.25
$Fe(Dhfpd)_3$	106.000	114.82	97.155	94.85
$Fe(Hdbm)_3$	124.900	125.64	120.06	104.89

4.90 SEMI-EMPIRICAL PM3 AND DENSITY FUNCTIONAL THEORY (DFT) STUDIES OF MIXED METAL BETADIKETONATES.

4.91 MIXED IRON (III) BETADIKETONATES

4.911 RESULTS AND DISCUSSION

More light has been thrown on the bonding and structural aspects of trivalent metal β-diketonate complexes of Al(III) [Case, 1971, Fortman *et al.*, 1967], Cr(III), Co(III) [Palmer, 1964] and Fe(III) [Adimado,1983]. The bis $(acac)_2$ complexes have been reported to exhibit all the features present in the IR spectra [Gupta and Theriot., 1979]. However, the tris complexes of mixed ligands do not strictly behave in the same manner but with a broadening of bands in the 1600-1550cm^{-1} region for all the complexes [Adimado and Patel, 1983]. The broadening has been exptlained to be due to strong multiple absorptions and the probable superimposition of bands in the region. The theoretical results from this study shown in table 4.34 below for mixed iron (III) betadiketonates, however, reveals the C - O and C - C bands from 1780-1580cm^{-1} region of the spectrum showing some marked differences in IR. The spectra of the complexes with substituents containing a higher number of fluoro groups are well resolved than those without or with fewer fluoro groups. These findings are consistent with experiment.

Table 4.35 some relevant infra red bands (cm^{-1}) for mixed Iron (III) metal betadiketonates computed at the PM3 level of theory.

Compound	$\upsilon_{as\ C-O}$		$\upsilon_{as\ C-C}$		υ_{sM-O}	
	Ext	Cal	Expt	Cal	Expt	Cal
$Fe(fbd)_2(bzac)$	1583	1774	1550	1633	467;430	426
$Fe(fbd)(bzac)_2$	1590	1760	1550	1620	458;427	432
$Fe(tbd)_2(fbd)$	1571	1704	1550	1625	450;432	407
$Fe(tbd)(fbd)_2$	1583	1583	1544	1642	463;430	462;431
$Fe(bzac)_2(tftbd)$	1592	1668	1541	1641	504;433	506;437
$Fe(bzac)(tftbd)_2$	1588	1772	1542	1644	550;458	512
$Fe(bztfac)_2(tftbd)$	1588	1586	1571	1676	538;444	541;445
$Fe(bztfac)(tftbd)_2$	1592	1591	1575	1645	525;429	541;425
$Fe(tfnac)_2(tbd)$	1574	1739	1550	1649	475;429	455;430
$Fe(tfnac)(tbd)_2$	1583	1584	1567	1644	475;417	454;417
$Fe(tfnac)_2(bzac)$	1575	1726	1550	1654	535;467	544; 470
Fe(bzac)(fbd)(tbd)	1588	1588	1560	1617	446;429	438; 428
Fe(tfnac)(bzac)(tbd)	1580	1588	1562	1622	470;417	454; 407

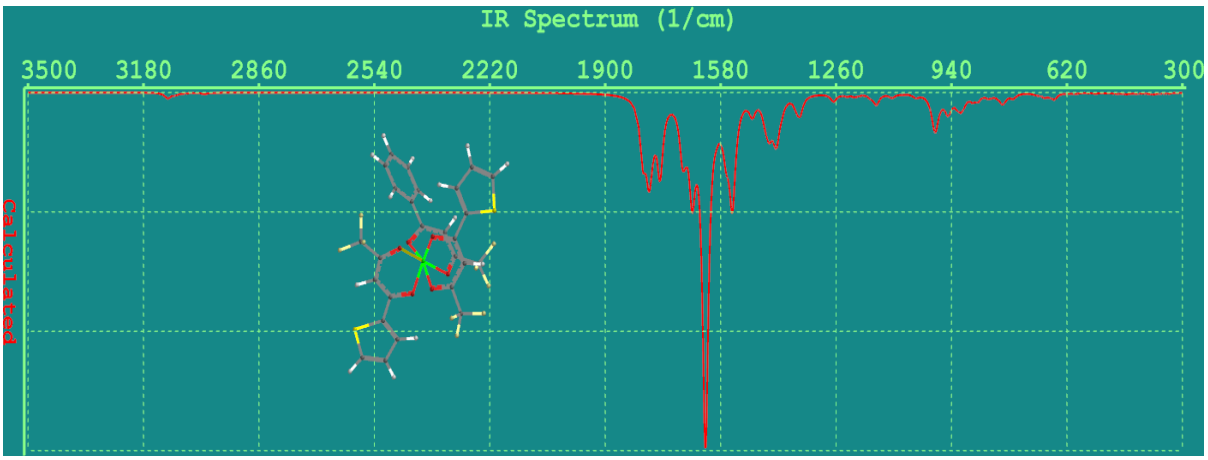

Figure 4.47 IR spectrum of Fe(Bztfac) $(tftbd)_2$ in the gas phase of the molecule.

4.912 MIXED ALUMINIUM (III) BETADIKETONATES

Table 4.36 some relevant infra red bands (cm^{-1}) for mixed Aluminium (III) metal betadiketonates computed at the PM3 level of theory.

Compound	$\upsilon_{as\ C-O}$	$\upsilon_{as\ C-C}$	υ_{sM-O}
$Al(fbd)_2(bzac)$	1833	1646	510,474
$Al(fbd)(bzac)_2$	1834	1644	471,448
$Al(tbd)_2(fbd)$	1829	1646	464,432
$Al(tbd)(fbd)_2$	1834	1648	478,458
$Al(bzac)_2(tftbd)$	1825	1646	516,434
$Al(bzac)(tftbd)_2$	1825	1644	500,435
$Al(bztfac)_2(tftbd)$	1843	1658	549,458
$Al(bztfac)(tftbd)_2$	1854	1648	546,410
$Al(tfnac)_2(tbd)$	1850	1650	489,470
$Al(tfnac)(tbd)_2$	1854	1648	546,447
$Al(tfnac)_2(bzac)$	1849	1655	549,492
Al(bzac)(fbd)(tbd)	1833	1647	478,458
Al(tfnac)(bzac)(tbd)	1850	1631	483,456

4.913 MIXED COBALT (III) BETADIKETONATES

Table 4.37 some relevant infra red bands (cm^{-1}) for mixed Cobalt (III) metal betadiketonates computed at the PM3 level of theory.

Compound	$\upsilon_{as\ C-O}$	$\upsilon_{as\ C-C}$	υ_{M-O}
$Co(fbd)_2(bzac)$	1800	1658	517,367
$Co(fbd)(bzac)_2$	1801	1659	512,403
$Co(tbd)_2(fbd)$	1769	1646	504,365
$Co(tbd)(fbd)_2$	1770	1644	465,367
$Co(bzac)_2(tftbd)$	1789	1658	483,401
$Co(bzac)(tftbd)_2$	1786	1632	408, 372
$Co(bztfac)_2(tftbd)$	1788	1648	486,376
$Co(bztfac)(tftbd)_2$	1785	1632	450,378
$Co(tfnac)_2(tbd)$	1793	1646	401,370
$Co(tfnac)(tbd)_2$	1793	1647	483,370
$Co(tfnac)_2(bzac)$	1789	1647	398,371
Co(bzac)(fbd)(tbd)	1767	1643	493,368
Co(tfnac)(bzac)(tbd)	1795	1643	407,368

4.914 MIXED CHROMIUM (III) BETADIKETONATES

Table 4.38 some relevant infra red bands (cm^{-1}) for mixed Chromium (III) metal betadiketonates computed at the PM3 level of theory.

Compound	$\upsilon_{as\ C-O}$	$\upsilon_{as\ C-C}$	υ_{M-O}
$Cr(fbd)_2(bzac)$	1800	1658	517,367
$Cr(fbd)(bzac)_2$	1701	1660	429,343
$Cr(tbd)_2(fbd)$	1666	1562	490,426
$Cr(tbd)(fbd)_2$	1770	1644	465,367
$Cr(bzac)_2(tftbd)$	1789	1658	483,401
$Cr(bzac)(tftbd)_2$	1712	1630	434, 369
$Cr(bztfac)_2(tftbd)$	1729	1677	445,332
$Cr(bztfac)(tftbd)_2$	1746	1595	480,386
$Cr(tfnac)_2(tbd)$	1790	1664	424,365
$Cr(tfnac)(tbd)_2$	1793	1647	483,370
$Cr(tfnac)_2(bzac)$	1717	1647	435,377
Cr(bzac)(fbd)(tbd)	1736	1673	432,416
Cr(tfnac)(bzac)(tbd)	1717	1647	436,410

4.915 MIXED MANGANESE (III) BETADIKETONATES

Table 4.39 some relevant infra red bands (cm^{-1}) for mixed Manganese (III) metal betadiketonates computed at the PM3 level of theory.

Compound	$\upsilon_{as\ C-O}$	$\upsilon_{as\ C-C}$	υ_{M-O}
$Mn(fbd)_2(bzac)$	1835	1705	480,411
$Mn(fbd)(bzac)_2$	1701	1660	429,343
$Mn(tbd)_2(fbd)$	1666	1562	490,426
$Mn(tbd)(fbd)_2$	1770	1644	465,367
$Mn(bzac)_2(tftbd)$	1789	1658	483,401
$Mn(bzac)(tftbd)_2$	1712	1630	434, 369
$Mn(bztfac)_2(tftbd)$	1729	1677	445,332
$Mn(bztfac)(tftbd)_2$	1746	1595	480,386
$Mn(tfnac)_2(tbd)$	1790	1664	424,365
$Mn(tfnac)(tbd)_2$	1851	1687	455,411
$Mn(tfnac)_2(bzac)$	1717	1647	435,377
Mn(bzac)(fbd)(tbd)	1736	1673	432,416
Mn(tfnac)(bzac)(tbd)	1717	1647	436,410

The spectra of mixed aluminium (III), cobalt (III), chromium (III) and manganese (III) betadiketonates had their C = O and C = C bands appearing at higher wavenumbers than are found in the corresponding iron (III) complexes. These frequencies appear between 1860-1700cm^{-1}for the C = O group and between 1680-1562cm^{-1} for the C = C group. The carbonyl frequencies of mixed aluminium betadiketonates showed the highest shift in band frequencies possibly due to the absence of d-electrons in its configuration.

The M-O vibrational frequencies for all the metal complexes studied were observed below 550cm^{-1} exhibiting all the features present in the corresponding tris-chelates [Adimado and Patel, 1983]. It is observed from the IR bands that, methyl substitution in place of an aromatic group shifts the C = O and C = C vibrational stretches to lower frequencies. This effect could be due to the mesomeric interactions of these aromatic groups by a methyl one (ie inductive effect). There is also an irregular shift in metal- ligand (M - O) bands as a result of unequal metal to ligand back bonding.

4.920 β–DIKETONATE, β-KETOIMINATE, β-DIIMINATE, β- KETOTHIOLATE, β-DITHIOLATE AND β- IMITHIOLATE COMPLEXES OF 4,4,4-TRIFLUORO-1-(2-FURYL)-1,3-BUTANEDIONE (htffbd).

4.921 RESULTS AND DISCUSSION.

The molecular structures of a representative β–Diketonate, β-ketoiminate, β- Diiminate, β-ketothiolate, β-Dithiolate and β-Imithiolate are given in, Figure 4.40 and Figure 4.41. Selected features of the intramolecular geometry of each derivative studied are presented in table 4.40and table 4.41

The M-S bonds (2.306 Å average) are significantly longer than the M-O bonds (1.895 Å average) which in turn is longer than the M-N bond (1.758 Å average). The M-O bonds are shorter in diketonates than in ketothiolates which are also shorter than the ketoiminates while

the M-S distance is longer in the thioiminate than the ketothiolate. The M-N bonds also show shorter distances in the thioiminates than the ketoiminates. The C = C bonds on the keto (O) side of the ring is longer than the C = C bonds on the imine (N) side with the C = C bonds on the thio (S) side of the ring having the shortest bond distance (ie C = C(O) > C = C(N) > C = C(S) in bond length). Perusal of the C-O, C-N and C-S bond lengths also reveals the order C-S > C-N > C-O which reverses the trend in C = C bond distances.

Substitution of the central metal influenced the bond distances with the Mn complexes mostly given the longest distances and the Al complexes the shortest. This might be as a result of the change in electron distribution within the compounds which distorts the shape of the chelate ring and subsequently influencing the bond lengths. It could also be as a result of the labile nature of Al as compared to the inert d^n metal ions.

Table 4.40 Selected bond distances of intramolecular geometry of structurally characterized 4,4,4-trifluoro-1-(2-furyl)-1,3 butanedione(Htffbd).

Compound	M-O	M-S	M-N	C-O	C-N	C-S	C=C(O)	C=C(S)	C=C(N)
Diketonate									
Al(Htffbd)	1.854	-	-	1.264	-	-	1.387	-	-
Co(Htffbd)	1.894	-	-	1.282	-	-	1.400	-	-
Cr(Htffbd)	1.883	-	-	1.325	-	-	1.400	-	-
Fe(Htffbd)	1.868	-	-	1.305	-	-	1.400	-	-
Mn(Htffbd)	1.975	-	-	1.400	-	-	1.400	-	-
Ketothiolate									
Al(Htffbd)	1.834	2.514	-	1.261	-	1.676	1.436	1.374	-
Co(Htffbd)	1.918	2.233	-	1.274	-	1.723	1.444	1.366	-
Cr(Htffbd)	1.909	2.243	-	1.297	-	2.243	1.446	1.357	-
Fe(Htffbd)	1.865	2.305	-	1.283	-	1.715	1.453	1.350	-
Mn(Htffbd)	1.889	2.234	-	1.299	-	1.658	1.411	1.383	-
Ketoiminates									
Al(Htffbd)	1.813	-	1.838	1.268	1.361	-	1.441	-	1.366
Co(Htffbd)	1.937	-	1.797	1.267	1.368	-	1.476	-	1.368
Cr(Htffbd)	1.931	-	1.788	1.313	1.325	-	1.406	-	1.401
Fe(Htffbd)	1.998	-	1.701	1.248	1.388	-	1.354	-	1.464
Mn(Htffbd)	2.098	-	1.667	1.262	1.413	-	1.481	-	1.354
Thioiminates									
Al(Htffbd)	-	2.620	1.793	-	1.268	1.755	-	1.367	1.472
Co(Htffbd)	-	2.267	1.815	-	1.289	1.811	-	1.360	1.467
Cr(Htffbd)	-	2.404	1.773	-	1.316	1.731	-	1.382	1.421
Fe(Htffbd)	-	2.440	1.803	-	1.277	1.752	-	1.348	1.453
Mn(Htffbd)	-	2.440	1.641	-	1.389	1.670	-	1.450	1.360

Table 4.41 Selected bond angles of intramolecular geometry of structurally characterized 4,4,4-trifluoro-1-(2-furyl)-1,3- butanedione(Htffbd).

Compound	S-M-O	N-M-O	S-M-N	S-M-S	N-M-N	O-M-O	M-S=C	M-N=C	M-O=C	C=C=C
Diketonate										
Al(Htffbd)	-	-	-	-	-	97.66	-	-	119.06	125.04
Co(Htffbd)	-	-	-	-	-	101.55	-	-	118.76	123.39
Cr(Htffbd)	-	-	-	-	-	90.60	-	-	131.06	119.14
Fe(Htffbd)	-	-	-	-	-	97.65	-	-	90.71	121.33
Mn(Htffbd)	-	-	-	-	-	97.01	-	-	116.19	123.05
Ketothiolate										
Al(Htffbd)	90.16	-	-	-	-	-	108.50	-	138.82	127.20
Co(Htffbd)	97.55	-	-	-	-	-	108.83	-	130.33	125.92
Cr(Htffbd)	92.66	-	-	-	-	-	109.06	-	132.70	124.11
Fe(Htffbd)	101.09	-	-	-	-	-	92.27	-	119.69	126.61
Mn(Htffbd)	102.63	-	-	-	-	-	104.53	-	123.72	127.83
Ketoiminates										

Al(Htffbd)	-	106.45	-	-	-	-	-	116.78	116.43	128.76
Co(Htffbd)	-	92.18	-	-	-	-	-	126.38	125.93	120.61
Cr(Htffbd)	-	88.10	-	-	-	-	-	137.06	128.14	120.26
Fe(Htffbd)	-	93.27	-	-	-	-	-	116.94	118.00	123.31
Mn(Htffbd)	-	91.52	-	-	-	-	-	117.07	114.20	123.92
Thioiminates										
Al(Htffbd)	-	-	81.58	-	-	-	108.78	145.76	-	126.09
Co(Htffbd)	-	-	91.25	-	-	-	113.21	137.44	-	125.76
Cr(Htffbd)	-	-	85.84	-	-	-	110.50	150.05	-	124.08
Fe(Htffbd)	-	-	94.08	-	-	-	104.65	133.92	-	126.47
Mn(Htffbd)	-	-	86.76	-	-	-	112.51	146.93	-	124.78

HOMO LUMO

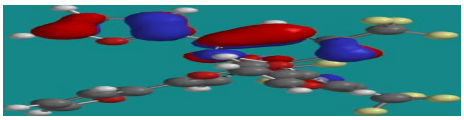
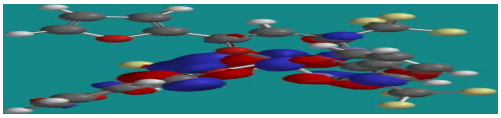

Ketoiminate (-1131.66) (-656.70)


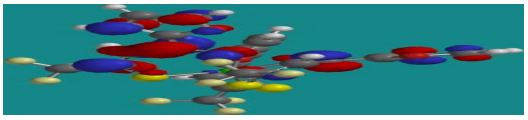

Ketothiolate (-1154.39) (-515.15)

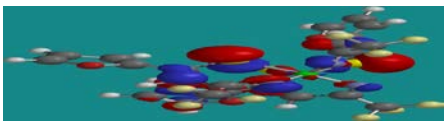
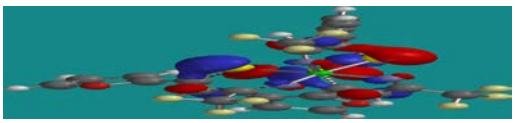

Thioiminate (-890.78) (-339.66)

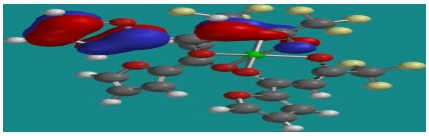
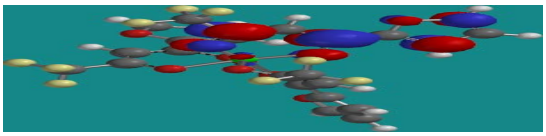

Diketonate (-1194.70) (-496.30)

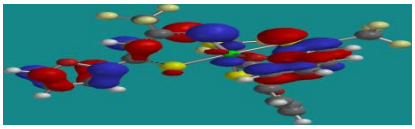
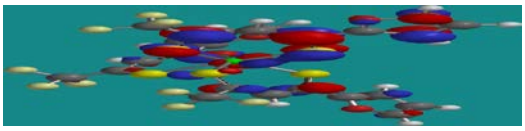

Dithiolate (-534.85) (76.10)

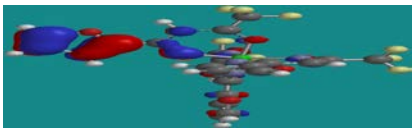
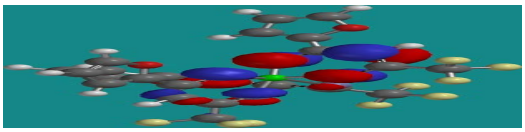

Diiminate (-1123.59) (-496.30)

Figure4.48 Frontier orbitals and their associated energies (in parenthesis) in kJ/mol for ketoiminate, ketothiolate, thioiminates, dithiolate and diiminate from PM3 calculations.

Figure 4.48 provides the relative HOMO and LUMO energies of a series of compounds with varying substitution patterns of heteroatom but with the same chelate ring substituents from which a number of features can be extracted. From the energy values shown in figure 4.48,

the HOMO and LUMO energies increase along the series: β– Diketonate < β– Ketothiolate < β– Ketoiminate < β– Diiminate < β– Thioiminate < β– Dithiolate, presumably due to the electron donating nature of sulphur compared to nitrogen and oxygen.

Substitution along the chelate ring backbone is greatest for the diketonates and smallest for the dithiolates. For chelate rings with only aliphatic substituents on the carbon backbone, the energy of the HOMO varies more than the LUMO on increasing the thiolate substitution. Replacing aliphatic groups on the carbon backbone of the chelate ring with aromatic groups is sufficient to substantially lower the HOMO-LUMO energy gap in the β– Diketonate series of compounds. Substitution of oxygen for an electron donating aniline group allows for fine-tuning of the absorption spectrum, since the HOMO and LUMO energies are destabilized by approximately the same extent [Felipe *et al.*, 2008]. Thus, within a series of chelates derived from the same diketonate, there is only a slight blue-shift in the absorption spectra with increasing aniline substitution, if it can be detected [Felipe *et al.*, 2008].

4.930 SEMI-EMPIRICAL PM3 STUDIES OF N6-TETRADENTATE MACROCYCLIC METAL COMPLEXES AND THEIR DERIVATIVES

4.931 IR Spectra

The spectra of all the complexes show a single band in the region 3031-3253cm^{-1} which is associated with the N-H stretching mode of amide group [Nakamato, 1978]. The amide I, amide II, amide III and amide IV groups [Ashu *et al.*, 2002] present in plane deformations are indicated by the bands at 1561-1785, 1441-1555, 1215-1271 and 632-674cm^{-1}, respectively. A clear identification of the metal–ligand vibrations is not straightforward due to the higher mixture of the different internal coordinates which take part in the description of the normal mode. The far infrared spectra show bands in the region 405- 515cm^{-1} corresponding to ν(M–

N) vibrations [Shakir *et al.*, 1996, 1999: Chandra and Kumar, 2004]. The presence of bands in all complexes in the region 405- 515cm^{-1}, originating from (M–N) azomethine vibrational modes, identifies coordination of the azomethine nitrogen [Rana *et al.*, 1982]. The bands present in the range 300–450cm^{-1} may be assigned to ν(M–Cl) vibration [Shakir *et al.*, 1996, 1999: Chandra and Kumar, 2004]. The infrared spectral data of the complexes are given in Tables 4.42 and 4.43 below.

Table4.42 Relevant IR bands (cm^{-1})

Complex	υ_s(C=N)		υ_{as}(C=N)		υ(C=C) + υ(C=N)		υ(M-N)	
					Skeletal vibrations		Azomethine	
	Expt	Cal	Expt	Cal	Expt	Cal	Expt	Cal
$HADCoCl_2$	1615	1697	1596	1556	1576,1560 1464,1412	1544,1476 1428,1412	510	514
$HADNiCl_2$	1630	1651	1608	1606	1590,1565 1480,1450	1593,1575 1490,1457	488	486
$HADCuCl_2$	1620	1664	1600	1586	1588,1548 1492,1460	1576,1543 1494,1458	456	475
$HBDCoCl_2$	1625	1701	1605	1606	1580,1560 1496,1464	1557,1546 1473,1465	504	508
$HBDNiCl_2$	1635	1657	1605	1606	1590,1576 1492,1464	1569,1538 1496,1464	460	460
$HBDCuCl_2$	1615	1718	1600	1604	1588,1580 1490,1462	1580,1572 1510,1434	425	417

Table4.43 Relevant IR bands (cm^{-1}) for CoR1R3 = CF_3

IR frequencies	assignment	IR frequencies	assignment
3031-3253w	CH_3 + NH	1419-1423w	Δ ring
1832-1837m	C=C-C	1405-1407w	CF_3 + CH_3
1780-1785s	C=N	1371-1387w	CH_3
1758-1760w	$C=N_{ring}$	634w	Co-N
1711-1715vs	C=N+ Δ ring	522w	Co-N
1561-1581w	Δ ring	495w	Co-Cl
1540-1555w	Γring	443w	Co-N
1441-1463w	C-C		

Table4.44 Relevant bond lengths (Å) and bond angles (degrees) for CoR1R3 = CF_3

Bond distance				Bond angles			
Co1-Cl1	2.206	N7-C8	1.483	N7-Co1-N6	107.24	Co1-N7-C2	103.58
Co1-Cl2	2.243	N7-C2	1.465	N3-Co1-N4	107.15	Co1-N6-C6	102.30
Co1-N6	2.052	N6-C6	1.443	N4-Co1-N7	74.16	N6=C15-C16	120.20
Co1-N7	2.016	N6=C15	1.325	N3-Co1-N6	72.44	N3-C14=C16	117.12
Co1-N4	2.025	N4=C1	1.330	Cl1-Co1-Cl2	179.01	N4=C1-C13	117.39
Co1-N3	2.067	N-C_{py}	1.349	Co1-N6-C15	135.45	N7=C8-C13	118.81
N3-C11	1.465	N=C_{py}	1.345	Co1-N3-C14	121.71	C1-C13=C8	117.91
N4-C12	1.441	C1-C20	1.483	Co1-N3-C11	102.80	C15-C16=C14	119.30
C8-C19	1.537	C15-C18	1.558	Co1-N4-C12	103.27		
C1-C13	1.471						

Table4.45 Relevant bond lengths (Å) and bond angles (degrees) for CoR1R3 = Phe

Bond distance				Bond angles			
Co1-Cl1	2.210	N7-C8	1.496	N7-Co1-N6	107.42	Co1-N7-C8	122.98
Co1-Cl2	2.243	N7-C2	1.464	N3-Co1-N4	107.43	Co1-N6-C14	120.39
Co1-N4	2.033	N6-C6	1.441	N4-Co1-N7	74.16	N6=C15-C16	118.77
Co1-N7	2.061	N6=C15	1.333	N3-Co1-N6	73.49	N3-C14=C16	118.01
Co1-N6	2.032	N4=C1	1.331	Cl1-Co1-Cl2	179.88	N4=C1-C13	117.39
Co1-N3	2.038	N-C_{py}	1.464	Co1-N6-C15	136.23	N7=C8-C13	118.81
N3-C11	1.464	N=C_{py}	1.464	Co1-N3-C14	120.39	C1-C13=C8	119.69
N4-C12	1.441	C1-C25	1.472	Co1-N3-C11	103.26	C15-C16=C14	119.31
C8-C19	1.479	C15-C16	1.462	Co1-N4-C12	103.13		
C1-C13	1.461						

Table4.46 Relevant bond lengths (Å) and bond angles (degrees) for CoR1R3 = CH_3

Bond distance				Bond angles	
Co1-Cl1	2.229	N3-C11	1.339	N5-Co1-N4	79.57
Co1-Cl2	2.244	N5-C2	1.418	N6-Co1-N3	77.74
Co1-N4	1.962	N5-C8	1.367	N3-Co1-N4	97.82
Co1-N5	1.991	N6=C15	1.391	N6-Co1-N5	104.94
Co1-N6	2.047	N4=C1	1.377	Cl1-Co1-Cl2	177.36
Co1-N3	1.957	C8=C13	1.398	Co1-N5-C8	138.00
N3-C14	1.447	N=C_{py}	1.464	Co1-N4-C1	138.24
N4-C12	1.418	C1-C25	1.472	Co1-N4-C12	105.62
C8-C19	1.479	C15-C18	1.486	Co1-N3-C1	116.93
C1-C13	1.391			Co1-N6=C15	134.80

4.940 Optimization of the Geometrical Parameters

A semi-empirical optimization of the geometrical parameters, and hence a structural analysis for the N6- tetradentate macrocyclic metal complexes were studied at the PM3 level of theory. The calculated bond lengths for the two Co–Cl were on the average 2.2245Å for trifluoro substituents, 2.2265Å for phenyl substituents and 2.2365Å for methyl substituents. The Co – N bond lengths on the average for the CF_3, phenyl and CH_3 substituents are respectively 2.040Å, 2.041Å and 1.989Å.

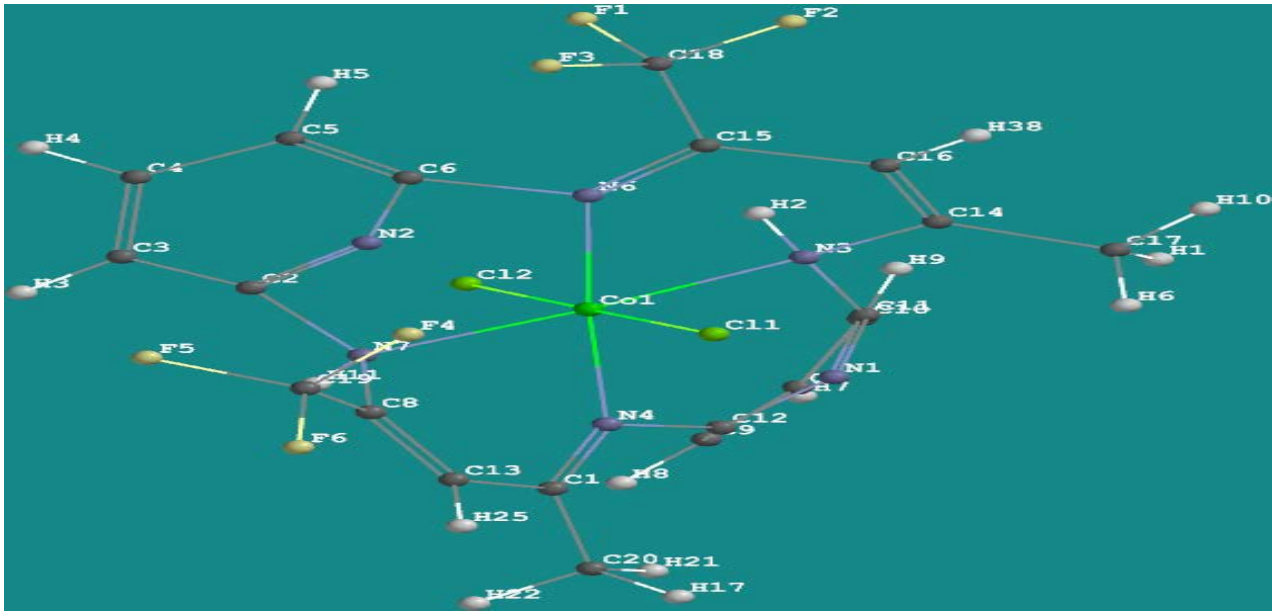

Figure 4.49 PM3 optimized structure of Co N6 macrocycle with CF3 substituents as derivative of the other metal β-ketoiminates showing atomic numbering.

CHAPTER FIVE

5.0 CONCLUSION AND RECOMMENDATION

5.1 CONCLUSION

Theoretical structural analysis through the PM3 and DFT procedures have shown that the most probable and stable structures for the $[M(acac)_3]$ (where M = Al, Co, Cr, Fe, or Mn) complexes and their derivatives are the fluorinated ones. The vibrational spectra were calculated starting from the most probable structure, with the aim of assisting in the vibrational assignment.

For the best interpretation of the PM3 and DFT vibrational analysis through the Spartan program, we thought that the visual computerized picture of each normal mode gives only a rough approach of its own characterization, and hence we studied relevant bonds and angles of the structures for a best indication of which bond or angle within the definition of an internal coordinate has a higher participation in the molecular vibration. The results of the bonding studies show that both methods, B3LYP and PM3, overestimate bond lengths compared to X-ray crystal structure data because of Coulomb repulsion in the gas phase.

The results of this study exhibit that the increase in the size of metal atom from the main group (Al) to the first role transition metals (Co, Fe, Cr and Mn) leads to an increase in the M-O bond length and a decrease in O-M-O bond angle. However, all other geometry parameters of the complexes remain almost unaffected.

The fundamental vibrational modes of acetylacetone and each of its complexes with the main group and first role transition metals together with the substituted derivatives have been successfully assigned based on the expterimentally observed IR vibrational spectra and the calculated frequencies and intensities.

5.2 RECOMMENDATIONS

1. From our work, all spectroscopic determinations were done in the gas phase. We suggest studies of the behaviour of these complexes in different solvents to ascertain the solvent effect on the spectroscopic and other bonding parameters.
2. Future work on these interesting complexes should include alternate computational treatments such as MP2 and MO6.

REFERENCES

Adams H., Baileyand A.N. and Fenton D.E. (1987); Organometallic Anticancer Compounds. J. Chem. Soc. Dalton Trans, 207.

Afshari S. (2010); a theoretical investigation of substituent effects on structure and NQR parameters of phenacyl phenyl sulfide derivatives.

Ahmed, M. A. K.; Fjellvåg, H.; Kjekshus, A.; Dietzel, P. D. C. Z. (2007); Mixed Ligand Complexes of Cobalt(II)-Synthesis, Structure, and Properties of $Co_4(thd)_4(OEt)_4$. Anorg.Allg. Chem., 633, 1371-1381.

Albertin G., Bordighon E. and Orio A.A. (1975); Five-Coordinate Copper(I1) Complexes. Synthesis and Properties of $[Cu(tren)L]^{2+}$ Cations. lnorg. Chem., 14, 1411.

Anant P., Mukesh P. G., Singh K.K. (2011) Int.J. ChemTech Res.,3(1)

Andrew D .Burrows,.; Frost, Christopher G.; Mahon, Mary F.; Raithby, Paul R.; Renouf, Catherine L.; Richardson, Christopher; Stevenson and Anna J. (2010); Dipyridyl beta-diketonate complexes: versatile polydentate metalloligands for metal-organic frameworks and hydrogen-bonded networks, 5067-5069.

Adimado A. A. and Patel K. S. (1983); Mixed Iron (III) β-diketonates; J. Coord.Chem., Vol. 13, 79-82.

Adimado A. A., AbaidooR. C. and Bondzi C. (1991);The antimicrobial effect of N_6 – tetradentate macrocyclic metalcomplexes and their precursors. Transition Met. Chem. 16, 407-409.

Asare D. N. (1999); Theoretical studies on mechanisms of some transition metal organometallic reactions. MSc. Thesis, KNUST.

Asbell, P.A.; Epstein, S.P.; Wallace, J.A.; Epstein, D.; Stewart, C.C.; Burger,R.M.(1998); Efficacy of cobalt chelates in the rabbit eye model for epithelial herpetic keratitis. Cornea, 17, 550–557.

Ashu C, Jaroli D. P. and Singh R.V.(2002); antimicrobial, antifertility and anti-inflammatory approach to tetradentate macrocyclic complexes of iron(II) and manganese(II). Metal Based Drugs Vol. 8, No. 6.

Baidina, I. A.; Krisyuk, V. V.;Stabnikov, P. A. (2006); Structure and Properties of Heterocomplex Compounds Based on Lead(II) Hexafluoroacetylacetonate and Copper(II) β-Diketonates. J. Struc. Chem., 47, 1111-1116.

Ballhausen C.J. and Gray H. B. (1962); The Electronic Structure of the Vanadyl Ion, Inorganic Chem. 1, 111.

Barceloux, D.G. (1999); Clinical toxicology, Cobalt.Clin.Toxicol.,Topanga, California 37(2), 201 -216.

Bertini, I.; Gray, H.B.; Stiefel, E.I.; Valentine, J.S.(2007); Biological Inorganic Chemistry: Structure and Reactivity; University Science Books: Sausalito, CA, USA.

Bradley D. F. and Andrew R. B. (2000); Substituent Effects on the Volatility of β-diketonates; Adv. Mater. Opt. Electron 10, 223-232.

Braga D., and Dillon L. A. C. (1997); Nature, London 386, 377.

Braga D., L. Brammer, N.R. Champness (2005), Cryst. Eng. Commun. 7, 1.

Brittain H.G. (1975); Proton Magnetic Resonance Spectrum of Magnesium Acetylacetonate in Chloroform-d.Evidence for Conformational Equilibrium. Inorg. Chem., 14 (11), 2858-2860.

Camermar, A.; Mastropaolo, D.; Camerman, N.(1983); Molecular Structure of Acetylacetone. A Crystallographic Determination.J. Am. Chem. Soc.,105, 1584-1586.

Case D. A. and Pinnavaia T. J (1971); Kinetics of stereochemical rearrangement for mixed β-diketonate complexes of Aluminium(III). Inorg.Chem., 10,482.

Cassandra L. F. (2006) polymeric metal complexes.Metallo-biomaterials for medicine and biotechnology. Bio-inspired and sustainable design.Responsive nanoscale assemblies.

Chandra S, Jain Deepali , Sharma Amit Kumar and Sharma Pratibha (2009); Coordination Modes of a Schiff Base Pentadentate Derivative of 4-Aminoantipyrine with Cobalt(II), Nickel(II) and Copper(II) Metal Ions: Synthesis, Spectroscopic and Antimicrobial Studies, Molecules,14 ,174-190.

Clark M., Cramer R. D.(III), and Opdenbostch N. V.(1989); Validation of the general purpose tripos 5.2 force field. J. comput Chem., 10, 982.

Clark, M.J.E.(1989); Ruthenium and Other Metal Complexes in Cancer Chemotherapy; Springer-Verlag:Heidelberg, Germany.

Collen S. A. J, Everaerts F. M. , Huf F. A. (1997); Characterization of ^{60}Co γ-Radiation Induced Radical Products of Antipyrine by Means of High-Performance Liquid Chromatography, Mass Spectrometry, Capillary Zone Electrophoresis, Micellar Electrokinetic Capillary Chromatography and Nuclear Magnetic Resonance Spectrometry, J. Chromatogr. A, 788, 95-103.

Cowan, J.A.(1997); Inorganic Biochemistry, 2nd ed.; Wiley-VCH: New York, NY, USA.

Do Couto, P.C.; Cabral, B. J. C.; Simões, J. A. M.(2006). Chem. Phys. Lett.,419(4-6), 486- 491.

Dreizler R.M., da Provincia J.(1984) Eds.; Density functional methods in physics, Plenum New York.

Eddie L. Chang , Christa Simmers and Andrew D. Knight (2010). Cobalt Complexes as Antiviral and Antibacterial Agents; J. pharm., 3, 1711-1728.

Eshraq A. A.A. (2007); Structure and Spectra of Acetylacetone and Some of Its complexes with Alkaline Earth Metals, 2-3.

Evans G.W. (1989); The effect of chromium picolinate on insulin controlled parameters in humans. Int J Biosoc Med Res;11:163, 80.

Felipe P. M., Chengeto G., Sergy V. L., Mark D. S. and James R. G.; β – Diketonate, β – ketoiminate, and β – Diiminate complexes of Difluoroboron. Eur. J. Inorg. Chem.. 2008, 3200-3211

Fenton, D. E.; Casellato, U.; Vigato, P.A.; Vidali, M. (1984); Electrochemical behaviour of acyclic and macrocyclic complexes of nickel(II), copper(II) and Uranyl(VI). Inorg. Chim.Acta, 95,187.

Fischer E. Rivera, B. A., Kohse-H. K. (2001); Chemical vapour deposition of Co_3O_4 on honeycomb substrates for catalytic applications oinghaus, J. Phys. IV 11 629.

Fortman J. T. and Sievers R.E.(1967); Determination of Rates of Optical Inversion of Aluminum β-Diketonate Complexes by Nuclear Magnetic Resonance Studies of Racemic Mixtures.Inorg. Chem., 6, 2022.

Frenking G., Antes I., Bohme M., Dapprich S., Ehler A.W.., Jonas V., Neuhaus A., Otto M., Stegmann R., Veldkamp A., Vyboishchikov S. F.(1996); Reviews in Computational Chemistry, eds. Lipkowitz K. B and Boyd D.D.VCH, New York, vol.8.

Furuta H, Kubo N, Maeda H, Ishizuka T, Osuka A, Nanami H and OgawaT (2000);N-confused double-decker porphyrins. Inorg. Chem. 39, 5424-5425.

Gaber M., Rehab A. and Badr-El-deen D.F.,(2008); Spectral and thermal studies of new Co(II) and Ni(II) hexaaza and octaazamacrocyclic complexes.J. Therm. Anal. Calor., 91.

Ghosh A. and Jynge K. (1997); *Cis-Trans* Isomerism in Porphyrin Isomers.J. Phys. Chem. B,101, 5459-5462.

Granquist C.G. (1995), Handbook of Inorganic Electrochromic Materials,Elsevier, Amsterdam.

Haitao zhang (2010); Heterometallic *β*-diketonates and oxo diketonates as single source precursors for the synthesis of oxide materials.UMI 3389998.

Hatchikian, E.C.(1981); A cobalt porphyrin containing protein reducible by hydrogenase isolated from Desulfovibrio desulfuricans (Norway). Biochem.Biophys.Res. Commun.,103, 521–530.

Herlinger A.W., Funk E.M., Chorak R.F.,Siebert J.W. and Roco E., (1994). Polyhedron, 13 69.

Hohenberg P. and Kohn W.; Inhogeneous electron gas. Phys. Rev. 136, B864 (1964).

Jackman L. M. and Sternhell S.(1969); Applications of nuclear magnetic resonance spectroscopy in organic chemistry. *Pergamon Press, Oxford*. Second Edition.134, 80.

Jalbout, A. F.; Nazari, F.; Turker L. *J. Mol. Struct.(THEOCHEM)*, **2004**, *1*, 627.

Jeffrey P. M., Damian M., and Leo R. (2007); An Evaluation of Harmonic Vibrational Frequency Scale Factors. J. Phys. Chem. A, 111, 11683-11700.

Karlin K.D. and Zubieta J. (1983); Copper Coordination Chemistry Biochemical and Inorganic Perspective, Academic Press, New York, 43.

Katz S. A.and Salem H.(1994); The Biological and Environmental Chemistry of Chromium, Eds.,VCH Publishers, New York.

Keegan,G.M., Learmonth,I.D.; Case C.(2008). A systematic comparison of the actual, potential, and theoretical health effects of cobalt and chromium exptosures from industry and surgical implants. Crit. Revs. Toxicology,38, 645–674.

Kodas T, Hampdem- Smith M.(1996); The Chemistry of Metal CVD. VCH: New York.

Koen Binnemans (2005); Handbook on the Physics and Chemistry of Rare Earths, Vol. 35

Kohn W. and Sham L. J. (1965); Self-Consistent Equations Including Exchange and Correlation Effects Phys. Rev. 140, A1133.

Kohn W., Y. M., and. Makarov D. E. (1998), ibid. 80, 4153.

Lecomte C., Rohmer M-M and Benard M. (2000); The porphyrin handbook (eds) K M Kadish, K M Smithand R Guilard, 2, 39– 78; Shelnutt J. A. (2000); The porphyrin handbook (eds) K M Kadish, K MSmith and R Guilard, 7, 167–223.

Lehn, J. M. (1978); Cryptates: inclusion complexes of macropolycyclic receptor molecules. Pure Appl. Chem. 50,No.9-10, 871-892.

Liang J. H., Jian F. F., and Tang M.(2009); DFT study of gaseous conformers of aspartic acid. J. of Theor.and Comp. Chem. (JTCC), 9, 687-700.

Lindoy, L. F.; Lip, H. C.; Louie, H. W.;Drew, M. G. B.; Hudson, M.(1977); Interaction of Lanthanide Shift Reagents with Coordination Complexes; Direct Observation of Nuclear Magnetic Resonance Signals for Free and Complexed Tris(pentane-2,4-Dionato) cobalt(III) at Ambient Temperature, and X-Ray Crystal and Molecular Structure of the 1:1 Adduct Formed J. Chem. Commun., 778-780.

Liu X., Qui Y., Sun S., Liu C. and Su Z. (2009); DFT study on second- order nonlinear optical properties of the derivatives of disubstituted seven-vertex cobaltacarborane metallocenyl.

Macklin, J.W.(1976); Mercury β-diketonato complexes-I. Vibrational spectra and structure of mercury acetylacetonato compounds. Spectrochimica Acta, 32A, 1459-1470.

Maeda H. (2005); Synthesis and Properties of Multiply N-Confused Porphyrins. 2005 winner of the IUPAC prize for young Chemistry.

Maryam S. A. and Alireza F. (2010); DFT study on metal cationization and o_6-protonation on 2′-deoxyguanosine configuration: changes on sugar puckering and strength of the n-glycosidic bond. J. of theo. and comp, chem. (jtcc) , 9, 585-609.

Maverick, A. W.; Ivie, M. L.; Waggenspack, J. H.; Fronczek, F. R.(1990); Intramolecular Binding of Nitrogen Bases to a Cofacial Binuclear Copper(11) Complex. Inorg. Chem., 29, 2403.

Mehrotra, R.C., Bohra, R., Gaur, D.P., (1978); Metal *β*- Diketonates and Allied Derivatives. Academic Press, London.

Mertz W. (1975); Effects and metabolism of glucose tolerance factor. Nutr Rev; 33:129–35.

Mruthyunjayaswamty B.H.M., Omkar B. Ijare and Y. JadegoudJ.Braz. Chem. Soc., Vol. 16, No. 4, 783-789, 2005.

Mulliken R. S.(1955); Electronic Population Analysis on LCAO-MO Molecular Wave Functions, J. chem. Phys., 23, 1833.

Natalia E. F., Nikolai V. G., Igor K. I., Alexander N. M., Natalia B. Morozova and Robert H. T. (2001);International Journal of Thermal Sciences, 40(5), 469-477.

Neilsen S.A, Izan, R.M. Brandshaw J.S., Lamb J.D., Christensen J.J. and. Sen D, (1985). Chem. Rev., 85, 271.

Nielsen F.H. Chromium. In: Shils M.E., Olson J.A., Shike M, (1993) eds. Modern nutrition in health and disease. 8th ed. Philadelphia: Lea & Febiger,:264–268.

O'Neill, P. M.; Hindley, S.; Pugh, M. D.; Davies, J.; Bray, P. G.; Park, B. K.; Kapu, D. S.; Ward,S. A.; Stocks, P. A. (2003); Co(thd)2: a Superior Catalyst for Aerobic Epoxidation and Hydroperoxysilylation of Un-Activated Alkenes: Application to the Synthesis of Spiro-1,2,4-Trioxanes. Tetrahedron Lett.,44, 8135-8138.

Oluwatola Omoregie (2011); Synthesis and Physicochemical Studies of Nickel(II) Complexes of Various 2-Alkyl-1-phenyl-1,3- butanediones and Their 2,2'-Bipyridine and 1,10- Phenanthroline Adducts.Int. J. of Chem. Vol. 3, No. 1.

Ozgur A. and Cemal P.(2010); vibrational spectroscopic investigation and conformational analysis of 1-pentylamine: a comparative densityfunctional study. J. of Theor.and Comp. Chem. (JTCC), 9,667.

Palmer R. A., Fay R. C. and Piper T. S. (1964); Stereochemistry of Metal β-Diketonates Complexes with Two Different Ligands, Inorg.Chem., 3, 875.

Pasko, S.; Hubert-Pfalzgraf L. G.; Abrutis A.(2004); Synthesis and Molecular Structures of Cobalt(II) β -Diketonate Complexes as New MOCVD Precursors for Cobalt Oxide Films. Vaissermann, J. Polyhedron, 23, 735-741.

Patel K. S. and Adimado A. A.(1980); Physicochemical studies of metal β-diketonates – V; Spectral and magnetic properties of the Al(III), Cr(III), Mn(III), Fe(III) and Co(III) complexes of 1-(2-Thienyl)- 1,3-butanedione and 4,4,4-Trifluoro-1-(2-Thienyl)-1,3- butanedione. J. inorg.Nucl.Chem..vol.42, 1241-1246.

Perdew J. P.(2005), Prescription for the design and selection of density functional approximations: More constraint satisfaction with fewer fits J. Chem. Phys. 123, 062201.

Purdy AP, Berry AD, Holm RT, Fatemi M, Gaskill DK, inorg. Chem. (1989); 2799.

Raissi, H.; Nowroozi, A.; Roozbeh, M.; Farzad, F.(2006).J. Mol. Struct.,787(1-3), 148.

Raman N., Joseph J., Senthil A. K. V. and Pothiraj C.(2006). Mycrobiology, 34(4): 214-218. Rees W.S. Jr (1996); Chemical Vapour Deposition: An Integrated Engineering Design for Advanced Materials (Engineering Materials and Processes).VCH: New York.

Ritu S., Prabhat, Randhir S., Swati P. and Avnish C.(2010); Studies of Transition Metal Complexes and Their Antibacterial Activities; J. of Ame. Sci.; 6(9):559-564.

Rosenberg, B.(1978); Platinum complexes for the treatment of cancer. Interdiscipl.Sci. Rev.,3, 134–147.

Rosu T , Pasculescu S, Lazar V, Chifiriuc C, Cernat R. (2006); Copper(II) Complexes with Ligands Derived from 4-Amino-2,3- dimethyl-1-phenyl-3-pyrazoline-5-one. Molecules, 11, 904-914.

Sadler, P.J.(1984); The biological chemistry of gold. Struct. Bond, 29, 171–214.

Salahub D. R., and Zerner M. C.(1989); The challenge of d and f electrons. Ed. Salahub D. R. and Zerner M. C. ACS Washington D.C., 1.

Samuels J.A., Folting K., Huffman J.C., Caulton K.G. (1996); Synthesis and characterization of fluorinated β-ketoiminate and imino- alcoholate Pd complexes: precursors for palladium chemical vapor deposition. Chem. Mater. 1996; 7: 929.

Sorokin, M. F.; Shode, L. G.; Nogteva, S. I. Tr.-Mosk.Khim(1980); Tekhnol. Inst. Im. D. I. Mendeleeva.,110, 132-134.

Sosa, C.; Andzelm, J.; Elkin, B. C.; Wimmer, E.; Dobbs, K. D.; Dixon, D. A. (1992).; A local density functional study of the structure and vibrational frequencies of molecular transition-metal compounds." *J. Phys. Chem.*96, 6630-6.

Spartan ’08 (2008) for Windows; Wavefunction, Inc.: Irvine, CA, USA.

Sylvester Burton (2006); synthesis, characterization and properties of copper(II) betadiketonate macrocycles.

Tabellion, F. M.; Seidel, S. R.; Arif, A. M.; Stang, P. J.(2001); Discrete Supramolecular Architecture vs Crystal Engineering: The Rational Design of a Platinum-Based Bimetallic Assembly with a Chairlike Structure and Its Infinite, Copper Analogue.J. Am. Chem.Soc., 123, 7740-7741.

Takimoto, M.; Mori, M.(2002); Novel Catalytic CO_2 Incorporation Reaction: Nickel-Catalyzed Regio- and Stereoselective Ring- Closing Carboxylation of Bis-1,3-dienes. J. Am. Chem. Soc., 124 (34), 10008-10009.

Takimoto, M.; Nakamura, Y.; Kimura, K.; Mori, M.(2004); Novel Catalytic CO_2 Incorporation Reaction: Nickel-Catalyzed Regio- and Stereoselective Ring-Closing Carboxylation of Bis-1,3-dienes .J. Am. Chem. Soc., 126 (19), 5956-5957.

Tayyari S.F., Milani-Nejad F., Rahemi H.(2002); Structure and vibrational spectra of the enol form of hexafluoro- acetylacetone.A density functional theoretical study. Spectrochim Acta A Mol Biomol Spectrosc. 58(8):1669-79.

Tayyari, S. F.; Raissi, H.; Milani-Nejad, F.; Butler, I. S. (2001); Vibrational assignment of α-cyanoacetylacetone.Vib.Spectrosc.,26, 187-199.

Téllezs, G. A.; Hollauer, E.; De Silva, M. I. P.; Mondragon, M. A.; Haiduc, Wang R.H., F.L. Jiang, Y.F. Zhou, L. Han, M.C. Hong, Inorg. Chim. Acta 358 ws(2005) 545.

Troyanov, S. L.; Gorbenko,O. Y.; Bosak, A. A. (1999); Synthesis, Crystal Structure and Properties of Manganese(II) Hexafluoroacetylacetonates $Mn(hfa)_2(H_2O)_2$ and KMn(hfa)3. Polyhedron, 18, 3505-3509.

Vincent J.B. (1999); Mechanisms of chromium action: low-molecular- weight chromium-binding substance. J.Am.Coll.Nutr.;18:6–12.

Warren J. Hehre (2003); A Guide to Molecular Mechanics and Quantum Chemical Calculations, 48.

Weber, U.; Thiele, H.(1998); NMR Spectroscopy: Modern Spectral Analysis.WILEY-VCH. Weinheim.

Wexler D. and Zink J. I. (1996); Luminescence and Resonance Raman Studyof Molecular Distortions Caused by Ligand-Centered Transitions in Metal Acetylacetonate ComplexesInorg.Chem. 35, 4064-4066.

Wu Y-D, Chan K. W. K., Yip C-P, Vogel E., Plattner D. A. and Houk K. N. 1997 J. Org. Chem. 62, 9240.

Ziegler, Tom. (1995); Density Functional Theory as a Practical Tool in Studies of Organometallic Energetics and Kinetics. Beating the Heavy metal Blues with DFT. Can.J.Chem ; 73, 743.